DEVELOPMENT OF NOVEL THERAPEUTICS FOR STROKE: PRECLINICAL INVESTIGATIONS OF OSTEOPONTIN AND 3-IODOTHYRONAMINE

By

Kristian Paul Doyle

A DISSERTATION

Presented to the Department of Molecular Microbiology & Immunology

at the Oregon Health & Science University

in partial fulfillment of

the requirements for the degree of

Doctor of Philosophy

School of Medicine
Oregon Health & Science University

CERTIFICATE OF APPROVAL

This is certify that the Ph.D thesis of

Kristian P. Doyle

has been approved

Mentor/Advisor – Mary Stenzel-Poore, Ph.D.

Member – David Grandy, Ph.D.

Member – Fred Heffron, Ph.D.

Member – Klaus Frueh, Ph.D.

Member – Roger Simon, M.D.

CONTENTS

LIST OF FIGURES

LIST OF TABLES

ACKNOWLEDGEMENTS

All of my grandparents died as a result of stroke, including my grandmother Rosemary Nash, who suffered a series of strokes while I was working on this thesis that took away her dignity, memories and ability to enjoy life. This personal disaster strengthened my resolve to pursue a career in stroke research and develop treatments for this devastating disease. This thesis is dedicated to her memory.

I would like to acknowledge Tao Yang and Nik Lessov who performed all of the rodent stroke surgeries included in this thesis. They are both endowed with tremendous patience and skill and it has been a privilege to work with each of them. I am also indebted to David Grandy and Thomas Scanlan for providing me with the novel compounds thyronamine and 3-iodoythyronamine and Katherine Suchland, without whom the thyronamine project would not have been possible.

I would also like to thank my mentor Mary Stenzel-Poore. She has always listened to me and taken my ideas seriously, no matter how unusual. She has always offered encouragement and given me the freedom to explore new directions. She has always demanded excellence and I could not have chosen a better scientist to learn from. I am also grateful to Roger Simon, a gentleman, a scholar and a role model to emulate as I pursue a career in stroke research.

PREFACE

I have prepared my dissertation in accordance with the guidelines set forth by the Graduate program of the School of Medicine, Oregon Health & Science University. My thesis is comprised of a general introduction, three chapters of original data, a chapter of perspectives, a final chapter consisting of materials and methods and an appendix describing a new primate model of stroke. The references throughout the entire thesis are listed together at the end of the manuscript and conform to the style of *Stroke*.

Chapter 2 consists of work that resulted in two manuscripts, one already published in the *Journal of Cerebral Blood Flow and Metabolism* (February 2005 issue) and the other submitted to the same journal. Chapter 3 consists of data from a manuscript that has been accepted for publication in the journa*l Stroke* and will be published in August of 2007. Chapter 4 pertains to data from a combinatorial experiment using both OPN and T_1AM that has not been submitted for publication. The appendix is currently being adapted into a manuscript and will be submitted to a currently unspecified journal.

ABSTRACT

The goal of my research has been to develop new treatments for ischemic stroke. In pursuit of this goal I have performed a preclinical investigation of osteopontin (OPN) and 3-iodothyronamine (T_1AM), two novel drug candidates that could be developed into therapies for stroke patients.

Osteopontin (OPN) is a secreted extracellular phosphoprotein involved in diverse biological functions, including inflammation, cell migration, and anti-apoptotic processes. In this thesis I investigate the neuroprotective potential of OPN using both *in vitro* and *in vivo* models of ischemia. I show that primary cortical neuron cultures exposed to OPN are protected against cell death from oxygen and glucose deprivation (OGD) and that the effect of OPN depends on the Arg-Gly-Asp (RGD) motif, and an increase in Akt and p42/p44 MAPK phosphorylation. Intra-cerebral ventricular administration of OPN caused a marked reduction in infarct size following transient middle cerebral artery occlusion in a murine stroke model and together these data suggest that OPN is a potent neuroprotectant against ischemic injury.

I sought to increase the neuroprotective potency of OPN and improve the method of delivery. Data presented here shows that thrombin cleavage of OPN improves its ability to ligate integrin receptors and improves its neuroprotective capacity in models of ischemia. I also tested whether OPN could be administered by intranasal administration and found that OPN is efficiently targeted to the brain via this delivery route and confers

robust protection against ischemic brain injury. OPN mimetics based on the peptide sequences located N or C terminal to the thrombin cleavage site were generated and tested in models of ischemia. Treatment with successively shorter N terminal peptides and a phosphorylated C terminal peptide provided significant neuroprotection against ischemic injury. These findings show that OPN mimetics offer promise for development into powerful new drugs for the treatment of stroke.

Mild hypothermia confers profound neuroprotection in ischemia. Two recently discovered natural derivatives of thyroxine, 3-iodothyronamine (T_1AM) and thyronamine (T_0AM) have been shown to lower body temperature in rodents for several hours without induction of a compensatory homeostatic response. Here I tested whether T_1AM- and T_0AM-induced hypothermia protects against brain injury from experimental stroke. I administered T_1AM and T_0AM 1 hour *after* stroke to test for an acute protective effect and 2 days *prior* to stroke to test whether they could be used as a preconditioning stimulus. T_1AM and T_0AM administration reduced body temperature from 37^oC to 31^oC. Mice given T_1AM or T_0AM after the ischemic period had significantly smaller infarcts compared to controls. Mice preconditioned with T_1AM prior to ischemia displayed significantly smaller infarcts compared to controls. Pre- and post-ischemia treatments required a drop in body temperature to achieve subsequent neuroprotection. These findings show that T_1AM and T_0AM, are potent neuroprotectants in acute stroke and T_1AM can be used as antecedent treatment to induce neuroprotection against subsequent ischemia.

The failure of any single neuroprotectant to be advanced to clinical use has led to considerable interest in combinatorial therapy. This thesis concludes with a combinatorial experiment using both OPN and T_1AM with T_1AM applied as an antecedent treatment and OPN as an acute neuroprotectant.

LIST OF ABBREVIATIONS

AADC	Aromatic amino acid decarboxylase
ACA	Anterior cerebral artery
aCSF	Artificial cerebrospinal fluid
AMPA	α-amino-3-hydroxy-5-methyl-4-isoxazolepropionic acid
ASA	American Stroke Association
BBB	Blood brain barrier
CNS	Central nervous system
CSD	Cortical spreading depression
COX-2	Cyclooxygenase-2
ECM	Extracellular matrix
FAK	Focal adhesion kinase
FDA	Food and Drug Administration (United States)
FGF	Fibroblast growth factor
GPCR	G-protein coupled receptor
ICV	Intracerebroventricular
IGF-1	Insulin like growth factor 1
IL-6	Interleukin 6
ILK	Integrin linked kinase
IN	Intranasal
IP	Intraperitoneal
KO	Knockout mouse

MAPK	Mitogen activated protein kinase
MCA	Middle cerebral artery
MCAO	Middle cerebral artery occlusion
MMP	Matrix metalloprotease
MCP-1	Monocyte chemoattractant protein-1
MRI	Magnetic resonance imaging
NGF	Nerve growth factor
NMDA	N-methyl-D-aspartate
NO	Nitric oxide
NOS	Nitric oxide synthase
OGD	Oxygen-glucose deprivation
OPN	Osteopontin
PARP1	Poly(ADP-ribose)polymerase-1
RGD	Arginine, glycine, aspartate (integrin binding sequence)
RNS	Reactive nitrogen species
ROS	Reactive oxygen species
SAR	Structure activity relationship
SLAYGLR	Cryptic integrin binding sequence (mouse)
SVVYGLR	Cryptic integrin binding sequence (human)
rt-PA	recombinant tissue plasminogen activator
T3	3,5,3,’-triiodothyronine
T4	Thyroxine
T_0AM	Thyronamine

T_1AM	3-Iodothyronamine
TAAR1	Trace amine associated receptor 1
TH	Thyroid hormone
TIA	Transient ischemic attack
TNFα	Tumor necrosis factor alpha
TTC	Triphenyltetrazolium chloride
VEGF	Vascular endothelial growth factor

CHAPTER 1

STROKE AND NEUROPROTECTION

1.1 Introduction

Each year in the United States approximately 700,000 individuals are afflicted with a stroke. Currently there are approximately 2 million survivors of stroke living in the US with prolonged disability, many unable to work or resume personal relationships. In China 1.5 million people die from stroke each year and in developed nations stroke is the third leading cause of death, only surpassed by heart disease and cancer. In the US health care costs reach 45 billion dollars annually. The economic, social and psychological costs of stroke are substantial [1-5].

There are very few treatments for stroke and the development of new therapeutics is imperative. My research goal has been to address this need and identify new therapeutics that could one day be used to treat this disease. I have chosen to investigate two potential therapeutics: osteopontin (OPN) and 3-iodothyronamine (T_1AM). Below, I discuss the underlying pathophysiology of stroke, the current state of treatment, my rationale for investigating OPN and T_1AM and the foundations upon which my hypotheses were built.

1.2 Brief History of Stroke

The first to write about the medical aspects of stroke was Hippocrates 2400 years ago, where he used the original common term for stroke, “apoplexy”, which in Greek literally means “struck suddenly with violence”. Hippocrates noted, “persons are most subject to apoplexy between the ages of forty and sixty” and attacks of numbness might reflect “impending apoplexy.” He also gave an accurate description and prognosis of sub-arachnoid hemorrhage: “when persons in good health are suddenly seized with pains in

the head and straightaway are laid down speechless and breathe with stertor, they die in seven days when fever comes on" [6]. Following Hippocrates the next to give an accurate treatise on stroke was Johann Jakob Wepfer in 1658. Johann Wepfer examined the brains of patients who died from apoplexy and was the first to recognize that blockage of the carotid and vertebral arteries and bleeding into the brain were causes of apoplexy [6].

Over the next few centuries, clinical and anatomical descriptions of stroke became more sophisticated but it was not until the latter half of the twentieth century that knowledge was appreciably advanced. In these decades, progress in technology allowed better visualization of the anatomy and functional aspects of the brain and new surgical treatments such as intracranial microsurgery became possible. Databases were built containing information from large numbers of stroke patients and therapeutic trials began that systematically evaluated the efficacy and safety of new treatments. As a result of these trials, numerous therapeutic strategies have been pioneered and introduced for clinical use. These include:

- Anticoagulant therapy (with heparin and aspirin) as prophylactic treatment for patients with symptoms of occlusive cerebrovascular disease [7].
- Treatment with corticosteroids, mannitol and glycerol to reduce edema and control increased intracranial pressure [5].
- Anti-hypertensive treatment using beta-adrenergic blocking agents, angiotensin-converting enzyme inhibitors, and calcium channel blocking agents to control

arterial hypertension and reduce the incidence of brain parenchymal hemhorrages and the frequency of ischemic stroke [5].

- Thrombolytic therapy with streptokinase and recombinant tissue plasminogen activator (rt-PA) to treat cerebrovascular thrombosis acutely [8].

Despite the aforementioned advances, research into stroke therapeutics has lagged behind research into other diseases such as heart disease, cancer, diabetes and AIDS. Of the treatments mentioned only rt-PA has been approved by the US Food and Drug Administration (FDA) for use in stroke, while the other treatments are applied based on the reports and shared experience of clinicians [5]. Lack of financial support partly explains why only rt-PA has the approval of the FDA. In 1996 the Department of Health and Human Services concluded that stroke was "first in disability, third in death, last in funding" [5]. There are other reasons to explain why there are so few treatments for stroke and I will address these in future sections of this thesis.

1.3 Stroke Pathophysiology

Stroke can be subdivided into two categories, ischemic and hemorrhagic. Ischemic strokes are more prevalent than hemorrhagic making up approximately 80% of all cases and have been the target of my thesis research. A thrombosis, an embolism or systemic hypo-perfusion, all of which result in a restriction of blood supply to the brain, can cause an ischemic stroke, which results in insufficient oxygen and glucose delivery to support cellular homoestasis. This triggers at least five processes that lead to cell death:

excitotoxicity and ionic imbalance, oxidative/nitrative stress, inflammation, apoptosis and peri-infarct depolarization [9].

Each of the above pathophysiological processes has a distinct time frame, some occurring over minutes, others over hours and days (Fig 1.1). These processes share overlapping and redundant features and cause injury to neurons, glia and endothelial cells. Within the core of the ischemic territory, where blood flow is most severely restricted, excitotoxic and necrotic cell death occurs within minutes. In the periphery of the ischemic area, where collateral blood flow can buffer the full effects of the stroke, the degree of ischemia and the timing of reperfusion determine the fate of individual cells. In this ischemic penumbra cell death occurs less rapidly via active cell death mechanisms such as apoptosis. Targeting these mechanisms provides a therapeutic opportunity.

Excitotoxcity, Acidotoxicity and Ionic Imbalance

The human brain constitutes approximately 2% of body weight but accounts for 20% of total oxygen consumption [10]. The brain requires this large amount of oxygen to generate sufficient ATP by oxidative phosphorylation to maintain and restore ionic gradients. One estimate suggests that the Na^+/K^+ATPase found on the plasma membrane of neurons, consumes 70% of the energy supplied to the brain [10]. This ion pump maintains the high intracellular K^+ concentration and the low intracellular Na^+ concentration necessary for the propagation of action potentials. After global ischemia mitochondrial inhibition of ATP synthesis leads to ATP being consumed within two minutes, this causes neuronal

plasma membrane depolarization, release of potassium into the extracellular space and entry of sodium into cells [5]. Energy failure also prevents the plasma membrane Ca^{2+} ATPase from maintaining the very low concentrations of calcium that are normally present within each cell.

The extracellular calcium concentration is approximately 1.2mM and most cellular processes regulated by calcium have a Km value in the range of 0.1 to 1μM. During ischemia intracellular calcium levels rise to 50-100μM, activating many, if not all calcium dependent proteases, lipases and DNAses [10]. Activation of these enzymes causes many cells in the ischemic core to die from simple catabolism. Because no ATP is available for the re-synthesis of cellular constituents these catabolic enzymes cause the disintegration of essential cellular structures.

Membrane depolarization also leads to neurotransmitter release, with the release of the excitatory neurotransmitter glutamate playing a critical role in ischemic pathology. A large concentration gradient of glutamate is maintained across the plasma membrane by sodium dependent glutamate transporters located on presynaptic and postsynaptic membranes. The synaptic glutamate concentration is in the micromolar range, whereas the cytosolic concentration of glutamate is approximately 10mM [11]. Membrane depolarization and accumulation of sodium inside cells during ischemia causes reversal of glutamate transporters and allows glutamate to exit cells along its concentration gradient.

The effect of an increase in synaptic glutamate concentration is the activation of N-

methyl-D-aspartate (NMDA) and α-amino-3-hydroxy-5-methyl-4-isoxazolepropionic acid (AMPA) receptors. The opening of these calcium permeable channels leads to further membrane depolarization and greater calcium influx, exacerbating intracellular calcium overload (excitotoxicity) [12]. Blocking glutamate binding sites on NMDA and AMPA receptors has repeatedly been shown to provide robust neuroprotection in models of focal ischemia, although protection is restricted to the penumbra, where receptor blockade is thought to prevent calcium entry from reaching a toxic threshold [11].

Calcium overload is further exacerbated by acidosis, one of the hallmark neurochemical elements of ischemia. Hyperglycemia and the switch from aerobic to anaerobic respiration increases lactate in the ischemic environment. Dissociated protons activate sodium selective acid sensing ion channels (ASICs) that are permeable to calcium. There are 4 ASIC genes encoding 6 polypeptides (ASIC1a, ASIC1b, ASIC2a, ASIC2b, ASIC3 and ASIC4), each of which has a distinct pH sensitivity. The $pH_{0.5}$ of ASIC1a is 6.2 and because the pH in ischemic brain falls to 6.0 to 6.5 it is likely that in ischemia this channel opens and allows further calcium into the cell (acidotoxicity) [13]. This phenomenon is glutamate independent, thus it is not prevented by administration of NMDA antagonsists, however, administration of the ASIC1a blocker PcTx1 can prevent ASIC1a activation has been shown to reduce lesion volume in experimental stroke [14].

Oxidative and Nitrative Stress

High levels of intracellular Ca^{2+}, Na^{2+} and ADP cause mitochondria to produce deleterious levels of reactive oxygen species. Unlike other organs the brain is especially vulnerable to reactive oxygen species due to neurons having relatively low levels of endogenous antioxidants. Overly abundant oxygen radicals cause the destruction of cellular macromolecules and participate in signaling mechanisms that result in apoptotic cell death [15, 16]. Ischemia activates nitric oxide synthase (NOS) and increases the generation of nitric oxide (NO), which combines with superoxide to produce peroxynitrite, a potent oxidant. The production of NO and oxidative stress is also linked to over-activation of poly(ADP-ribose)polymerase-1 (PARP-1), a DNA repair enzyme. In response to DNA strand breaks PARP-1 catalyzes the transformation of β-nicotinamide adenine dinucleotide (NAD+) into nicotinamide and poly(ADP-ribose). When PARP-1 is over-activated it depletes cells of NAD+ and ATP. This further increases levels of ADP, leading to additional production of reactive oxygen species thereby completing a destructive positive feedback loop [9].

Apoptosis

Mild ischemic injury preferentially induces cell death via an apoptotic-like mechanism rather than necrosis[17, 18]. Because the ischemic penumbra sustains milder injury, apoptosis predominates in this region. Triggers of apoptosis include oxygen free radicals, death receptor ligation, DNA damage, protease activation and ionic imbalance.

The release of cytochrome c from the outer mitochondrial membrane plays a central role in mediating apoptosis in response to ischemia. Release of cytochrome c is caused by

ionic imbalance and mitochondrial swelling or by formation of a pore in the outer mitochondrial membrane. The complex interplay of the Bcl-2 family of proteins either promotes (Bax, Bak, Bad, Bim, Bid) or prevents (Bcl-2, Bcl-XL, Bcl-w) pore formation. The pore is formed by oligomerization of Bax and/or Bak in the outer membrane, with Bax transcriptionally induced by p53, which in turn is activated by DNA damage. The anti-apoptotic Bcl-2 proteins, Bcl-2 and Bcl-XL, can form heterodimers with Bax, thereby preventing pore formation [19-24].

Bad, Bim and Bid also influence pore formation, although the exact manner by which they do so is unclear. Bim is bound to dynein and actin and is released by dissociation of the cytoskeleton. Upon mobilization, Bim translocates to the mitochondrial membrane and promotes the release of cytochrome c. Bid is present in a proform in the cytosol and is cleaved by caspase 8 after TNF/Fas receptor activation. Once cleaved, it too translocates to the mitochondrial membrane and promotes the release of cytochrome c. In its phosphorylated form Bad is bound to protein 14-3-3. Bad is dephosphorylated by calcineurin, a calcium dependent serine/threonine phosphatase. When Bad is dephosphorylated it is released from 14-3-3 and translocates to the mitochondria where it also promotes cytochrome c release. Unlike Bax and Bak, Bid, Bad and Bim do not have the ability to directly mediate cytochrome c release by forming a pore. Instead they appear to function as sensors of cell stress that may promote apoptosis by heterodimerizing and antagonizing the function of anti-apoptotic Bcl-2/Bcl-XL and/or activating the function of Bax and Bak [20-23].

Cytochrome c release activates downstream caspases through formation of the apoptosome, a complex of dATP, cytochrome c, procaspase 9 and Apaf1. Effector caspases 3 and 7 then target substrates that dismantle the cell by cleaving homeostatic, cytoskeletal, repair, metabolic, and cell signaling proteins. These caspases also cause further DNA fragmentation by activating capase-activated deoxyribonuclease (CAD) by cleaving the inhibitor protein ICAD. Caspase activation can be modulated by protein inhibitors of apoptosis (IAP) and indirectly by secondary mitochondria-derived activator of caspase (Smac/Diablo).

Activation of the extrinsic pathway of death receptors can induce caspase activation independent of the release of cytochrome c. Death receptor ligation results in activation of caspase-8 and caspase-10, which in turn can activate effector caspase 3 [25]. Activation of death receptors like Fas/CD95, TNFR1, and the TRAIL receptor is promoted by the TNF family of ligands, including FASL, TNF, LT-alpha, LT-beta, CD40L, LIGHT, RANKL, and TRAIL, which are released as part of the inflammatory response to ischemia [26, 27].

Susceptibility to ischemia often correlates with expression of Bcl-2. For example in the hippocampus, basal Bcl-2 immunoreactivity is high in ischemia resistant pyramidal neurons of the CA3 region, but very low in the ischemia sensitive CA1 region [28]. Bcl-2 expression is also high in the brainstem where autonomic function is often preserved following ischemia and low in the selectively vulnerable neurons of the cortex [28]. This correlation of Bcl-2 expression and resistance to apoptosis may be explained by recent

findings that suggest in addition to physically trapping pro-apototic proteins, Bcl-2 has other properties that enable it to attenuate cell death. For example, Ellerby et al find that Bcl-2 is sensitive to redox changes and has antioxidant properties during calcium stress [29]. As Bcl-2 is found in the ER, the plasma membrane, and the nuclear membrane, additional Bcl-2 functions may be revealed.

Several experimental studies, particularly relevant to the work in this thesis, have shown that inhibition of apoptosis reduces ischemic injury [30]. For example, activation of the extracellular signaling protein kinase (ERK) pathway and the phosphatidylinositol-3 (PI3) kinase pathway has been found to be neuroprotective. These pathways activate transcription factors such as CREB and NFκB related to cell survival and phosphorylate Bax and Bad, thereby preventing the release of cytochrome c. Additionally, caspase 3 inhibitors, gene deletions of Bid, the use of peptide inhibitors and viral vector mediated gene transfer of Bcl-2 and Bcl-XL are strategies that are known to be neuroprotective [31-34].

A summary of the most salient features of mitochondria-dependent and mitochondria-independent activation of cell death is provided in figure 1.2.

Inflammation

Inflammation contributes to stroke related brain injury [35]. In response to ischemic stroke glial cells release inflammatory cytokines such as TNFα, IL-6 and IL-1β and stimulate

the expression of chemokines and adhesion molecules. This promotes the recruitment of peripheral leukocytes into the brain which release pro-inflammatory mediators such as cyclooxygenase-2 (COX-2), interleukin-1 (IL-1) and monocyte chemoattractant protein-1 (MCP-1). TNF-α is expressed in ischemic brain and contributes to ischemic damage, as demonstrated by the finding that administration of a TNF-α neutralizing antibody reduces brain injury after focal ischemia in rats [36, 37]. TNF-α stimulates acute-phase protein production, increases the permeability of the blood brain barrier and induces the expression of endothelial adhesion molecules and other inflammatory mediators [38]. Some components of the inflammatory cascade are beneficial, for example IL-6 can protect neurons from NMDA toxicity and vascular endothelial growth factor (VEGF) promotes vascular remodeling during stroke recovery [39, 40]. Effects of the inflammatory cascade may be detrimental or beneficial depending on factors such as the stage of tissue injury and predominance of a single signaling pathway among multiple divergent pathways [36, 41, 42].

Peri-infarct Depolarizations

Cortical spreading depression (CSD) is a self-propagating wave of electrochemical activity that progresses through neural tissue following acute ischemia. Cortical spreading depression causes sustained (1-5 minutes) cellular depolarization, depressed neuro-electrical activity, increased glutamate release and loss of membrane ionic gradients [43]. In the penumbra CSD may exacerbate tissue damage by impairing restoration of ionic equilibrium. Peri-infarct depolarizations are known to occur in

mouse, rat and cat stroke models and the incidence and duration of spreading depression correlates with infarct maturation [44, 45]. Inhibition of spreading depression using a therapeutic approach such as hypothermia, could be an important strategy to limit expansion of an ischemic lesion within the penumbra [46].

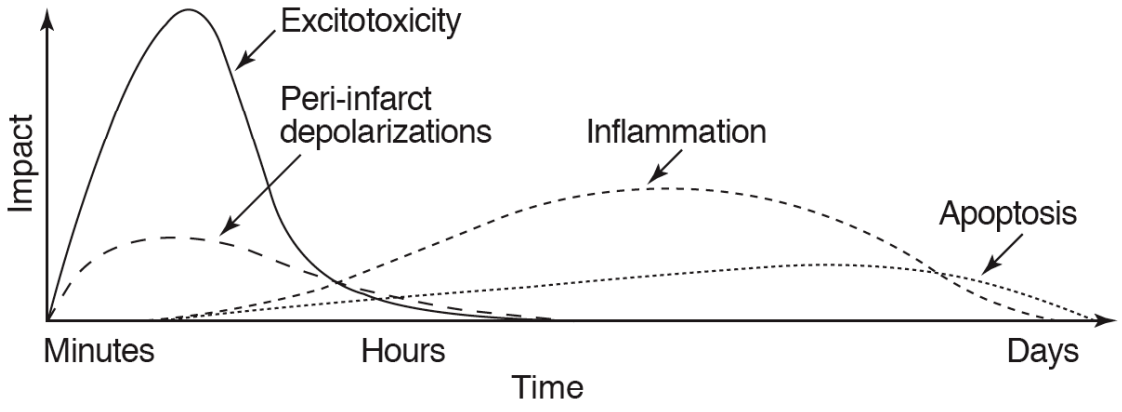

Figure 1.1. Cascade of damaging events in focal cerebral ischemia. Very early after the onset of ischemia, excitotoxic mechanisms kill neurons and glia. In addition,

exticotoxicity triggers a number of events that can further contribute to the demise of the tissue. Such events include peri-infarct depolarizations and the more delayed mechanisms of inflammation and apoptosis. The x-axis reflects the evolution of the cascade over time, while the y-axis illustrates the impact of each element of the cascade on the final outcome. (From Dirnagl et al., *Trends Neurosci* 1999; 22: 391-397 [47])

Figure 1.2. Cell death pathways relevant to apoptosis in cerebral ischemia. The proapoptotic protein Bax (and/or Bak) mediates the release of cytochrome c (cyt c) from the mitochondria. Bax can be induced by p53, which in turn is activated by DNA damage. Apoptosis is activated by translocation of Bad to the mitochondria. Dephosphorylation of Bad by calcineurin (CaN) causes release of BAD from 14-3-3 and translocation to the mitochondria. The antiapoptotic proteins Bcl-XL and Bcl-2 prevent Bax mediated cyt c release. When released into the cytosol, cyt c binds Apaf-1 and procaspase 9 forming an apoptosome complex, which than cleaves and activates caspase 3. Activation of caspase 3 leads to cell death by degradation of DNA repair enzymes,

degradation of the cytoskeleton, and activation of endonucleases. The apoptosis-inducing factor (AIF) can also be released from the mitochondria, causing degradation of DNA and contributing to cell death. Caspase 3 may also be activated by caspase 8, which is activated by TNF receptor ligation. Caspase 8 can also activate mitochondria-induced cell death by limited proteolysis of Bid. Truncated Bid (t-Bid) translocates to the mitochondria promoting Bax induced cyt c release. Calpains can activate cathepsins that degrade Bid, thereby promoting apoptosis (adapted from Cerebral Blood Flow and Metabolism [10]).

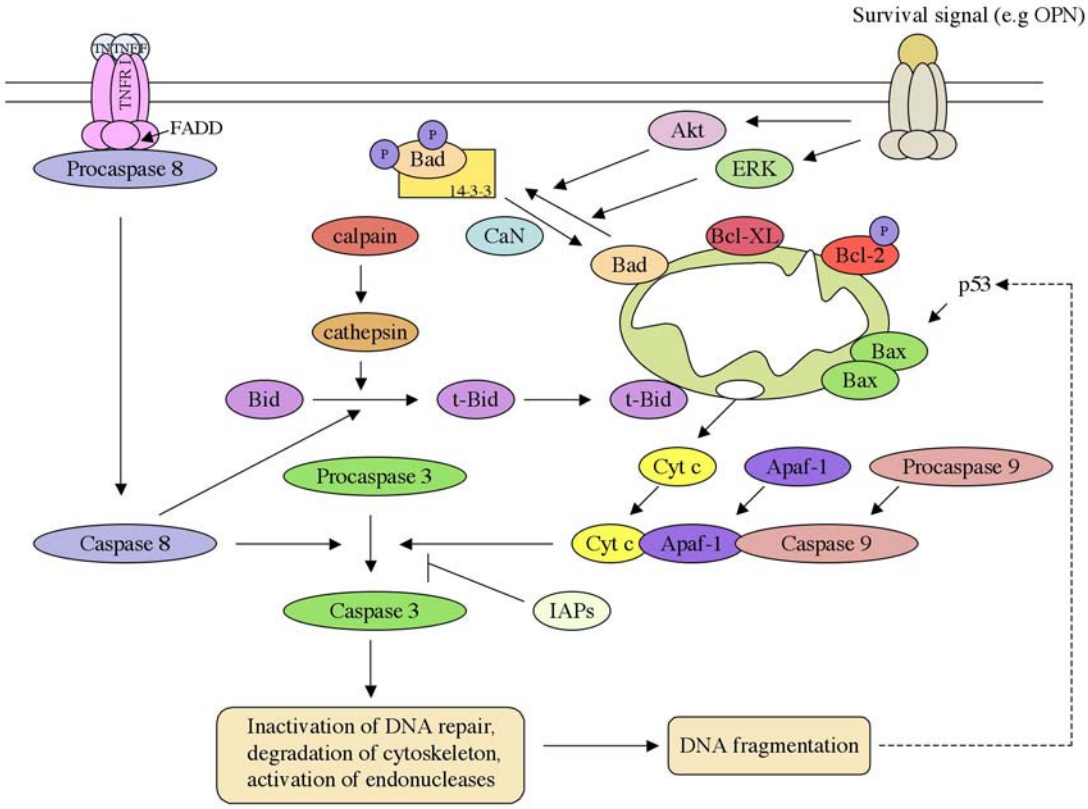
Survival signal (e.g OPN)
TNF
TNFR
FADD
Procaspase 8
P
Bad
14-3-3
Akt
ERK
calpain
CaN
Bad
Bcl-XL
Bcl-2
P
p53
cathepsin
Bax
Bax
Bid
t-Bid
t-Bid
Cyt c
Apaf-1
Procaspase 9
Procaspase 3
Caspase 8
Cyt c
Apaf-1
Caspase 9
Caspase 3
IAPs
Inactivation of DNA repair, degradation of cytoskeleton, activation of endonucleases
DNA fragmentation

1.4 Neuroprotection

Neuroprotection refers to strategies that protect neurons from injury or degeneration [35]. Neuroprotection can be achieved by indirect (rt-PA, cerebral angioplasty), physiological (hypothermia) or pharmacological therapies, each of which target one or all of the mechanisms of damage described above.

Neuroprotection by indirect therapy is used clinically. For ischemic stroke the American Stroke Association (ASA) recommends cerebral angioplasty or the administration of rt-PA. Neuroprotection by physiological therapy (hypothermia) is used for protection against brain injury following cardiac arrest as demonstrated by two landmark prospective randomized controlled studies demonstrating the benefit of mild hypothermia in improving neurologic outcome in patients suffering from cardiac arrest [48, 49]. In contrast, although pharmacological neuroprotection is possible in experimental models of stroke, all prior research has failed to translate into new treatments for patients [50, 51]. No trial using a pharmacological neuroprotective agent over the last 25 years has been successful.

Notable pharmacological neuroprotective agents that have failed at phase III clinical trial include the lipid peroxidation inhibitor tirilazad mesylate, the ICAM-1 antibody enlimomab, the calcium channel blocker nimodipine, the γ-aminobutyric acid (GABA) antagonist clomethiazole, the glutamate antagonist and sodium channel blocker

lubeluzole, the competitive NMDA antagonist selfotel, and several noncompetitive NMDA antagonists (dextrophan, gavestinel, aptiganel and eliprodil)[52-58].

There are several reasons to explain why these pharmacological neuroprotective agents have failed to be efficacious in patients. Preclinical experiments are often conducted on healthy, young, genetically similar animals whereas trials are conducted on patients with advanced age and co-morbidities such as diabetes and hypertension. While there are similarities in the basic pathophyisology of stroke between species, there are significant differences in brain structure, function and vascular anatomy. Unlike the rodent brain the human brain is gyroencephalic and has greater neuronal and glial density. As a result there are important differences in size, spatial distribution and temporal evolution of ischemic damage between experimental models and humans. Also, outcome in animal models is often assessed within days to weeks, whereas in humans neurological function is typically assessed after 3-6 months.

The relatively short time window available for administration of most drugs also impedes success at clinical trial. For example the time window available for administration of rt-PA is only 3 hours. The short time window is compounded further by the length of time it takes to transport patients to the hospital and difficulty in making an accurate diagnosis. In a recent study of 356 patients, investigators using computerized tomography (CT), the standard means of imaging the brain of suspected stroke patients, were able to give an accurate diagnosis of stroke in just 54% of cases. In the therapeutically relevant subset of

patients that sought care within 3 hours of the onset of symptoms, CT imaging detected evidence of an ischemic stroke in 7% of patients [59].

Another major factor to account for past failure of pharmacological neuroprotection is that patients with different stroke pathophysiology and subtype are often combined in a trial, whereas the drug being tested may have efficacy limited to a certain stroke subtype, (e.g. strokes with mainly white matter involvement). Pharmacokinetic properties of a drug and changes in cerebral blood flow may also account for failed efficacy. Blood flow can drop to 5-10% of normal in the core of an infarct and to 30-40% of baseline in the penumbra [60]. In addition, the blood brain barrier restricts access to the brain parenchyma, rendering useless many potential neuroprotective drugs that are unable to reach the brain.

1.5 Ischemic Preconditioning

Ischemic preconditioning, in which brief ischemic insults induce tolerance to subsequent injurious ischemia, is a powerful adaptive defense that involves an endogenous program of neuroprotection [61, 62]. Ischemic preconditioning is widely conserved in biology. The phenomenon was first described in the heart and has since been observed in liver, intestine, lung, muscle, kidney, retina, and brain. In the brain tolerance to ischemia develops at 48 hours, is maximal at 72 hours, and persists for about 7 days [63]. The protection induced is substantial, with infarct volume reduced by 50-70% [62, 64-67].

Ischemic preconditioning offers novel insights into endogenous mechanisms of neuroprotection and provides a therapeutic opportunity as an antecedent therapy for patients at risk of ischemic injury, such as those scheduled for cardiac artery bypass surgery (CABG) and arterectomy.

Regulation of gene transcription plays a vital role in the process. Our laboratory has shown that ischemic preconditioning reprograms the genomic response to injury by downregulating genes involved in metabolism and ion channel activity and upregulating transcription factors and survival proteins [68, 69]. For example, preconditioning entails new synthesis of proteins such as heat shock proteins, Bcl-2, hypoxia inducible factor, and mitogen activated protein kinases (MAPKs) [62, 70, 71]. Of particular interest is the upregulation of the protein osteopontin (OPN), known to play a role in cell survival and thus a potential neuroprotectant [72].

Emerging human data indicate that transient ischemic attacks (TIAs) reduce the severity of a subsequent stroke and may represent a natural example of ischemic preconditioning. In a study of 65 patients, those with a prior history of TIA were found to have smaller infarcts (assessed by MRI) and milder neurological deficits than those with no history of TIA [73]. Although the clinical induction of TIAs is an inappropriate preconditioning stimulus for humans, alternative stimuli may be viable alternatives for patients. Tolerance to ischemia can be induced by other preconditioning stimuli such as chemical induction [74, 75], hypoxia [76], cytokines [77], endotoxin priming [78-81] and hypothermia [82]. Thus, multiple

stimuli that convey distinct signals lead to a common endpoint, namely protection against ischemic injury and some of these could be adapted for therapeutic use.

1.6 Research Goal

The goal of my research has been to develop new treatments for ischemic stroke. In pursuit of this goal I have investigated OPN and 3-iodothyronamine (T_1AM), two novel drug candidates that could be developed into drugs for stroke patients. OPN is a ligand for integrin receptors that could potentially confer neuroprotection by activating integrin coupled survival pathways, and thus counter the apoptotic response to ischemia. T_1AM is an endogenous cryogen that can rapidly induce hypothermia. In the setting of stroke T_1AM could confer neuroprotection by inducing a depth and duration of hypothermia that has been shown to be therapeutic as both a preconditioning stimulus and an acute treatment. The following is a discussion of my research to advance these candidate treatments towards a clinical application.

CHAPTER 2

OSTEOPONTIN

INTRODUCTION

2.1 An introduction to OPN

Osteopontin is a multifunctional cytokine and adhesion protein that contains sequences that bind to integrin receptors and CD44v3/6 [83, 84]. OPN is a secreted protein in all body fluids, but exists as an immobilized protein in mineralized tissue and an intracellular protein in macrophages. Many of the functions of OPN were discovered by studies of OPN deficient mice. These mice reveal that OPN plays a role in bone remodeling, tissue debridement, cellular immunity, wound healing and cancer metastasis [85, 86]. OPN is chemotactic for various cell types, including macrophages and is essential for cell-mediated immunity and a normal Th1 cytokine response. OPN attaches bone cells to bone matrix and can activate numerous signal transduction pathways downstream of integrin receptors and CD44, including pathways that promote cell survival.

2.2 The structure of OPN

OPN contains a thrombin cleavage site and an RGD motif that is important in its interactions with integrin receptors [87-90]. OPN is rich in aspartic acid, glutamic acid and serine residues and contains ~30 monosaccharides, including 10 sialic acids. Carbohydrate is attached to OPN as one N-glycosyl and 5-6 O-glycosyl side chains. Phosphorylation occurs to a variable extent at up to 28 sites distributed throughout the molecule [60]. Phosphorylation at key residues is essential for OPN to bind to certain

integrin receptors. OPN also contains a calcium binding region and a heparin binding domain. The calcium binding region of OPN allows it to bind to calcium phosphate and inhibit or promote mineralization in bone and urine. Whether OPN is soluble or immobilized determines the specific modulatory effect of OPN on mineralization. Soluble OPN inhibits mineralization, while immobilized OPN draws calcium phosphate out of solution and promotes crystal formation [86]. The functional significance of the heparin binding region of OPN is unknown and heretofore, the purpose of the glycosylation was unrecognized. Studies described in this thesis suggest that glycosylation may influence cleavage of OPN by thrombin.

The thrombin cleavage site of OPN consists of the conserved sequence RSK and is in close proximity to the RGD sequence. Thrombin cleavage is a prerequisite for efficient engagement of the RGD sequence to the $\alpha v\beta 3$ integrin receptor. Thrombin cleavage also reveals the cryptic integrin binding sequence SLAYGLR. This sequence binds to $\alpha 9$ and $\alpha 4$ integrins but only when thrombin cleavage has generated a free carboxylic acid on the arginine residue at the end of the sequence [91, 92] (Fig 2.1A). These sequences are conserved in mouse and human with the exception that in humans the SLAYGLR sequence is SVVYGLR (Fig 2.1B).

Figure 2.1 A.) Schematic of mouse OPN. Top: The functional domains of OPN. Bottom: The relative locations within OPN necessary for binding to different integrin receptors and CD44 splice variants. Note: A more complete account of integrin subunits and their respective binding site on OPN (SLAYGLR or RGD) can be found in Figure 2.2. **B.)** The sequence of mouse and human OPN. The RGDSLAYGLR/RGDSVVYGLR sequence is shown in bold. Mouse OPN is 70% homologous to the human protein.

A

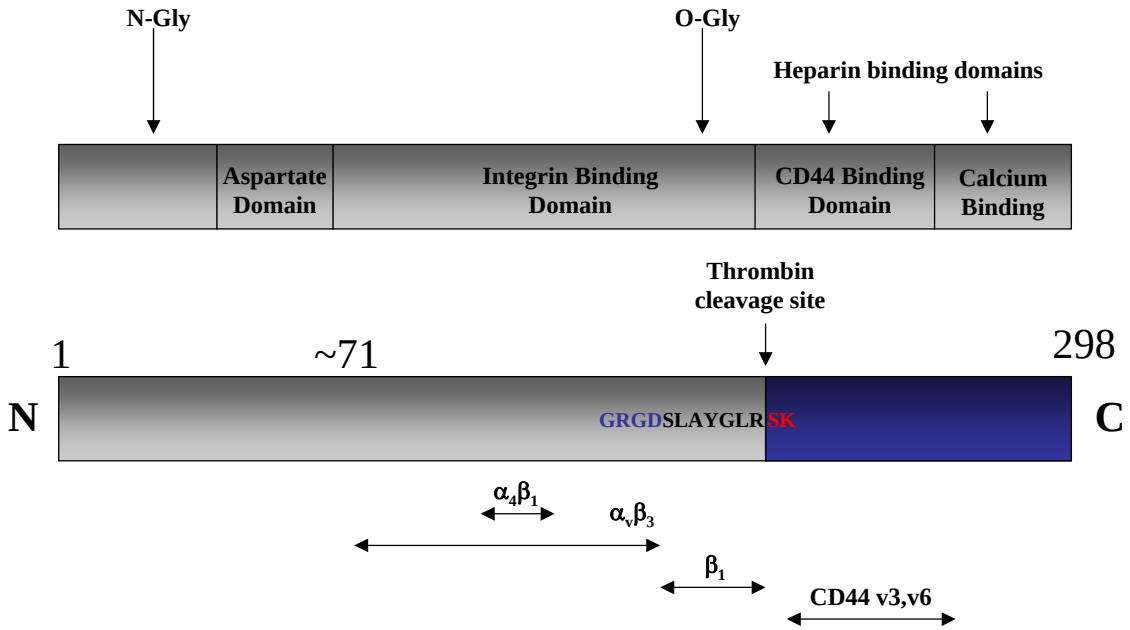

B

Murine Osteopontin Sequence (UniProt entry P10923):

MRLAVICFCL FGIASSLPVK VTDSGSSEEK LYSLHPDPIA TWLVPDPSQK
QNLLAPQNAV SSEEKDDFKQ ETLPSNSNES HDHMDDDDDD DDDDGDHAES
EDSVDSDESD ESHHSDESDE TVTASTQADT FTPIVPTVDV PNG**RGDSLAY**
GLRSKSRSFQ VSDEQYPDAT DEDLTSHMKS GESKESLDVI PVAQLLSMPS
DQDNNGKGSH ESSQLDEPSL ETHRLEHSKE SQESADQSDV IDSQASSKAS
LEHQSHKFHS HKDKLVLDPK SKEDDRYLKF RISHELESSS SEVN

Human Osteopontin Sequence (UniProt entry P10451):

MRIAVICFCL LGITCAIPVK QADSGSSEEK QLYNKYPDAV ATWLNPDPSQ
KQNLLAPQNA VSSEETNDFK QETLPSKSNE SHDHMDDMDD EDDDDHVDSQ
DSIDSNDSDD VDDTDDSHQS DESHHSDESD ELVTDFPTDL PATEVFTPVV
PTVDTYDG**RG DSVVYGLR**SK SKKFRRPDIQ YPDATDEDIT SHMESEELNG
AYKAIPVAQD LNAPSDWDSR GKDSYETSQL DDQSAETHSH KQSRLYKRKA
NDESNEHSDV IDSQELSKVS REFHSHEFHS HEDMLVVDPK SKEEDKHLKF
RISHELDSAS SEVN

2.3 OPN, integrins and survial signaling

Integrins comprise a large family of cell surface receptors that are present in species as divergent as sponges and humans. They are composed of two subunits, α and β and each αβ combination has its own binding specificity and signaling properties (Fig 2.2). Most integrins recognize multiple ECM proteins. Conversely, individual integrin ligands, such as fibronectin, laminin, collagen, vitronectin and osteopontin, bind to several integrin receptors. Integrins can signal through the plasma membrane in either direction. The extracellular binding activity of integrins is regulated from the inside of the cell (inside out signaling) while the binding of ligands to integrins elicits signals that are transmitted into the cell (outside in signaling) [93].

The cytoplasmic tails of integrins are generally short and always devoid of enzymatic features. To transmit signals, integrins use adaptor proteins such as focal adhesion kinase (FAK) and integrin linked kinase (ILK) that connect the integrin to the cytoskeleton, cytoplasmic kinases, and transmembrane growth factor receptors. Signaling pathways activated by integrin receptors promote complex biological functions, including cell adhesion, proliferation, migration, differentiation and survival (Fig 2.3).

Protein kinases activated by integrins including FAK, Src family kinases, and ILK, are all capable of triggering cell survival pathways. The FAK pathway is activated by most integrins and can lead directly to cell survival by binding to PI3-kinase. PI3-kinase activates Akt, which promotes cell survival by phosphorylating and inactivating pro-

apoptotic proteins such as Bad and caspase-9. The activation of Src family kinases by integrins can lead to cell survival by activating the transcription factor NF-κB, which translocates to the nucleus and promotes expression of pro-survival genes [93, 94].

OPN, acting through integrins, could activate these and other intra-cellular signaling pathways that promote cell survival. Evidence that such pathways may be activated when OPN is present in the brain can be derived from the effects of two other integrin ligands, laminin and fibronectin. Laminin was shown recently to protect neurons against glutamate-induced excitotoxicity, acting through β1 integrin receptors. This protection was mediated via FAK-PI3K-AKT and Bcl-2 upregulation [95], a pathway shared by OPN when it binds β1 integrin receptors. Fibronectin has also been shown to protect cells from ischemic damage after stroke. Mice deficient for plasma fibronectin show increased neuronal apoptosis and larger infarction following transient focal ischemia [96, 97]. Similar to OPN, laminin and fibronectin share the RGD sequence necessary to bind to most integrin receptors. Thus when the brain is exposed to ischemic insult, ligating integrin receptors appears to be a viable means of enhancing neuronal survival.

2.4 OPN and ischemic injury

OPN is expressed at low basal levels in neurons, [98, 99], endothelial cells [86] and microglia [100]. During pathological states it is also expressed by infiltrating immune cells such as macrophages [100]. Most CNS cells have integrin receptors, thus, OPN can act on endothelial cells, astrocytes, microglia, and neurons [93, 95, 101-104]. OPN expression is

modulated by cytokines and NO [86, 105-109]. During ischemic injury there is an acute upregulation of cytokines, such as IL-1β and TNFα, as well as inducible nitric oxide synthase (iNOS) [110-113]. Thus, proinflammatory signals induce OPN expression during ischemia.

OPN mRNA is upregulated as early as 3 hours and reaches maximum levels at 5 days following temporary middle cerebral artery occlusion (MCAO) [100]. This suggests early and delayed functions for OPN, a theory supported by studies of renal ischemia. In the kidney there is a differential sensitivity of distal and proximal tubules to ischemic injury, which correlates with OPN expression in those cell types [114-116]. Distal tubules express OPN in the normoxic state and early after ischemic insult [115]; these cells are much less sensitive to ischemic injury and have acute upregulation of anti-apoptotic molecules such as Bcl-2 [114]. In contrast, proximal tubules are less tolerant to ischemia/reperfusion injury [114] and OPN expression is not detected early. Rather, OPN is upregulated 5 days following ischemia in *regenerating* proximal tubule cells [115]. This suggests that early expression of OPN may increase the resistance of distal tubules to apoptotic signals and late expression of OPN may play a role in matrix remodeling. Similar processes may take place during brain ischemia.

OPN inhibits apoptosis of endothelial cells deprived of growth factors. Administration of OPN to endothelial cells causes an increase of Bcl-X_L, a Bcl-2 family member, which prevents apoptosis by binding to Apaf-1 and inhibiting the activation of the apoptosis

effector capsase-9 [72]. OPN could act in a similar fashion on neurons in the penumbra and increase resistance to apoptosis.

Experiments using OPN KO mice [86, 117] implicate a protective role for OPN in ischemia. OPN KO mice show increased cellular damage following renal ischemia compared with wildtype mice [118]. A similar finding has been reported in the brain. OPN KO mice exhibit greatly increased degeneration of the ipsilateral thalamus in response to cerebral ischemia compared to wild-type animals, although overall infarct volume is not changed [119, 120].

In support of a delayed protective role for OPN, increased expression of OPN is sustained for several days following focal cerebral ischemia [100, 121, 122]. OPN aids phagocytosing macrophages in removing cell debris [100, 121, 122] and serves as a chemoattractant to induce astrocyte and microglia migration to the site of glial scar formation [100, 104]. This process is necessary to reduce further damage to the viable tissue surrounding the ischemic core. In addition, during wound healing, OPN KO mice show poor extracellular matrix reorganization [117], an event critical after cerebral injury for proper tissue remodeling and glial scar formation [121].

In summary the increased presence of OPN in the brain in response to ischemia, the role of OPN in facilitating cell survival, and the phenotype of OPN KO mice in response to renal and brain ischemia, lend support for the notion that OPN is an endogenous factor released in response to stroke to protect against injury. Thus the addition of exogenous

OPN to the brain acutely after stroke offers an exciting new target for pharmacological neuroprotection.

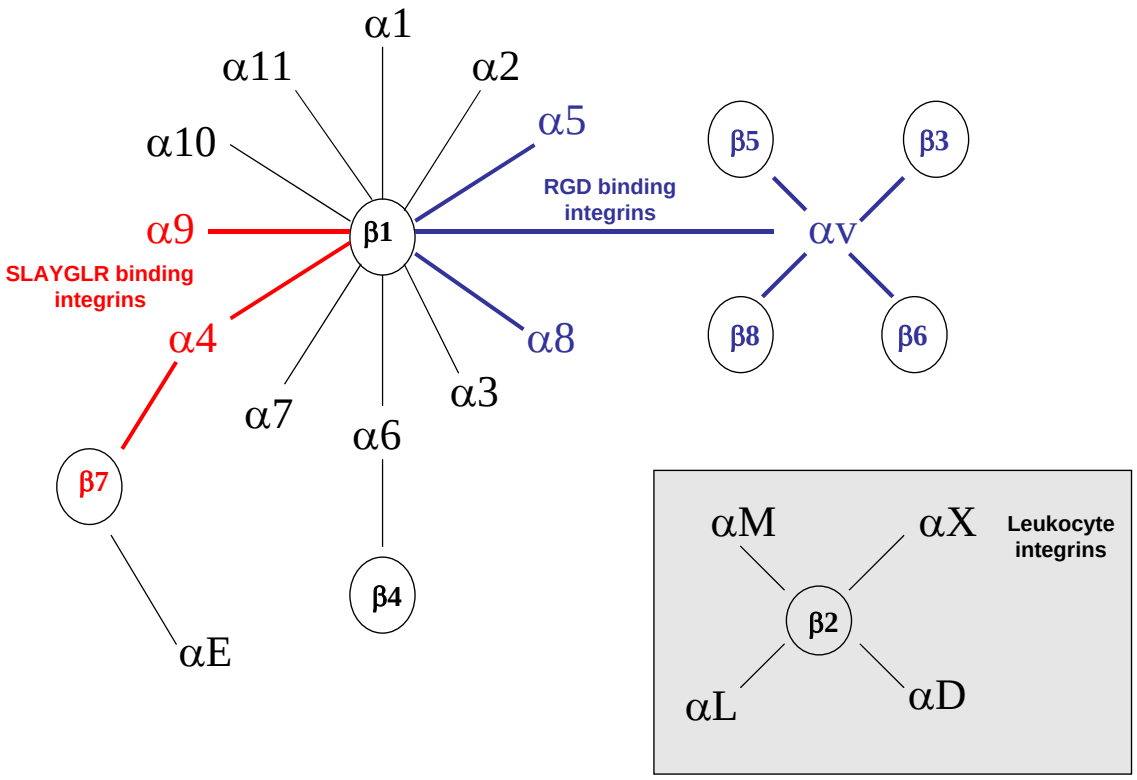

Figure 2.2. Integrins are heterodimeric transmembrane receptors composed of α and β subunits. Approximately 22 integrins have been identified thus far. This diagram shows the different combinations of integrin receptor subunits and their specificity for the sequences RGD and SLAYGLR. Blue α/β combinations bind to the sequence RGD, red α/β combinations bind to the sequence SLAYGLR. This diagram was adapted from Reddy and Mangale, 2003 [123].

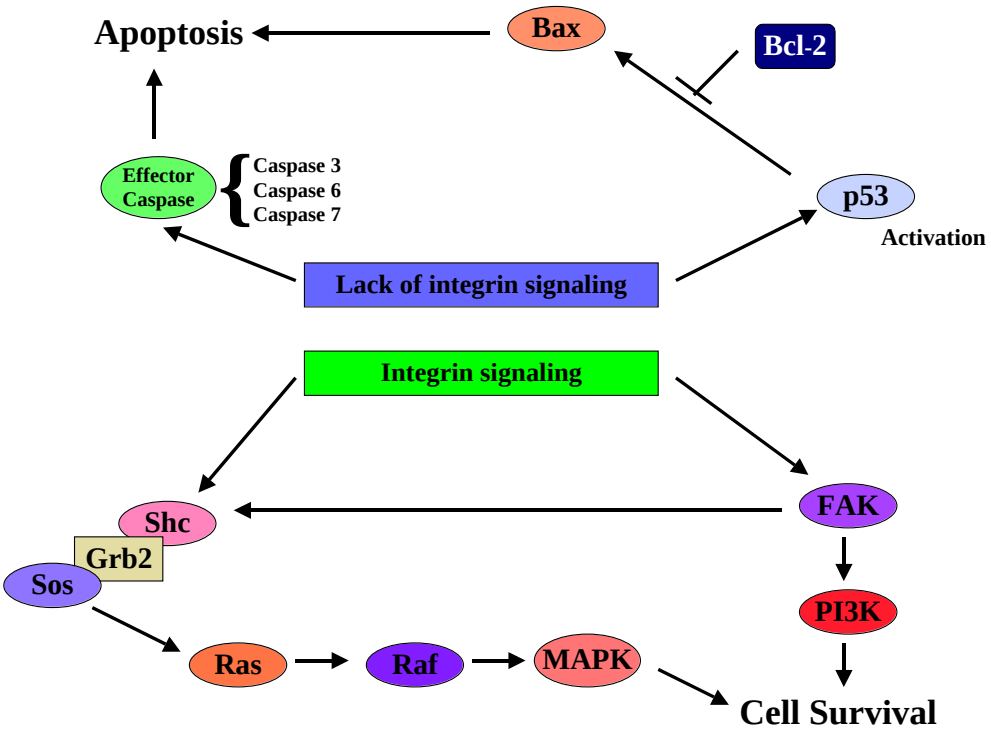

Figure 2.3 Cellular resistance to apoptosis can be increased through integrin interactions. Upon ligand binding, integrin signaling leads to the tyrosine phosphorylation of cytoskeletal and other signaling components. Focal adhesion kinase (FAK) is activated via autophosphorylation and a large array of other signaling molecules that promote cell survival are phosphorylated, including MAPK and PI3 Kinase.

2.5 Preclinical Development of OPN

An important goal of my research is the preclinical optimization of OPN for its advancement as a potential drug candidate in stroke therapy. As such, I have focused my attention on issues of drug delivery and improved potency of OPN. To facilitate the design of a final drug I have also performed a structure activity analysis to identify the regions within the parent molecule required for neuroprotection.

2.6 Optimizing delivery

Many effective pharmaceuticals have been rendered useless in the treatment of cerebral diseases due to an inability to deliver them to the brain [124]. The biggest impediment to drug delivery to the brain is the presence of the blood brain barrier (BBB). Drugs that are delivered via the blood must pass the BBB to reach the brain. The BBB is a membranous permeability barrier that tightly segregates the brain from the circulating blood. It is comprised of blood capillaries in the CNS that are structurally different from the blood capillaries found in other tissues. Capillaries of the brain and spinal cord lack the gaps between endothelial cells that allow the rapid movement of solutes from the circulation to other organs. Instead these capillaries are lined with a special layer of endothelial cells that lack fenestrations and are sealed with tight junctions. Only lipid soluble solutes can freely diffuse through the capillary endothelial membrane and enter the brain. As a result most drugs used currently for disorders of the brain are lipid soluble and can readily cross the BBB following oral administration [125-129].

The BBB also has an enzymatic component wherein solutes crossing the endothelial cell membrane are exposed to degradative enzymes present in large numbers inside the endothelial cells of the BBB. These enzymes recognize and rapidly degrade most peptides, including naturally occurring neuropeptides such as enkephalin [130]. The BBB is further reinforced by a high concentration of P-glycoprotein (Pgp), active-drug-efflux-transporter protein in the luminal membranes of cerebral capillary endothelial cells. This efflux transporter can actively remove a broad range of drug molecules from the endothelial cell cytoplasm before they can cross into the brain parenchyma [131, 132].

Drug delivery to the CNS that bypasses the BBB would represent a significant preclinical advance. Accordingly this thesis includes experiments that tested whether OPN can enter the brain by intranasal administration. This need was particularly important for OPN because its target for neuroprotective actions, integrin receptors, lie within the CNS.

Intranasal administration provides a simple, practical and rapid route of delivery into the CNS that circumvents the BBB. It has been known for many years that pathogens and toxic metals can be transported from the nasal mucosa to the CNS along neural pathways. However, it has only recently been appreciated that these same pathways can be used to deliver therapeutic agents to the CNS.

Intranasal delivery works by an intraneuronal and extraneuronal pathway into the brain. The intraneuronal pathway involves axonal transport and requires hours to days for drugs

to reach different brain regions. The extraneuronal pathway relies on bulk flow transport through perineural channels, and delivers drugs directly to the brain parenchymal tissue and the cerebrospinal fluid (CSF). This extraneuronal pathway allows therapeutic agents to reach the CNS within minutes [133].

A number of protein therapeutic agents have been successfully delivered to the CNS using intranasal delivery in a variety of species. Neurotrophic factors, such as nerve growth factor (NGF), insulin like growth factor-I (IGF-1), and fibroblast growth factor (FGF) have been delivered intranasally to the CNS in rodents [134-136]. Studies in humans with proteins, such as vasopressin, cholecystokinin, and insulin have demonstrated direct delivery to the brain from the nasal cavity along the olfactory neural pathway [137-140].

Studies in rodents have examined the effects of intranasally administered CNS therapeutic agents. In rodent stroke studies therapeutic benefit of intranasal delivery of IGF-1 has been demonstrated [135, 141]. Intranasal delivery of IGF-I reduces infarct volume and improves neurologic function in rats following middle cerebral artery occlusion (MCAO). A preliminary report indicates that this treatment is effective even when delayed for 4 hours after the onset of MCAO [135].

2.7 Improving the potency of Osteopontin

Enzymatic modification of OPN by treatment with thrombin is a potential means of improving its neuroprotective potency. The thrombin cleavage site of OPN is located near the RGD sequence. Thrombin cleavage alters the orientation of the RGD sequence improving its affinity for αvβ3 integrin receptors. Thrombin cleavage also affects the integrin binding ability of OPN by increasing the repertoire of integrins available for OPN binding. OPN contains a SLAYGLR sequence (SVVYGLR in humans) that is cryptic and unable to bind to integrins unless there has been prior cleavage by thrombin. Thrombin cleavage generates a free carboxylic acid in the arginine of the SLAYGLR sequence that is necessary for binding to α4 and α9 integrins. Thus treatment with thrombin represents a method of improving the neuroprotective potency of OPN by enhancing its ability to ligate integrin receptors and broadening the repertoire of cognate interactions.

2.8 Identifying the regions of OPN required for neuroprotection

Testing short peptide mimetics of OPN is an informative means of conducting a structure activity relationship. Peptide mimetics allow one to assess the importance of modifications (e.g glycosylation and phosphorylation) and assign neuroprotective function to specific regions of the OPN parent molecule. Accordingly this thesis includes experiments using OPN peptide mimetics to uncover the structural requirements for neuroprotection.

2.9 Hypothesis

I hypothesize that exogenous administration of OPN protects against cerebral ischemic injury and that protection occurs via activation of integrin-mediated pathways. I postulate that thrombin treatment of OPN improves its ability to confer neuroprotection and that specific domains of OPN can be identified that confer neuroprotection. This work was performed with the goal of providing sufficient evidence to warrant clinical testing.

2.10 Research Design

To test the hypothesis that OPN confers neuroprotection, I evaluated OPN in two models of ischemic stroke, an *in vivo* model of focal ischemia, middle cerebral artery occlusion (MCAO) and an *in vitro* model of ischemic stroke, oxygen glucose deprivation (OGD). Based on my findings that OPN is a novel neuroprotectant I tested whether the absence of OPN exacerbates stroke damage in OPN deficient mice.

Next I investigated basic mechanisms by which OPN confers neuroprotection. I hypothesized that OPN confers neuroprotection via ligation of integrin receptors on neurons and activation of integrin linked survival pathways. In conjunction with Dr Robert Meller, I used an *in vitro* model of stroke to probe the biochemical basis of neuroprotection. The completion of this aim allowed early assessment of the safety of OPN, and aided in the rational design of peptidomimetics.

My initial experiments that established for the first time that OPN is capable of conferring neuroprotection *in vivo,* relied on delivering OPN to the brain by icv injection. This method of administration is impractical for humans. In order to improve the method of OPN delivery to the brain I tested whether OPN can reach the brain by intranasal administration, a method that is feasible for humans and confer protection in the setting of ischemia.

Previous studies have shown that thrombin cleavage of OPN improves its ability to ligate integrin receptors. I verified this finding using an adhesion assay, a test of integrin binding ability, and then tested whether thrombin treatment of OPN enhances its neuroprotective function in models of stroke. Based on my findings that thrombin treatment of OPN improves neuroprotection I explored the structural requirements for neuroprotection with the goal of developing peptide mimetics with potential as drug therapeutics.

RESULTS

2.11 OPN has neuroprotective capability *in vivo* and *in vitro*.

To determine whether OPN is neuroprotective, rat cortical cultures were pre-treated with OPN for 24 hours prior to exposure to OGD. OPN significantly reduced cell death with the protective effect concentration-dependent and maximally protective at 0.1ug/ml, which is equivalent to 5nM (Fig 2.4a). This concentration reduced cell death by 47%. In the absence of OGD, there was no effect of OPN treatment on cell number or basal cell death, indicating that OPN treatment is not directly cytotoxic to neurons. These results demonstrate for the first time that OPN treatment of neuronal cells can provide marked protection against ischemic injury.

To test whether OPN confers neuroprotection when administered *post* exposure to ischemia, cortical cells were given an ischemic challenge followed by incubation with OPN for 24 hours. A 37% reduction in cell death was observed which is a similar amount of protection to that observed when cells are incubated with OPN prior to OGD (Fig 2.4b). These data show that OPN treatment following ischemia is neuroprotective and suggest that OPN may have therapeutic benefit *following* an ischemic event.

Given the neuroprotective effects of OPN observed *in vitro*, I tested whether the absence of endogenous OPN increases susceptibility to focal ischemia in a mouse model of

MCAO. Mice with a targeted disruption in the OPN gene [142] (OPN-/-, n=7) had similar infarct sizes compared to wildtype mice (OPN+/+, n=8). Following 60 min MCAO, OPN-/- mice had infarcts measuring 31.7% compared with wildtype infarcts, which measured 26.5% (Fig. 2.5). These results indicate that the absence of endogenous OPN does not pre-dispose the whole brain to greater injury in the setting of ischemia, however, this experiment does not address whether there is more extensive injury in selective brain regions following ischemia in OPN deficient mice.

To determine whether administration of exogenous OPN confers protection against ischemic injury *in vivo*, OPN or aCSF was injected into the lateral ventricle just prior to and immediately following 75 min MCAO. By administering OPN to the brain before and after stroke we ensured that OPN was present in the brain at the time of injury. For this experiment OPN was delivered in two 0.5µl injections each containing 50ng of OPN. Mice treated with OPN had significantly smaller infarcts (~ 2-fold) compared to mice treated with aCSF at 24 and 96 hours following MCAO (Fig. 2.6). Albumin, a protein with an equivalent weight to OPN, was injected as a control protein (2 x 50 ng) into the lateral ventricle prior and following 75 min MCAO. Infarct size in mice injected with albumin did not differ from infarct size in aCSF treated animals.

Temperature fluctuations are a source of variability in ischemic cell death. Historically this has confounded studies of neuroprotection. For example the neuroprotective effect of the NMDA antagonist MK-801 is mediated through its hypothermic effect and not due to NMDA receptor antagonism [143]. Stroke outcome is also affected by hypoglycemia and

hyperglycemia. For example drugs that cause hypoglycemia can exacerbate stroke damage by prolonging glucose deprivation post reperfusion and drugs that cause hyperglycemia can cause acidosis and intensify acidotoxicity. To determine whether OPN causes fluctuations in body temperature, I measured temperature in response to OPN administration in the presence or absence of focal ischemia (Table 2.1 and 2.2). Intracerebroventricular injection (icv) of OPN had no effect on body temperature compared to mice administered aCSF. Furthermore, no differences in blood glucose levels were observed following OPN administration (Table 2.3), hence the protective effect of OPN is unlikely to be due to changes in body temperature and blood glucose availability. Thus OPN can act as a potent neuroprotectant in focal ischemia.

Figure 2.4 a) Pretreatment of cells with OPN causes a concentration-dependent reduction in cell death following 120 minutes of OGD. Cells were pretreated with OPN (0.01-1.0 μg/ml) for 24 hours prior to 120 minutes of OGD. Cell death was determined by PI staining 24 hours later. Data shown are means ± SD (n=5); * denotes $P<0.05$ and ** $P<0.01$ vs. effect of 120 minutes of OGD (one-way ANOVA with Bonferroni's *post hoc* test). **b)** OPN is neuroprotective when incubated with cells following OGD. Cells were pretreated with OPN (0.1 μg/ml) for either 24 hours prior to 120 minutes of OGD, or 24 hours following 120 minutes of OGD. Cell death was determined by PI staining 24 hours later. Data shown are mean ± SD (n=5); * denotes $P<0.05$ and ** $P<0.01$ vs. effect of 120 minutes of OGD (one-way ANOVA with Bonferroni's *post hoc* test).

a

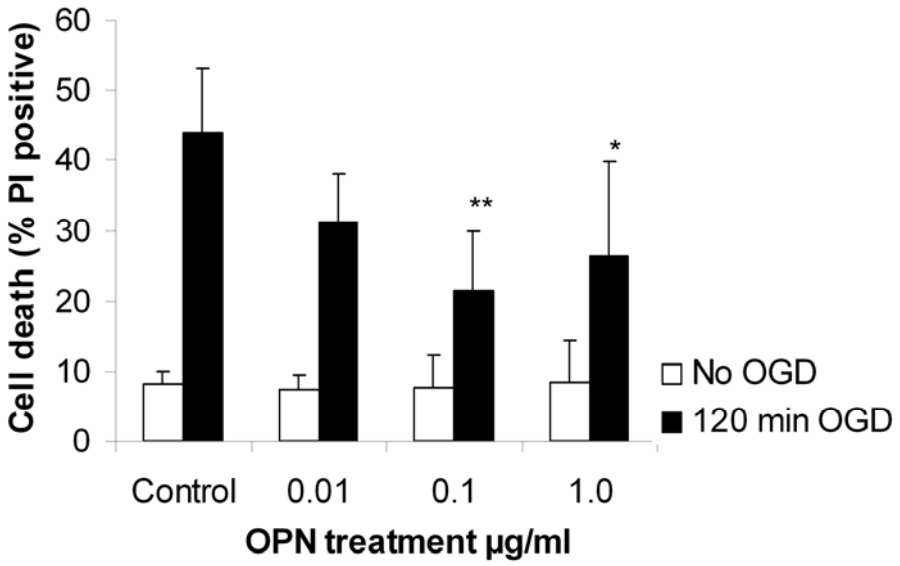
Cell death (% PI positive)
60
50
40
30
20
10
0
**
*
No OGD
120 min OGD
Control
0.01
0.1
1.0
OPN treatment µg/ml

b

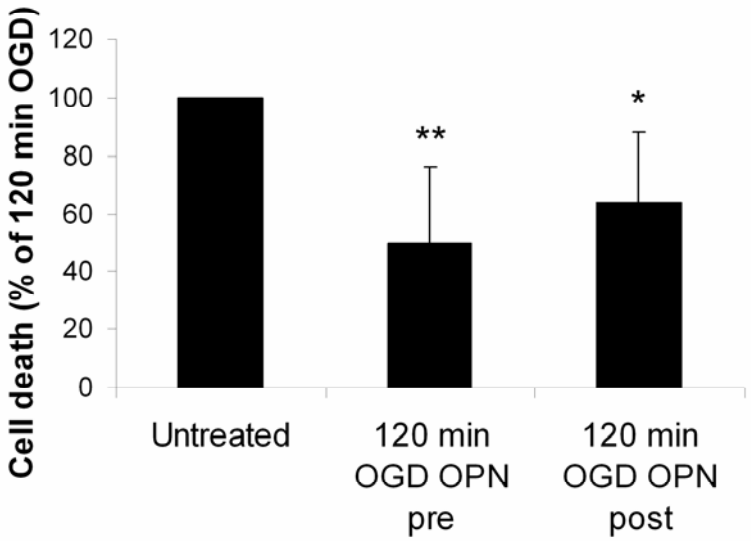
Cell death (% of 120 min OGD)
120
100
80
60
40
20
0
**
*
Untreated
120 min OGD OPN pre
120 min OGD OPN post

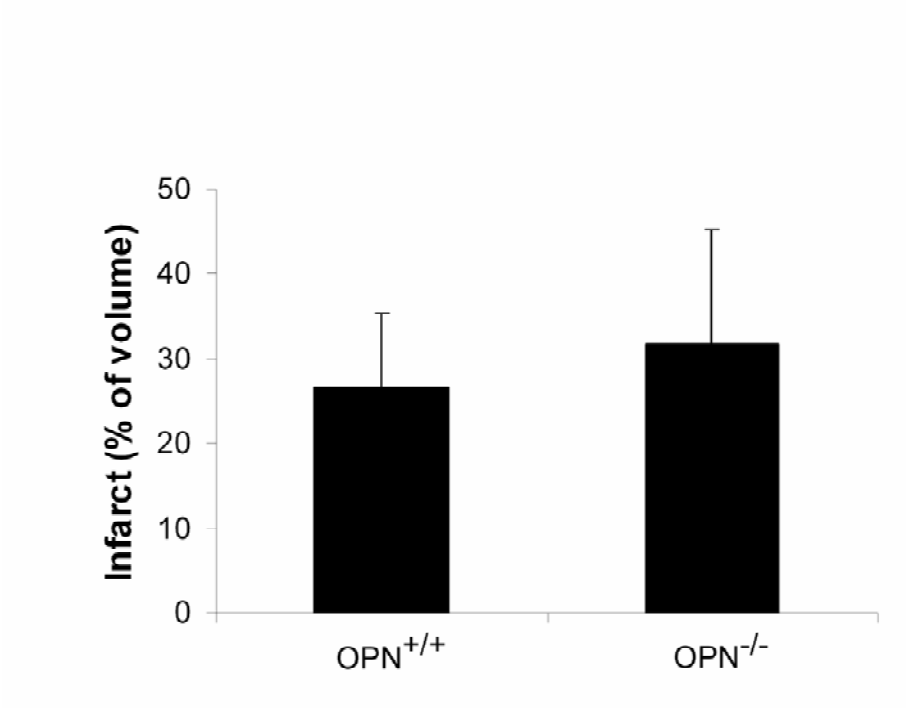

Figure 2.5 OPN deficient mice show similar infarct size to wildtype littermate controls. $OPN^{-/-}$ (n=7) and wildtype littermates (n=8) were subjected to 60 min MCAO. Infarct volume was measured 24 hr following stroke using TTC staining. Data shown are mean $\pm$ SD; p=0.4.

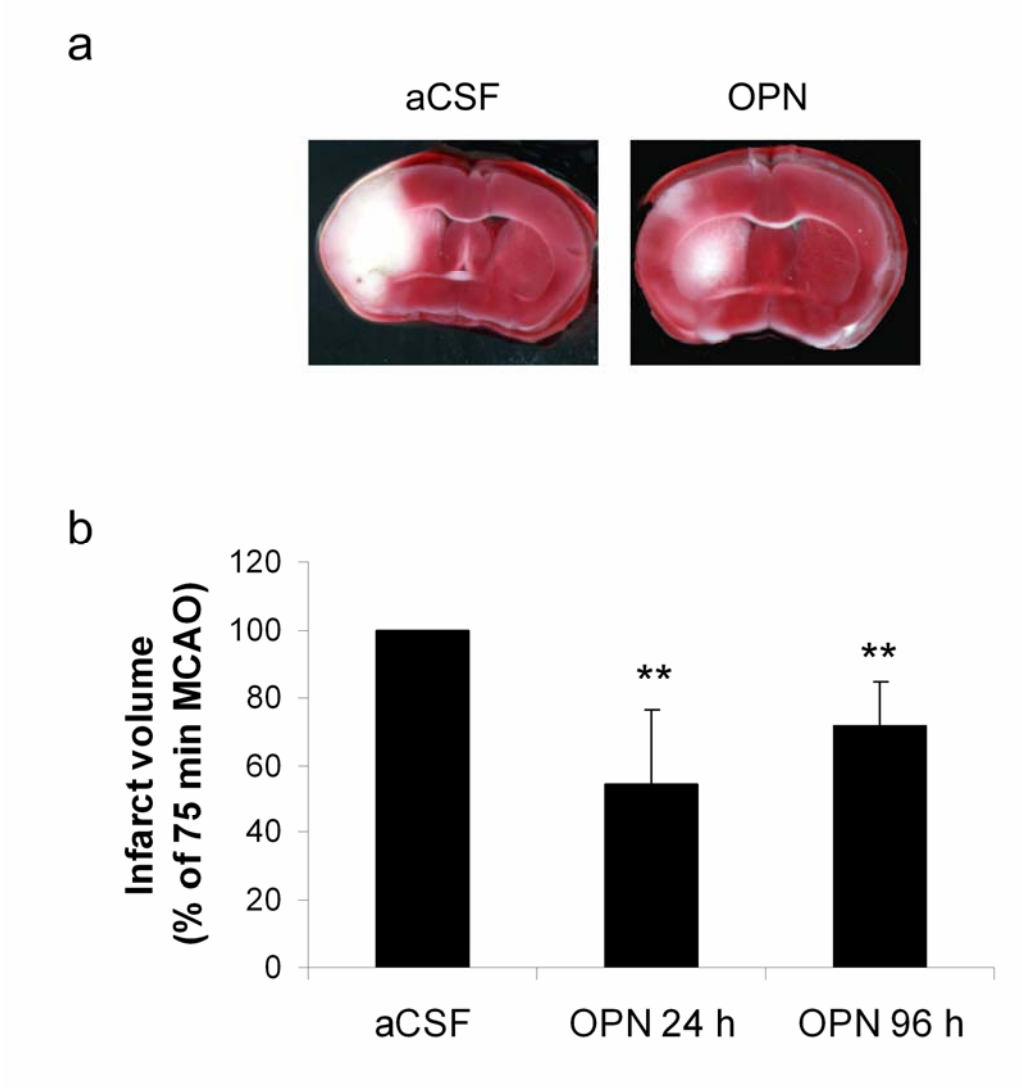

Figure 2.6 OPN reduces infarct volume following stroke. Mice were administered OPN (2 x 50 ng) or CSF and subjected to 75 minutes of MCAO. Infarct volume was measured 24 hours (OPN, n=9; aCSF, n= 15) and 96 hours (OPN, n=8; aCSF, n=8) following stroke using TTC staining. a) Representative images of TTC stained sections of mouse brain 24 hours following MCAO. b) Effect of OPN on infarct volume 24 hours and 96 hours post stroke. Data shown are mean $\pm$ SD; ** denotes $P<0.01$ vs. effect of aCSF (one-way ANOVA with Bonferroni's *post hoc* test).

	Body temperature (°C)					
Time post injection (h)	**24hrs pre inj.**	**1hr**	**3hr**	**6hr**	**24hr**	**48hr**
Treatment						
CSF	36.4 ± 0.4	36.0 ± 0.4	36.1 ± 0.3	36.4 ± 0.5	36.5 ± 1.0	36.2 ± 0.2
OPN	36.3 ± 0.9	36.1 ± 0.6	36.4 ± 0.4	36.2 ± 0.4	36.5 ± 0.9	35.7 ± 0.4

Table 2.1 Effect of OPN and aCSF intra-cerebroventricular administration on core body temperature in mice. Data shown are mean ± SD.

	Body temperature (°C)					
Time post stroke (h)	**3**	**6**	**24**	**48**	**72**	**96**
Treatment						
CSF	34.6 ± 1.1	35.0 ± 0.5	34.7 ± 0.4	34.7 ± 0.5	34.6 ± 0.8	34.6 ± 1.4
OPN	35.1 ± 1.3	34.7 ± 1.3	34.2 ± 0.5	34.3 ± 1.1	34.0 ± 2.2	34.5 ±1.3

Table 2.2 Effect of OPN and aCSF intra-cerebroventricular administration on core body temperature following 75 minutes of MCAO in mice. Data shown are mean ± SD.

Treatment	Number of animals	Blood glucose 1hr post injection (mg/dL)	Blood glucose 24hr post injection (mg/dL)
CSF	7	122.7 (±17.75)	114.6 (±15.86)
OPN	7	122.3 (±13.9)	112.1 (±19.3)

Table 2.3 Effect of OPN and aCSF intra-cerebroventricular administration on blood glucose concentration in mice. Data shown are mean ± SD.

2.12 The mechanism of neuroprotection by OPN.

To determine whether the neuroprotective effect of OPN involves an interaction with an integrin receptor we tested a peptide antagonist for the ability to block the capacity of OPN to reduce cell death due to ischemia. Cortical cultures were incubated with OPN in the presence of the competitor RGD-containing peptide, GRGDSP, which has been shown previously to competitively block OPN interactions with integrins [144]. Cortical cultures treated with OPN in the presence of GRGDSP (10nM) prior to OGD showed reduced protection against cell death (Fig 2.7). Incubation of cortical cultures with the GRGDSP peptide (10nM) for 24 hours had no effect on cell viability compared to control untreated cells (5.2% vs. 4.9% of PI positive cells, respectively). Furthermore, the GRGDSP peptide had no significant effect on 120 minutes of OGD-induced cell death (Fig 2.7). These data suggest that OPN exerts its neuroprotective effect through integrin receptors.

We next tested whether the neuroprotective actions of OPN occur through phosphatidylinositol 3-kinase (PI3K), a known downstream mediator of OPN's effects in certain cell types which, in turn, activates Akt (protein kinase B) [145-147]. We found that OPN treatment of cortical cells fails to protect against OGD-induced cell death in the presence of LY294002 (10μM), a PI3K inhibitor (Fig 2.8a). We also investigated the activation of the pro-survival protein kinase p42/p44 MAPK cascade following treatment with OPN. OPN-induced neuroprotection was reversed in the presence of the Mek inhibitor U0126 (10μM)(Fig 2.8a), which blocks activation of p42/p44 MAPK.

Incubation of cortical cells for 24 hours with either LY294002 (10μM) or U0126 (10 μM) had no effect on basal cell viability or on cell death following 120 minutes of OGD (Fig 2.8a). These data suggest that OPN mediates its neuroprotective effects via the activation of Akt or p42/p44 MAPK cascades.

To further test whether treatment of cells with OPN leads to activation of Akt or p42/p44 MAPK, we probed western blots with antibodies specific for phosphorylated Akt (Ser 473) and phosphorylated p42/p44 MAPK. Cortical cultures treated with OPN displayed increased Akt phosphorylation (Fig 3.5b). Phosphorylation of p42/p44 MAPK by OPN was biphasic, with an initial reduction, followed by an increased phosphorylation (Fig 2.8b). Further, the effect of OPN on p42/44 MAPK phosphorylation was reduced by LY294002 and GRGDSP peptide and abolished by U0126. Where as the effect of OPN on Akt phosphorylation was reduced by LY294002 and GRGDSP peptide (Fig 2.8c).

Additionally, the neuroprotective effect of OPN against OGD-induced cell death was blocked when cortical cultures were treated with OPN in the presence of the protein synthesis inhibitor, cycloheximide. These data suggest that the neuroprotective effects of OPN require the activation of the Akt and p42/p44 MAPK cascades, as well as new protein synthesis.

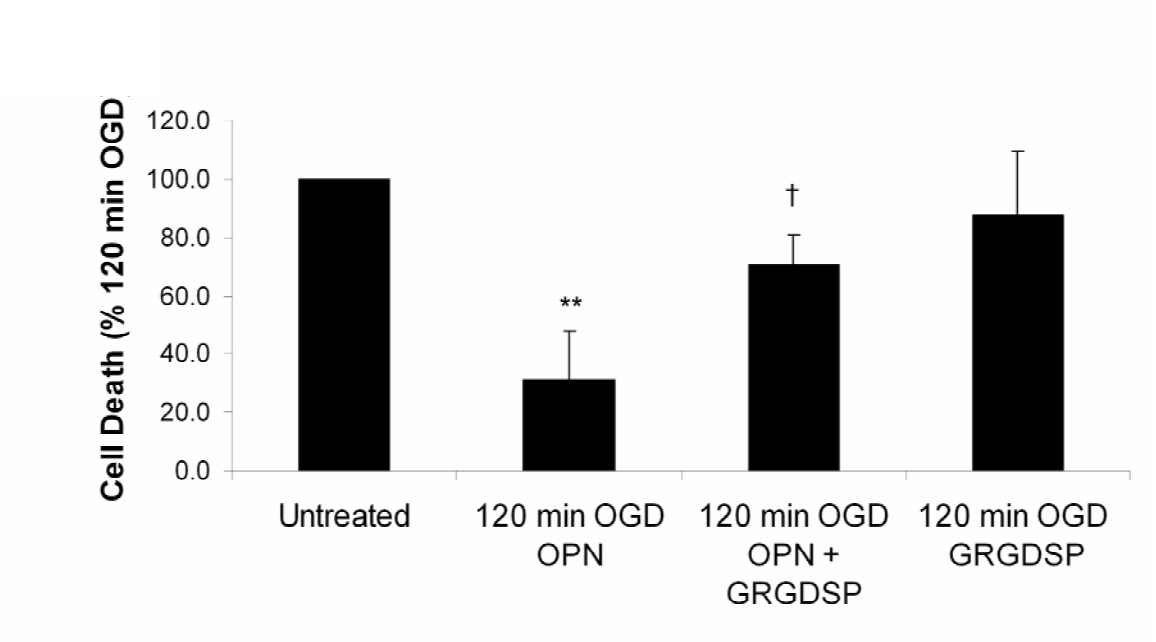

Figure 2.7 The neuroprotective effect of OPN is blocked by the RGD containing hexa-peptide GRGDSP. Cells were treated with GRGDSP (10 nM) for 10 minutes prior to addition of OPN (0.1 μg/ml) for 24 hours. Cells were then subject to 120 minutes of OGD. Data shown are means ± SD (n=4), ** denotes $P<0.01$ vs. effect of 120 minutes of OGD and † denotes $P<0.01$ vs. OPN-treated cells subjected to 120 minutes of OGD (one-way ANOVA with Bonferroni's *post hoc* test).

Figure 2.8 The neuroprotective effect of OPN is blocked by the PI3K inhibitor LY294002 and the Mek inhibitor U0126. **a)** Cells were treated with LY294002 (10 μM) or U0126 (10 μM) for 10 minutes prior to addition of OPN (0.1 μg/ml) for 24 hours. Cells were then subjected to 120 minutes of OGD. Data shown are a mean ± SD (n=4-6), * denotes $P < 0.05$ vs. effect of 120 minutes of OGD (one-way ANOVA with Bonferroni's *post hoc* test) and † denotes $P < 0.05$ vs. effect of OPN. **b)** Western blots showing increased phosphorylation of Akt and p42/p44 MAPK following incubation with OPN (0.1 μg/ml) for 1-24 hours. As a loading control, blots were re-probed for α-tubulin. Blots shown are representative blots of 3 independent experiments. **c)** Effect of U0126, LY294002 and GRGDSP peptide on OPN induced increase in Akt and p42/p44 MAPK phosphorylation. Cells were pretreated with inhibitors for 10 minutes prior to incubation with OPN for 24 hours. Levels of Akt and p42/p44 MAPK phosphorylation were determined by western blot. As a loading control, blots were re-probed for α-tubulin. Data shown are a representative blot of 2 independent experiments.

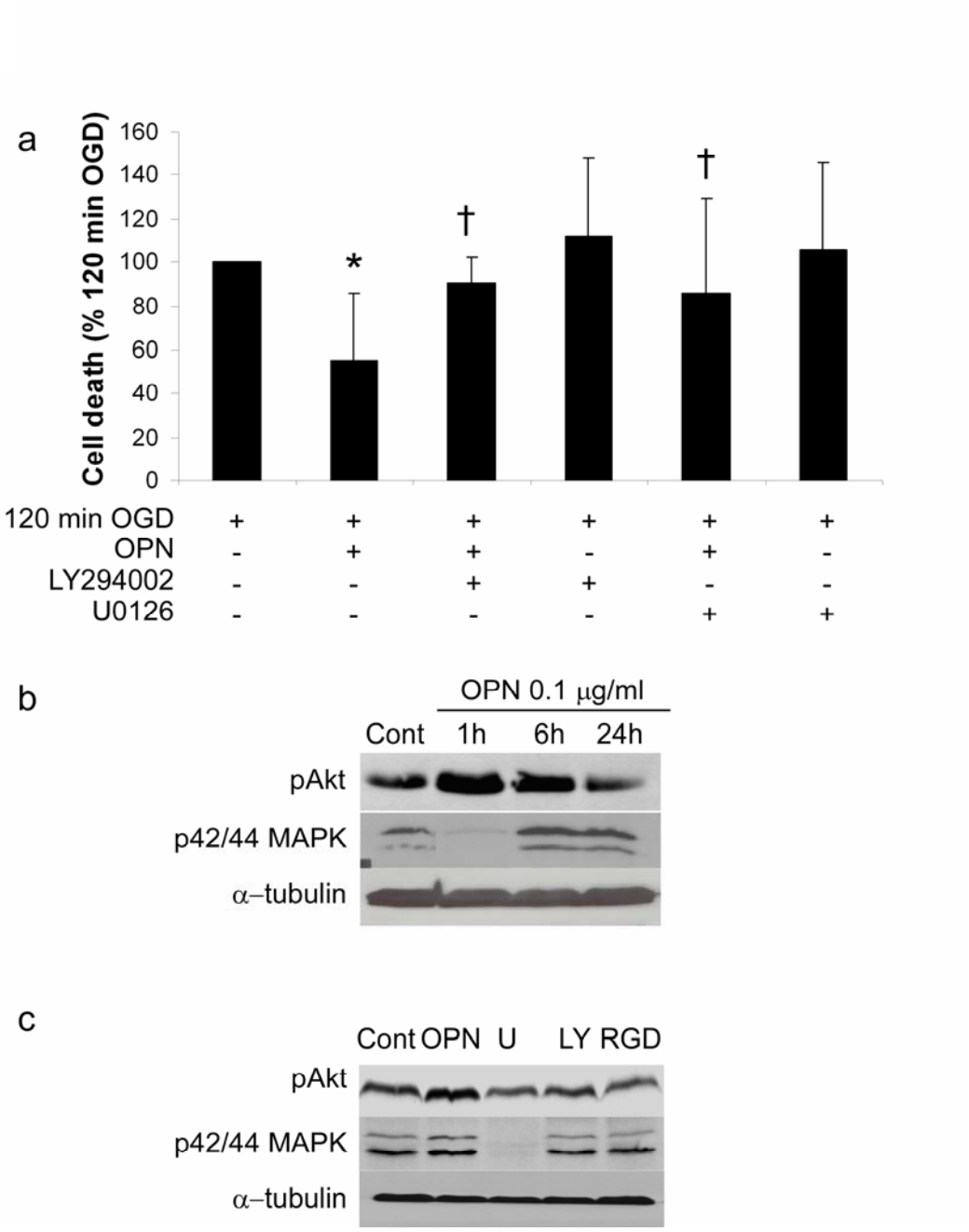
a
Cell death (% 120 min OGD)
160
140
120
100
80
60
40
20
0
*
†
†
120 min OGD + + + + + +
OPN - + + - + -
LY294002 - - + + - -
U0126 - - - - + +
b
OPN 0.1 μg/ml
Cont 1h 6h 24h
pAkt
p42/44 MAPK
α–tubulin
c
Cont OPN U LY RGD
pAkt
p42/44 MAPK
α–tubulin

2.13 OPN can be delivered to the brain via intranasal administration

The therapeutic efficacy of a neuroprotective drug can be improved by intranasal delivery. The unique anatomical and physiological characteristics of the nasal passages allow both intracellular and extracellular entry into the CNS [133, 148]. The axons of olfactory sensory neurons are situated in the olfactory bulb [149] but their dendritic processes are directly exposed to the external environment in the upper nasal passage. This provides an intracellular route into the brain via non-specific fluid phase endocytosis and anterograde axoplasmic transport from the dendritic processes to the olfactory bulb [148, 150]. A direct extracellular pathway also exists into the brain via the nasal passage. This has been demonstrated with horseradish peroxidase (HRP), a protein with a size of 40kDa [151], which is a similar size to OPN. It has been proposed that the extracellular route is via diffusion into the olfactory submucosa along open intercellular clefts in the olfactory epithelium, leading to the olfactory subarachnoid space and CSF circulation [148, 149]. When administered intranasally, HRP is detectable in the olfactory bulb within minutes of administration indicating that migration of relatively large molecules into the brain is quite rapid.

To develop a mode of administering OPN to the brain that would be viable for humans, I tested whether OPN could reach the brain via intranasal administration. Within two hours of intranasal administration of 2µg OPN, I detected the presence of OPN in the brain based on immunoreactivity staining. The pattern of staining showed high OPN immunoreactivity in the striatum and the cortex of the brain (Fig 2.9a). This pattern of

staining demonstrates that intranasal administration can deliver OPN to the territory made ischemic by MCAO. To quantify the amount of OPN that reaches the brain following intranasal delivery, CSF was sampled from mice treated with 5µg of OPN or aCSF at 30 minutes, 1 hour and 2 hours following administration. At 2 hours following OPN treatment there was a 50% increase in OPN concentration in the CSF (Figure 2.9b)

To allow adequate delivery and accumulation of OPN in the brain at the time of stroke injury, I administered 5µg of OPN intranasally 10 minutes following initiation of 60 minutes of MCAO. Mice were sacrificed 72 hours later. While the majority of infarct damage is evident within 24 hours of MCAO the infarct evolves further over the next several days. Hence, infarct measurements made 72 hours following MCAO can provide a more accurate picture of neuroprotection and distinguish whether treatment was truly neuroprotective or merely delayed damage [152]. I found that intranasal administration of OPN significantly reduced infarct volume by 33% compared to vehicle treated mice (Fig 2.9c).

Fig 2.9 OPN delivery to the brain through an intranasal route. **A.)** Immunofluorescence surrounding the region of the lateral ventricle of a mouse administered aCSF or OPN (2µg) intranasally. Red (Cy 3) = OPN, blue (DAPI) = nuclei. Mice were sacrificed 2 hr post administration. **B.)** OPN concentration in the CSF of mice administered OPN (5µg) or aCSF intranasally. Mice were sacrificed at the indicated time points post administration and OPN concentrations in the CSF were analyzed by ELISA. CSF from 3 mice was pooled for each time point. **C.)** Intranasal administration of OPN reduces infarct volume following MCAO. OPN (5µg) or aCSF was delivered intranasally 10 min after initiating 60 min MCAO. Mice were sacrificed 72 hr following surgery. Data shown are mean $\pm$ SD. *$p<0.05$ compared to aCSF administration ($n = 8$ each group).

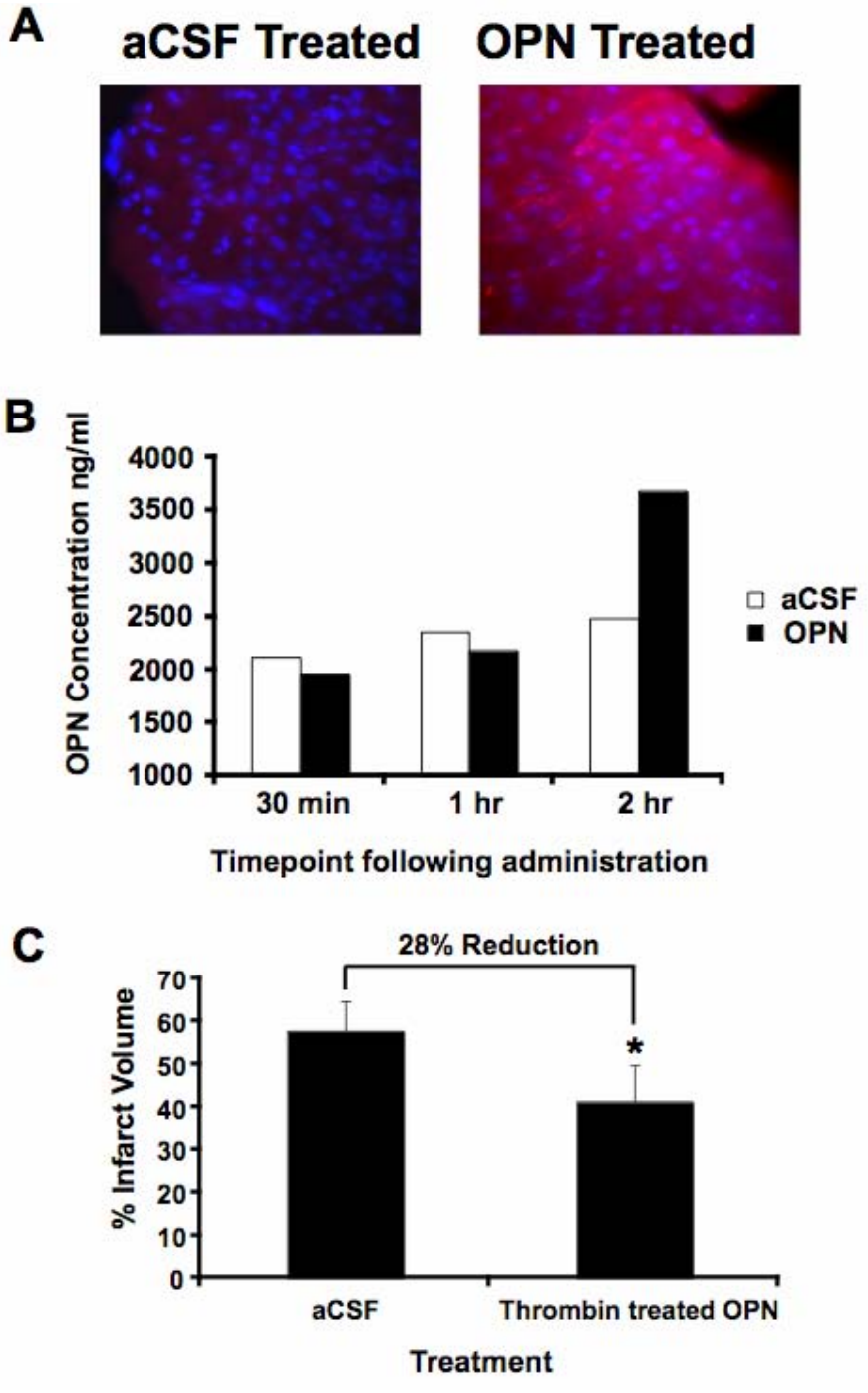
A
aCSF Treated
OPN Treated
B
OPN Concentration ng/ml
4000
3500
3000
2500
2000
1500
1000
30 min
1 hr
2 hr
Timepoint following administration
aCSF
OPN
C
28% Reduction
% Infarct Volume
70
60
50
40
30
20
10
0
*
aCSF
Thrombin treated OPN
Treatment

2.14 Enhancing the Neuroprotective capability of OPN

The ability of OPN to bind to integrin receptors is improved following thrombin cleavage. Senger and Perruzzi have shown by plating human fibroblasts onto human and rat OPN, that the cell adhesive properties of OPN are regulated by a naturally occurring thrombin cleavage site in close proximity to the RGD sequence [153]. This information coupled with our discovery that OPN confers neuroprotection by signaling through integrin receptors lead me to hypothesize that thrombin treatment of OPN would improve its neuroprotective capability. To test this hypothesis I first tested whether incubating recombinant mouse OPN with thrombin would cleave the protein.

Recombinant mouse OPN is produced as a mixture of glycosylated and non-glycosylated OPN proteins. I found that incubation with thrombin cleaves glycosylated OPN efficiently, but not non-glycosylated OPN (Figure 2.10a). The non-gylcosylated form of OPN remained resistant to cleavage despite incubation in thrombin for 72 hr at 37^{o}C. This suggests that glycosylation is required for recognition and/or cleavage of OPN by thrombin and is the first example where glyocosylation of OPN has functional significance.

Treatment of OPN with thrombin generated the following products: intact non-glycosylated OPN and two peptide fragments representing the C and N terminal fragments of glycosylated OPN. Thrombin cleavage led to a substantial enrichment of the cleaved fragments of OPN (Figure 2.10a). To verify that thrombin improves the ability of

OPN to ligate integrin receptors I tested whether thrombin treatment of recombinant mouse OPN improved cell adhesion using HEK 293 cells. I found that cells plated on thrombin-treated OPN displayed an improved ability to adhere to their substrate compared to cells plated on untreated, intact OPN (Figure 2.10b).

To test whether thrombin cleavage of OPN improves its neuroprotective capacity I exposed primary rat neuronal cultures to OGD followed by incubation with untreated or thrombin-treated OPN (5nM) for 24 hr post OGD. Intact OPN conferred significant protection against OGD induced cell death, however, thrombin-treated OPN provided substantially greater protection against OGD-induced cell death compared to untreated OPN (61% vs 29% reduction in cell death, Figure 2.11a).

To compare neuroprotection by untreated and thrombin-treated OPN *in vivo*, thrombin-treated OPN, untreated OPN or aCSF was administered icv immediately after MCAO (75min) and the degree of neuroprotection was compared 24 hr later. Thrombin-treated OPN reduced infarct volume two-fold more than untreated OPN (45% vs 22% reduction) relative to vehicle treated animals (Figure 2.11b). Untreated OPN provided protection against ischemic injury, as we had found previously, however in this experiment the effect did not reach statistical significance.

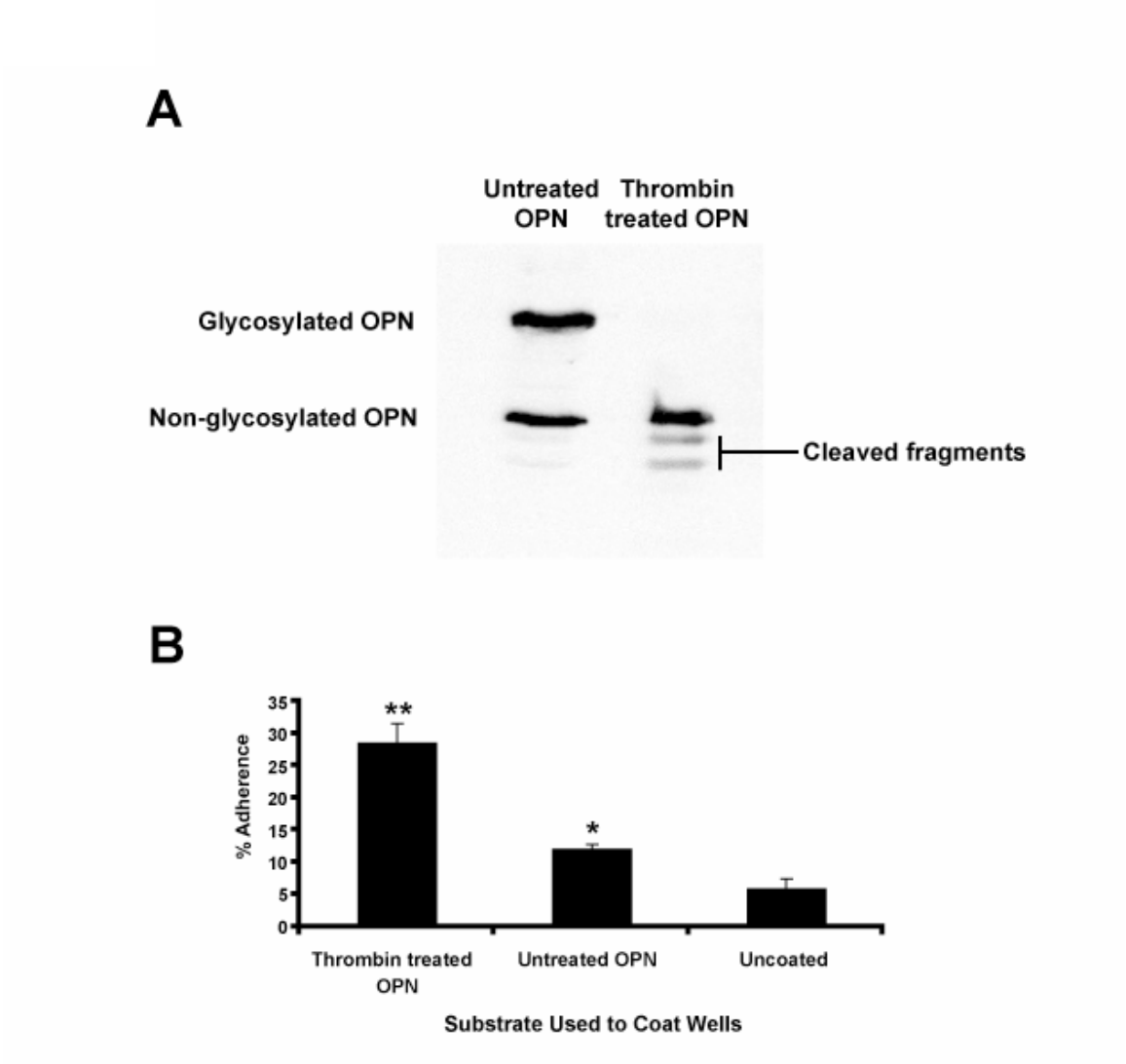

Fig 2.10 a.) Thrombin cleavage of OPN. Western immunoblot showing cleavage of glycosylated OPN after a 72 hr incubation in thrombin agarose. **b.)** Thrombin treated OPN is more effective at promoting HEK 293 cell adherence than untreated OPN. Data shown are means $\pm$ SD. Thrombin treated OPN significantly increased cell adherence relative to untreated OPN and uncoated wells **$p<0.05$. Untreated OPN significantly increased adherence relative to uncoated wells *$p<0.05$.

Figure 2.11. Thrombin treated OPN is more effective than untreated OPN at reducing neuronal death in response to ischemia. **a.)** Thrombin treated OPN conferred greater protection against OGD-induced cell death compared to intact OPN. *p <0.05 relative to OGD control. **p<0.05 compared to untreated OPN. Data shown are mean $\pm$ SEM. **b.)** Thrombin treated OPN is more neuroprotective than untreated OPN *in vivo*. Administration (icv) of thrombin treated OPN caused a greater reduction in infarct size than untreated OPN. Control mice received aCSF. *p<0.05 compared to aCSF and untreated OPN Data shown are mean $\pm$ SEM. n $\geq$ 9 per group. Images show representative sections from each treatment group.

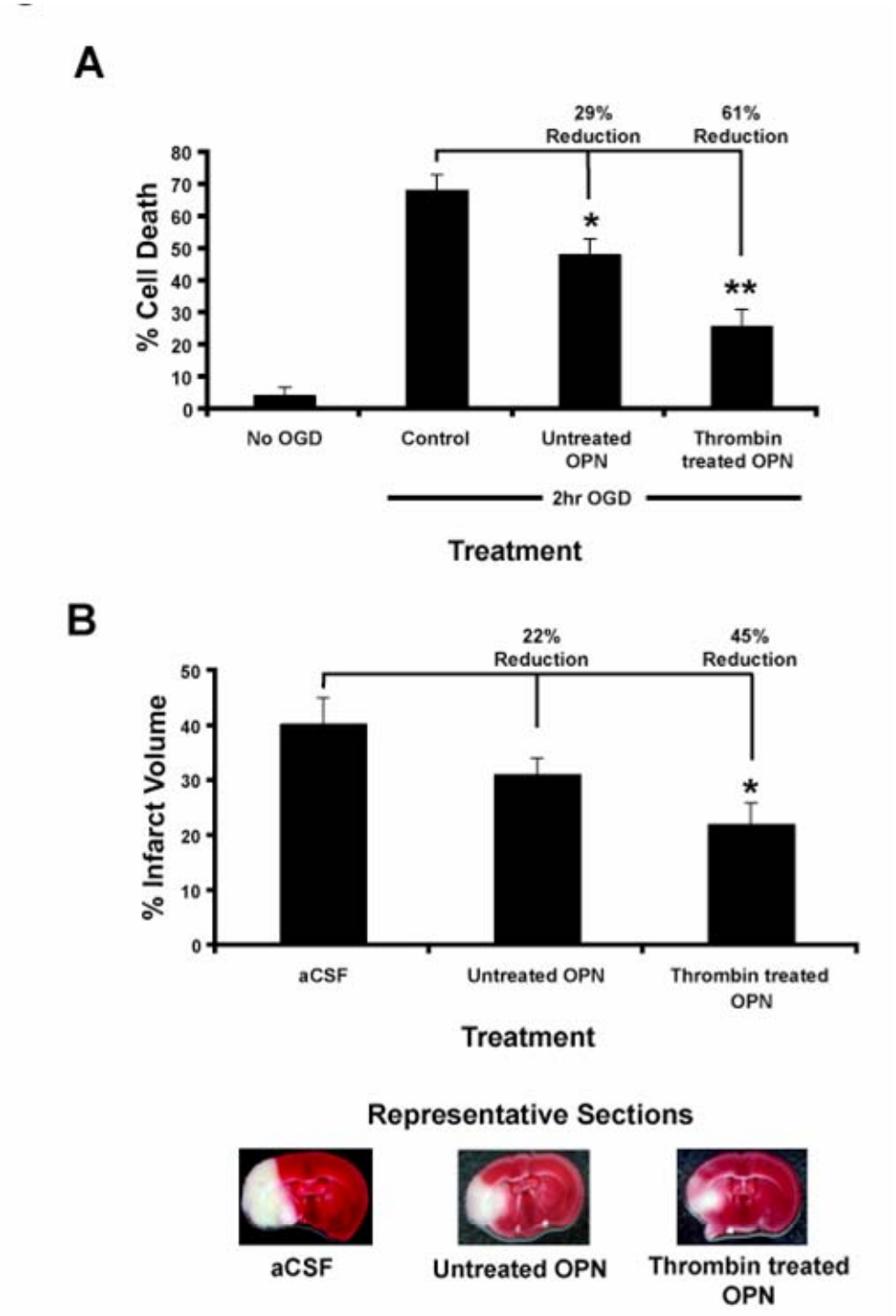
A
29% Reduction
61% Reduction
% Cell Death
80
70
60
50
40
30
20
10
0
*
**
No OGD
Control
Untreated OPN
Thrombin treated OPN
2hr OGD
Treatment
B
22% Reduction
45% Reduction
% Infarct Volume
50
40
30
20
10
0
*
aCSF
Untreated OPN
Thrombin treated OPN
Treatment
Representative Sections
aCSF
Untreated OPN
Thrombin treated OPN

2.15 Peptides based on the N and C terminal fragments of thrombin-cleaved OPN are neuroprotective

To determine whether one or both of the peptide fragments generated from thrombin cleavage of OPN have neuroprotective properties two 45 amino acid peptides corresponding to the sequence immediately N terminal and C terminal to the thrombin cleavage site of OPN were synthesized commercially (Figure 2.12). These peptides were generated with phosphorylated residues at sites reported to be phosphorylated in native OPN [60]. NT 109-153 (p), the N terminal peptide corresponding to amino acids 109 to 153 of native OPN, which contains the integrin binding sequences RGD and SLAYGLR, conferred greater neuroprotection than intact OPN in our *in vitro* model of stroke when compared to an equivalent molar dose of intact native OPN (5nM) (Figure 2.13). This supports the hypothesis that exposure of the SLAYGLR sequence improves the neuroprotective capability of OPN. Unexpectedly, I also found pronounced neuroprotection by the C terminal peptide, CT 154-198 (p) which is based on the sequence of the C terminal fragment of OPN. This result was surprising because we previously found that OPN mediates neuroprotection by interaction with integrin receptors, a property associated with the region of OPN located N terminal to the thrombin cleavage site.

Based on my finding that peptide NT 109-153 (p) and peptide CT 154-198 (p) confer neuroprotection *in vitro*, I tested each peptide in an *in vivo* model of stroke. Both peptides reduced infarct size compared to vehicle treated animals when delivered intranasally. NT

109-153 (p) reduced infarct volume by 36% and CT 154-198 (p) reduced infarct volume by 34% (Figure 2.14). For this experiment the peptides were administered 1 hr post MCAO validating a minimum time window of one hr post stroke available for OPN treatment.

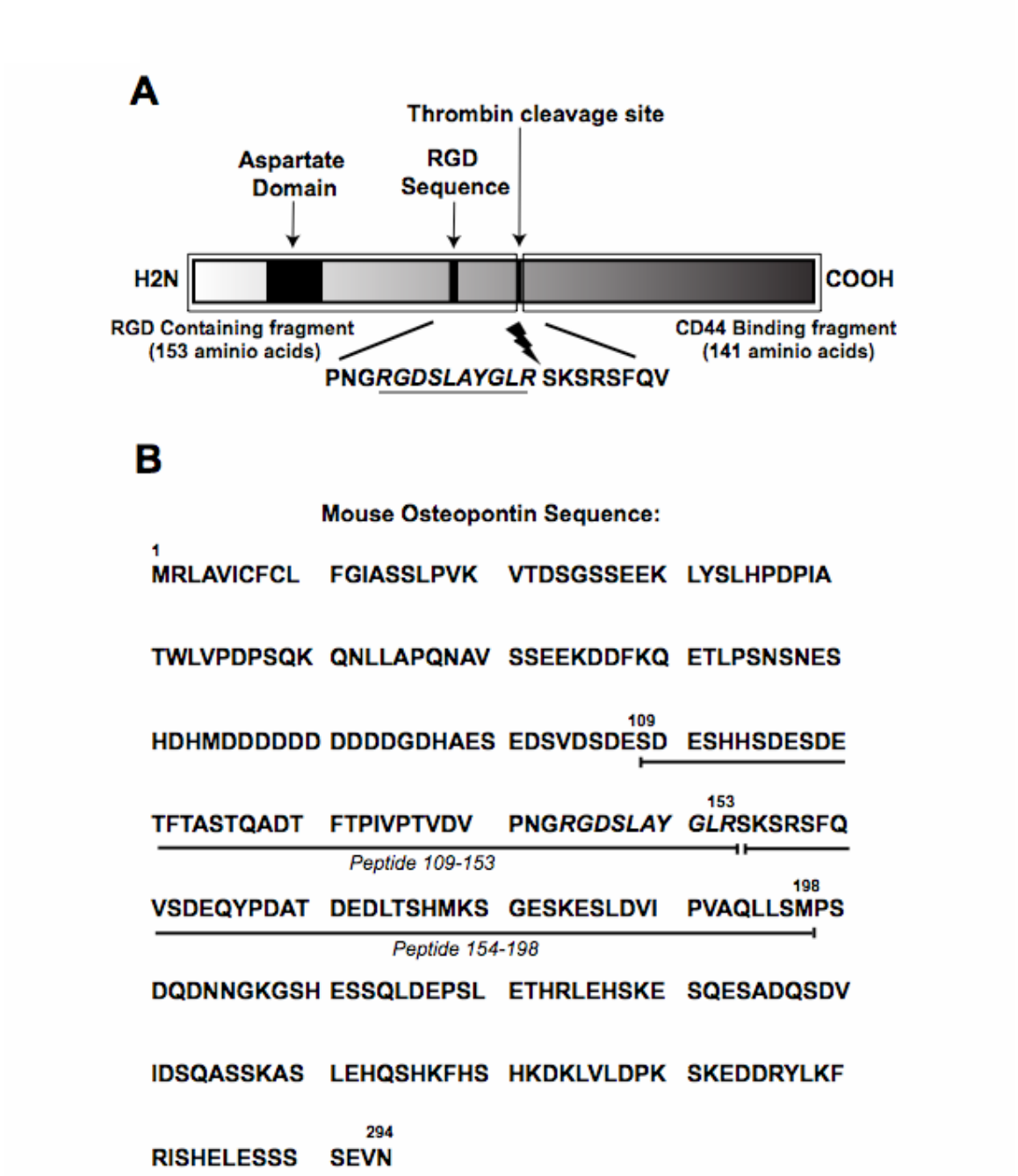

Fig 2.12 A.) Diagram of mouse OPN showing the location of the thrombin cleavage site, RGD sequence and SLAYGLR sequence. **B.)** Sequence of mouse OPN showing the relative location of peptide NT 109-153 and peptide CT 154-198 within the sequence.

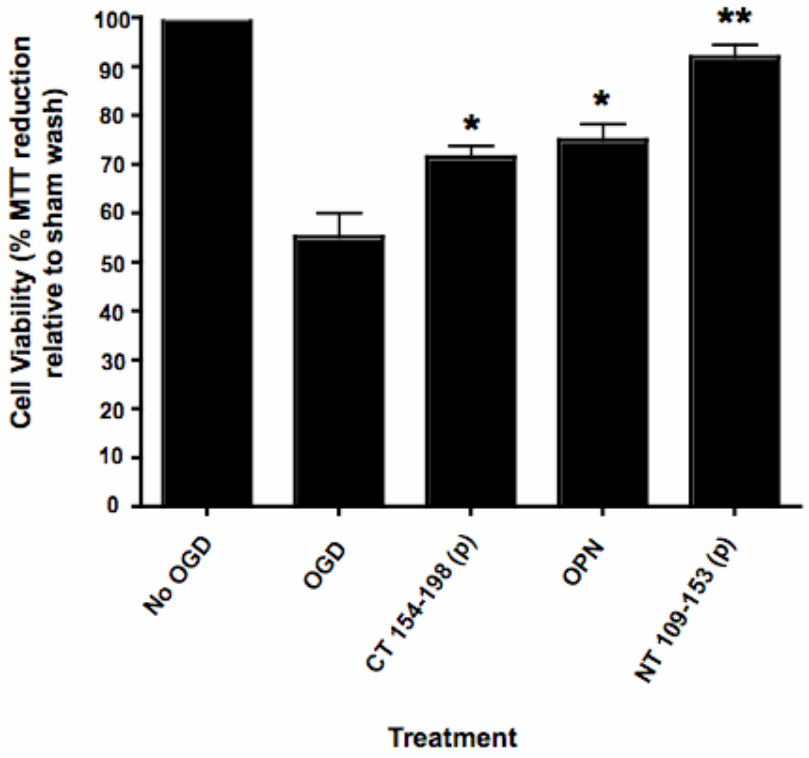

Fig 2.13 Peptides of OPN are neuroprotective *in vitro*. Cells were treated with 5nM intact OPN, peptide NT 109 – 153(p) or peptide CT 154 – 198(p) for 24 hr post 120 min OGD. Cell viability was assessed by MTT assay. n=3. Data shown are mean $\pm$ SEM. *p<0.05 relative to OGD control. **p<0.05 relative to OPN treatment.

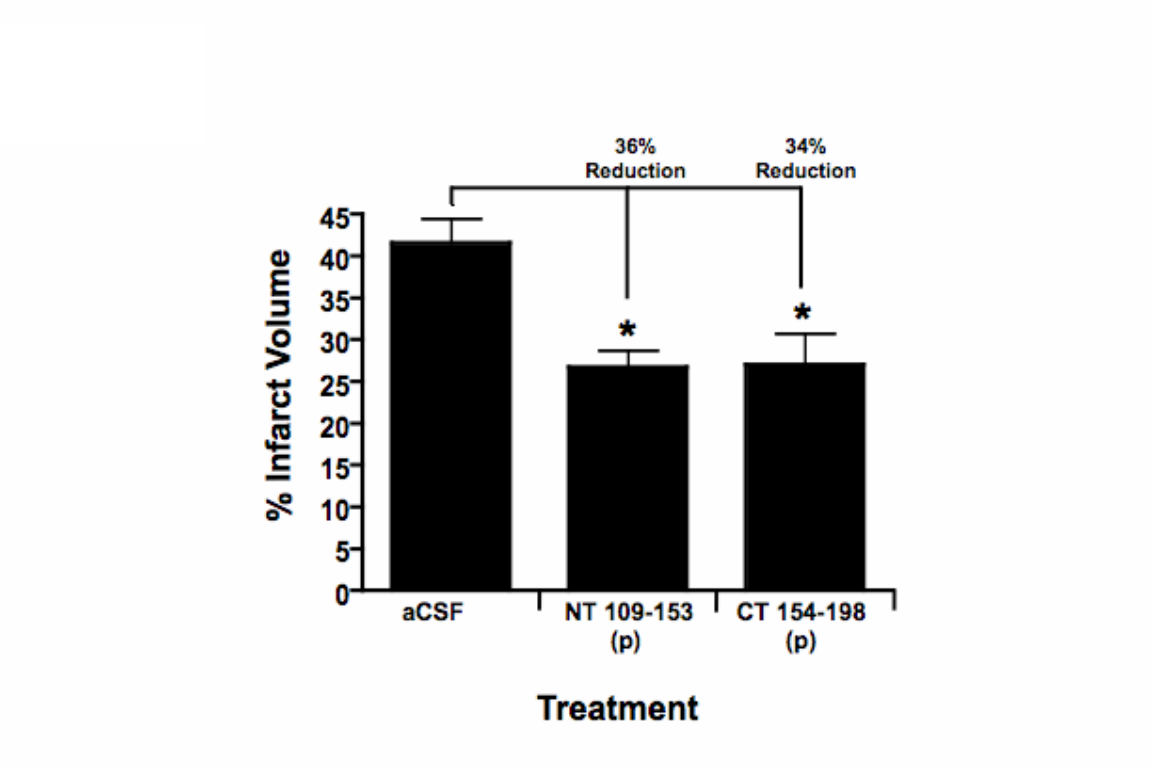

Fig 2.14. Intranasal administration of peptide NT 109 – 153(p) or peptide CT 154 – 198(p) reduces infarct volume following MCAO. One hr following MCAO, peptides were given intranasally at a dose equimolar to 5µg of OPN. Mice were sacrificed 24 hr later. Data shown are mean $\pm$ SEM. *$p<0.05$ compared to aCSF administration. n = 8 each group.

2.16 The C terminal peptide requires phosphorylation to be neuroprotective while the N terminal peptide does not require phosphorylation.

To determine whether peptides NT 109-153 (p) and CT 154-198 (p) require phosphorylation for their neuroprotective activity I tested non-phosphorylated versions of each peptide (peptides NT 109-153 and CT 154-198, Figure 2.12). These peptides were nasally administered 10 minutes after initiating MCAO at a concentration equimolar to our protective dose of OPN (5μg). The non-phophorlyated C terminal peptide failed to provide neuroprotection while the non-phosphorylated N terminal peptide retained neuroprotective capability. A scrambled 45 amino acid peptide based on the sequence of NT 109-153 also failed to provide neuroprotection (Figure 2.15).

The integrin binding sequence RGDSLAYGLR is located at the C terminal end of peptide NT 109-153 (p) and the phosphorylated residues are located at the N terminal end (Figure 2.15). Having discovered that this peptide does not require phosphorylation to confer neuroprotection I tested truncated versions, with residues removed from the N terminal end. The 30 amino acid peptide NT 124-153 and the 20 amino acid peptide NT 134-153 were nasally administered 10 minutes after initiating MCAO and mice were sacrificed 24 hr later. Each of these peptides conferred protection against ischemic injury. NT 124-153 reduced infarct volume by 31% and NT 134-153 reduced infarct volume by 61% (Figure 2.15). These data suggest that the neuroprotective sequence of the N terminal fragment of OPN lies between residues 134 and 153 and provides a relatively short sequence for future drug design.

2.17 Dose response and time window of NT 124-153

The above studies indicate that peptide NT 124-153 is the optimal choice for further preclinical testing. To investigate the relationship of dose and time on the efficacy of peptide NT 134-153 we tested this peptide at a dose ten fold higher and ten fold lower than the previously identified protective dose and at 1, 3 and 5 hrs post MCAO. When the peptide was delivered intranasally 1 hour post MCAO it conferred a similar amount of protection at 3500ng and 350ng, but was no longer neuroprotective at 35ng (Figure 2.16). When the peptide was tested at a dose of 350ng at the additional time points of 3 and 5 hours post MCAO it conferred a significant amount of protection at 3 hours but not at 5 hours (Figure 2.16). This indicates that there is a time window of at least 3 hours available for treatment with this peptide.

Fig 2.15. CT 154-198 (p) requires phosphorylation for neuroprotection, NT 109-153 (p) does not require phosphorylation for neuroprotection and a 20 amino acid version of NT 109-154 is neuroprotective. **a.)** Schematic of OPN and the relative location of each peptide within OPN (not to scale). **b.)** Infarct volume following peptide treatment. Ten minutes after initating MCAO, the indicated peptides were given intranasally at a dose equimolar to 5µg of OPN. Mice were sacrificed 24 hr later. Data shown are mean $\pm$ SEM. *$p<0.05$ compared to aCSF administration. n = $\geq$ 8 each group.

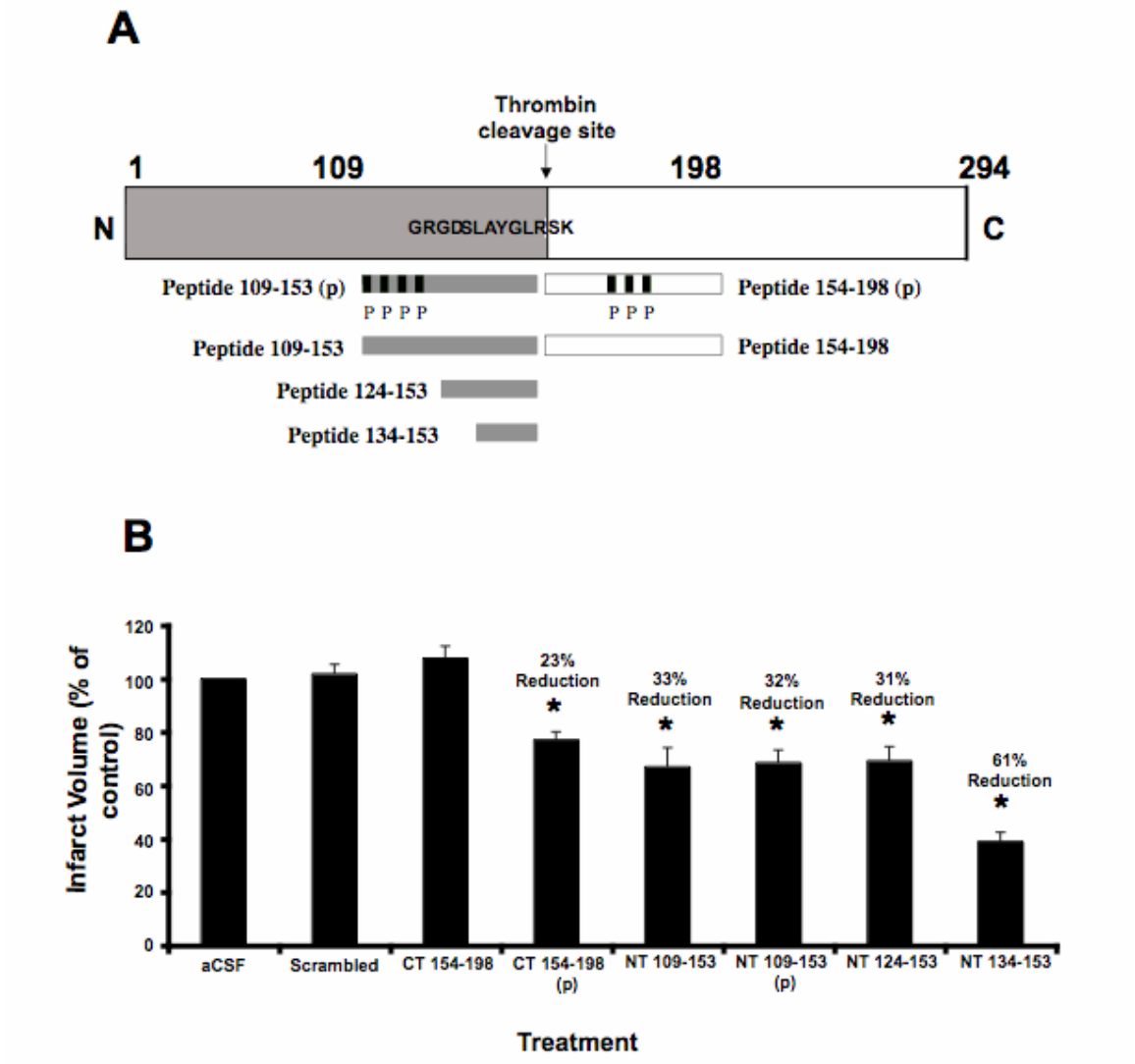
A
Thrombin cleavage site
1
109
198
294
N
GRGDSLAYGLRSK
C
Peptide 109-153 (p)
P P P P
P P P
Peptide 154-198 (p)
Peptide 109-153
Peptide 154-198
Peptide 124-153
Peptide 134-153
B
Infarct Volume (% of control)
120
100
80
60
40
20
0
23% Reduction
33% Reduction
32% Reduction
31% Reduction
61% Reduction
*
aCSF
Scrambled
CT 154-198
CT 154-198 (p)
NT 109-153
NT 109-153 (p)
NT 124-153
NT 134-153
Treatment

Fig 2.16. Time window and dose response of NT 134-153. **a.)** Infarct volume following administration of NT 134-153 during MCAO and at 1, 3 and 5 hrs post MCAO. At each time point the peptide was delivered intranasally at a dose of 350ng (equimolar to 5µg of OPN). Mice were sacrificed 24 hr after MCAO. Data shown are mean $\pm$ SEM. *$p<0.05$ compared to aCSF administration ($n = \geq 8$ each group). **b.)** Infarct volume following intranasal administration of 35ng, 350ng and 3500ng of NT134-153 at 1 hr post MCAO. Mice were sacrificed 24 hr after MCAO. Data shown are mean $\pm$ SEM. *$p<0.05$ compared to aCSF administration ($n = \geq 8$ each group).

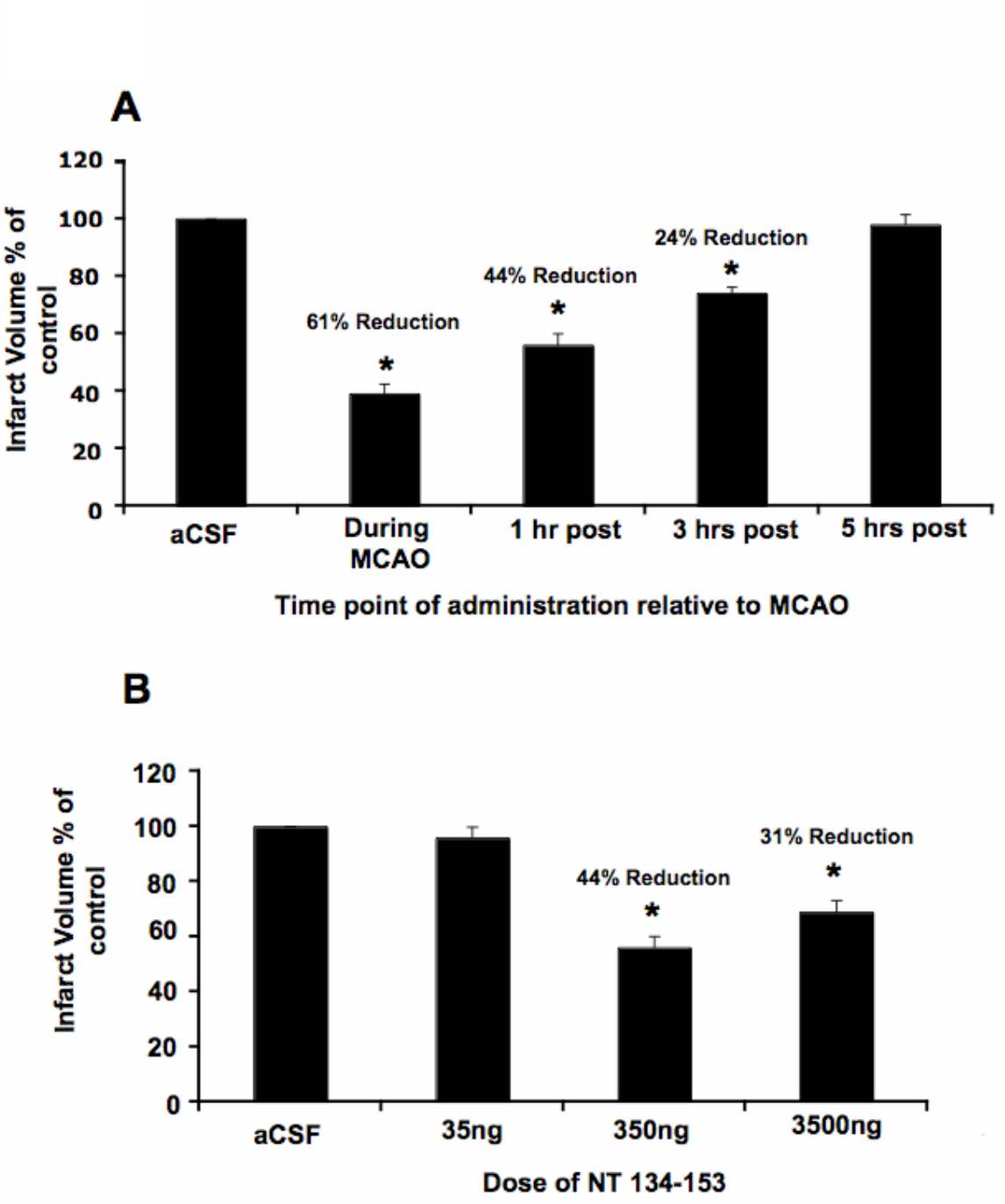
A
Infarct Volume % of control
120
100
80
60
40
20
0
61% Reduction
44% Reduction
24% Reduction
*
aCSF
During MCAO
1 hr post
3 hrs post
5 hrs post
Time point of administration relative to MCAO
B
Infarct Volume % of control
120
100
80
60
40
20
0
44% Reduction
31% Reduction
aCSF
35ng
350ng
3500ng
Dose of NT 134-153

2.18 Discussion

The work I present here shows that OPN is neuroprotective when administered before or after injurious 120 min OGD in cultured rat cortical cells. OPN also reduced infarct volume following MCAO-induced ischemia in mice. Taken together, these data suggest OPN has therapeutic potential as a stroke treatment.

A protective role for OPN in renal ischemia has been proposed [154, 155] due to its increased presence following ischemia and preferential localization with cells destined to survive [156]. Further, the absence of endogenous OPN appears to increase sensitivity to ischemia, as OPN knockout animals have greater kidney damage following renal ischemia [157]. Interestingly, I found that the absence of OPN did not appear to pre-dispose mice to greater overall injury in the CNS, as wild-type and OPN knockout mice had similar infarcts following MCAO. However, it has since been reported that the absence of OPN predisposes selective brain regions to greater injury following stroke [120]. Schroeter et al found increased thalamic neurodegeneration following ischemic stroke in OPN deficient mice, although they too found that infarct development at the site of ischemia was similar in OPN knockout and wildtype mice. Taken together these findings suggest a context dependent effect of OPN in ischemic brain injury. As a possible explanation it is conceivable that protective effects of endogenous OPN are overridden by hyperacute ischemic injury in the cortex but are sufficient to mitigate slowly evolving neurodegeneration in the thalamus.

Previous reports suggest that OPN may activate multiple pro-survival mechanisms including decreased induction of nitric oxide synthase [158], increased NF-κB and CREB activity [147], and increased PI3K activation [145]. Here I show that the neuroprotective action of OPN depends, in part, on PI3K activation, as neuroprotection is lost in the presence of LY294002. Blocking the activation of MAPK also reduced the neuroprotective effect of OPN. Subsequent phosphorylation and activation of Akt by PI3K or MAPK by Mek, appears to be involved in mediating the neuroprotection seen *in vitro.* This finding is consistent with previous studies wherein activation of Akt and MAPK leads to increased phosphorylation of Bad, a protein whose pro-cell death functions are blocked by such phosphorylation events [159]. Furthermore, the transcription factor CREB, which regulates the expression of a number of pro-cell survival proteins, is also a substrate for these protein kinases [159, 160].

Given that OPN's protective effects are also blocked by a protein synthesis inhibitor, it would appear that the activation of multiple intracellular neuroprotective protein kinase cascades may result in the synthesis of new proteins resulting in reduced cell death following ischemia. From this data I present the following model for the mechanism by which acute administration of OPN could confer neuroprotection following stroke:

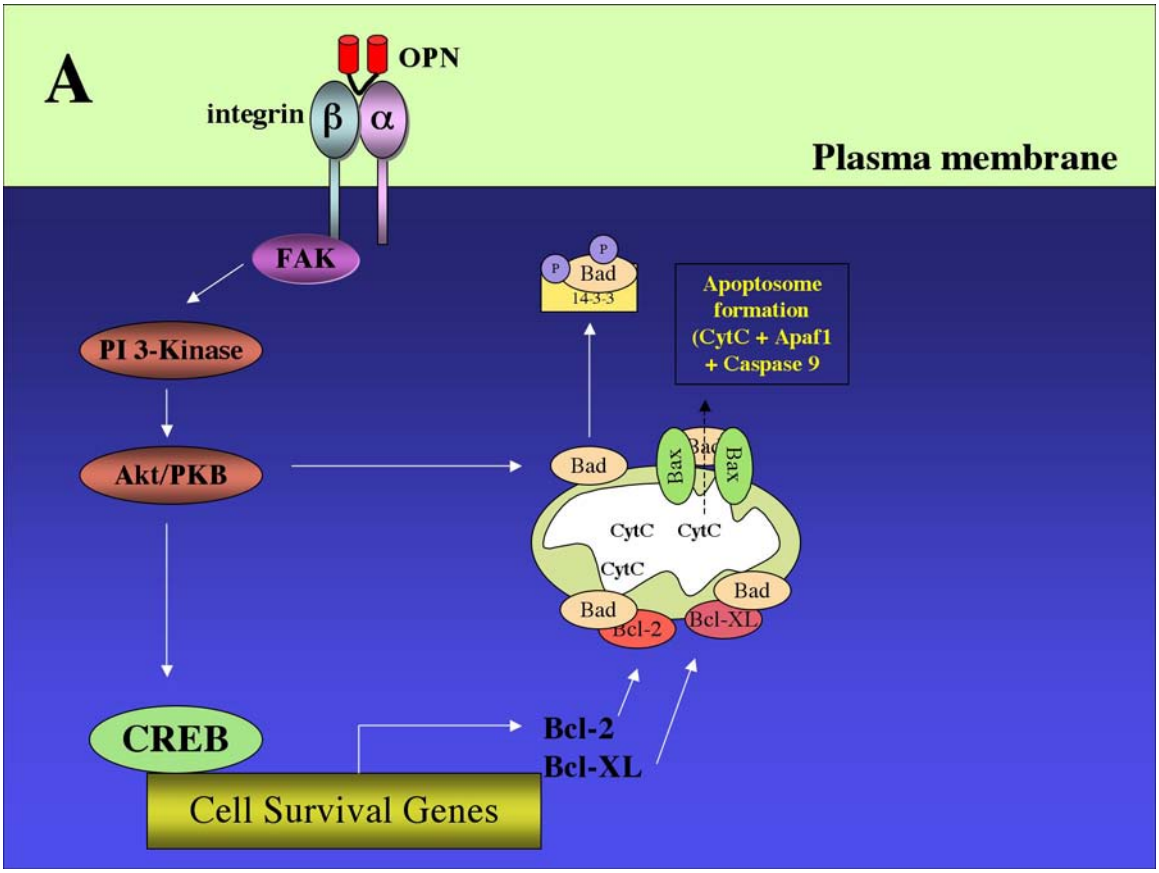

A.) OPN mediated resistance to ischemia-induced apoptosis via the integrin-PI-3-kinase-Akt pathway. Ischemia results in the localization of proapoptotic Bcl-2 family proteins such as Bad at the mitochondria, which leads to cytochrome C leakage and Apaf-1-mediated assembly of the apoptosome complex. Activation of PI-3-kinase by OPN/integrin ligation triggers the phosphorylation of Akt, which in turn serves as a central regulator of cell survival by phosphorylating CREB and Bad. Phosphorylated Bad is displaced from the mitochondria and sequestered by chaperones of the 14-3-3 family. Activation of CREB mediates the transcription of antiapoptotic proteins such as Bcl-2 and Bcl-XL, which can bind to Bad and further prevent pore formation and cytochrome C leakage.

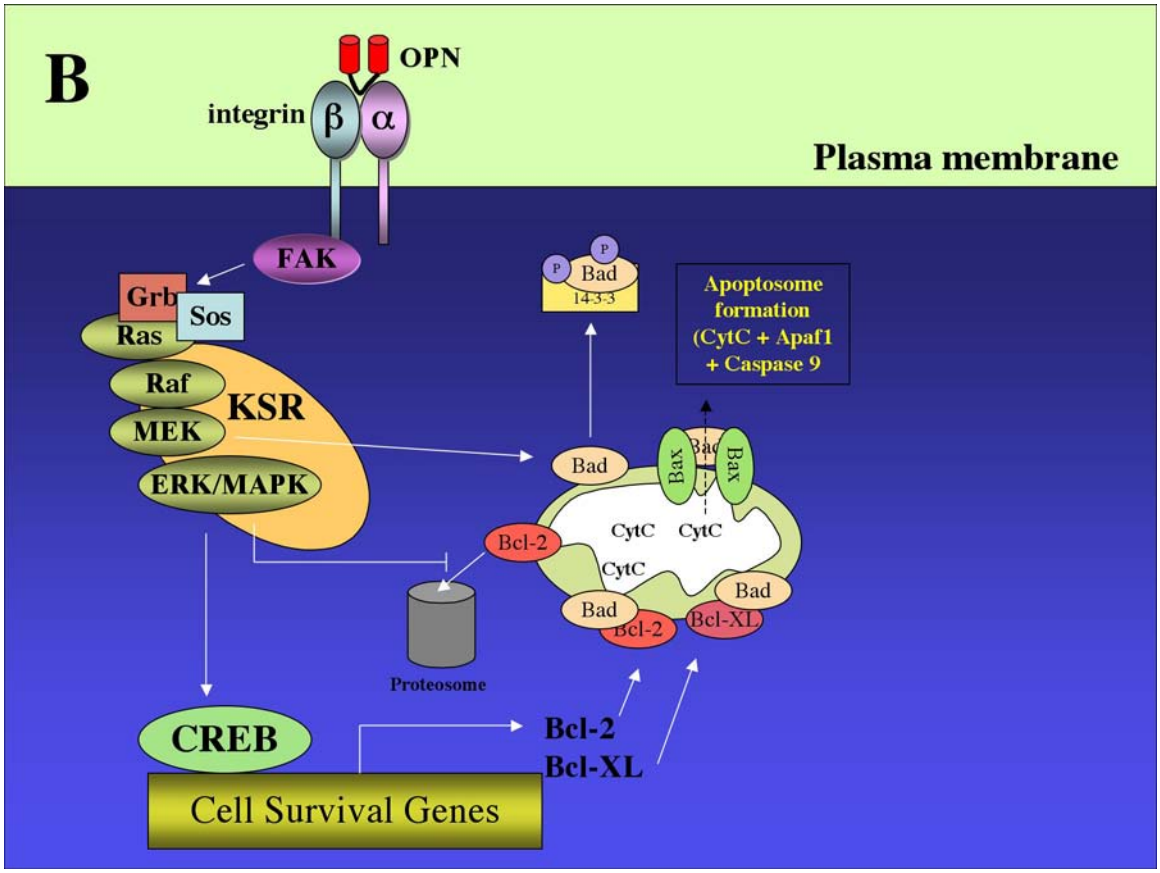

B.) OPN mediated resistance to ischemia-induced apoptosis via the MAPK pathway. Concomitantly with the activation of the Akt pathway, integrin ligation by OPN leads to the activation of the Ras-Raf-MEK-ERK cascade. Activated Ras can recruit Raf, which binds to and activates MEK and subsequently ERK, bound on a kinase suppressor of Ras (KSR) scaffold. Phosphorylation of Bcl-2 by activated ERK prevents its recognition by ubiquitin ligases. Of the proteins bound to KSR both Raf and MEK are capable of phosphorylating proapoptotic BAD, leading to its sequestration by 14-3-3 proteins. ERK activation of CREB also results in transcription of Bcl-2 and Bcl-XL providing another means of mitigating the activity of proapoptotic Bcl-2 family proteins induced by ischemia.

The therapeutic potential of OPN treatment in stroke is improved with intranasal administration [161]. Intranasal delivery is a non-invasive means of bypassing the blood-brain barrier that targets the CNS. Efficient delivery to the brain in animal models and humans has been achieved with a number of different proteins (e.g. IGF-1, FGF, NGF) and other molecules (DNA plasmids, flavenoids) [141, 150, 161-166]. Intranasal administration has several advantages over other forms of drug delivery. It is non-invasive and simple to perform. Moreover, intranasally administered molecules are not cleared by the liver prior to reaching the CNS. This approach has been used successfully with several proteins and peptides in the treatment of CNS diseases or injury [141, 150, 161-163, 165]. A recent study demonstrated a reduction in stroke volume and improved behavioral scores for rats that were given insulin-like growth factor-I intranasally following MCAO [141, 162]. An additional study showed that treatment of stroke was successful using the intranasal delivery of the anti-oxidant myricetin [166].

Based on this information I tested whether OPN could reach the brain via intranasal administration and found that OPN reaches the brain rapidly and protects against stroke injury when targeted to the CNS with this delivery method. This represents a significant preclinical advance for translating OPN to a treatment for stroke in humans.

Intact and thrombin cleaved OPN have distinct integrin binding properties [153]. I postulated that improved integrin binding would improve OPN's neuroprotective potency, thus I tested the effect of treating OPN with thrombin. Thrombin cleaves OPN at Arg168, and alters the orientation of the RGD sequence making it an improved ligand for

the integrins αvβ3, αvβ1, αvβ5, α8β1 and α5β1. Thrombin cleavage also reveals a SLAYGLR (SVVYGLR in humans) binding site for the integrins α9β1, α4β7 and α4β1 [167, 168].

Thrombin treatment of glycosylated OPN yielded 2 fragments: a 30kD fragment that contained the RGD sequence and a 28kD fragment that contained a CD44 binding region [85]. Non-glyocosylated OPN appears to be resistant to thrombin proteolysis, which implies that glycosylation is a structural requirement for the recognition and/or cleavage of OPN by thrombin. This is the first demonstration that glycosylation of OPN has functional significance.

Cell adhesion is largely mediated by integrin receptors as evidenced by the fact that monoclonal antibodies raised against integrins prevent cells from attaching to substrates [153]. The studies presented in this thesis show that thrombin treated OPN promoted greater cell attachment compared to full length OPN, which suggests that thrombin treated OPN is an improved ligand for integrin receptors.

Compared to intact OPN, thrombin treated OPN provides 2-fold more protection from cell death in primary rat neuronal cultures subjected to 120 min of OGD. Cells were incubated in equimolar amounts of thrombin treated or full length OPN for 24 hours prior to OGD. For these preliminary studies the two fragments of OPN were not separated. Thus, the improved potency may have been due to an alteration in the structure of the N terminal or C terminal half of OPN, or indeed due to a combined effect of alterations in

both halves. However, these data confirmed that fragments of OPN are more active than intact OPN in promoting cell attachment and protecting neuronal cultures against cell death. I then compared the effect of treating with intact OPN or thrombin treated OPN *in vivo* using our mouse MCAO model of stroke. I found that, similar to our *in vitro* finding, thrombin treated OPN provides 2-fold more protection from ischemic injury.

The improved neuroprotection conferred by thrombin treated OPN lead to further testing of the neuroprotective capacity of synthetic peptides representing the N and C terminal halves of thrombin cleaved OPN. Use of synthetic peptides allowed the evaluation of fragments of OPN individually and without the contaminating presence of the intact non-glycosylated molecule found in recombinant OPN preparations. The N terminal peptide, NT 109-153 (p), which contains the RGD motif, conferred marked neuroprotection in the setting of ischemia. Moreover when this peptide was tested *in vitro* it conferred significantly more neuroprotection than intact OPN when tested at an equal molar dose. This is consistent with my hypothesis that thrombin treatment of OPN improves the ability of the RGDSLAYGLR sequence to bind to integrin receptors. It is somewhat surprising, however, that the C terminal peptide, CT 154-198 (p) which lacks a RGD motif, also displayed neuroprotective activity *in vitro* and *in vivo*. Thus, the improved neuroprotective capacity of thrombin treated OPN may not be solely due to improved integrin binding ability. It is possible that increased potency may be due to the mobilization of the C terminal end of OPN following thrombin cleavage, thereby permitting the C terminal fragment to become untethered from the N terminal fragment and allow more receptors to be bound by thrombin cleaved OPN. The free peptide form of the C terminal fragment may adopt a new conformation that allows it to bind to

receptors involved in neuronal survival. For example, in addition to binding integrin receptors, OPN is a ligand for CD44, a receptor that mediates a diverse array of functions including cell migration, leukocyte activation and cell to cell and cell to extracellular matrix communication [169]. More recently a new role for CD44 has emerged in mediating cell survival. CD44 has been reported to have an anti-apoptotic effect in lymphocytes and the loss of CD44 promotes colon carcinoma apoptosis [170, 171]. As the C terminal fragment of OPN contains a CD44 binding site such cell survival properties may underlie the neuroprotective role of peptide CT 154-198 (p) [172].

To test whether peptides CT 154-198 (p) and NT 109-154 (p) require phosphorylation for their neuroprotective activity I tested non-phosphorylated versions of both peptides and found that CT 154-198 did not confer neuroprotection in the absence of phosphorylated residues at sites threonine 170, serine 176 and serine 180, while NT 109-153 was neuroprotective in the absence of phosphorylation, indicating that the N terminal fragment of OPN does not require phosphorylation to enhance neuronal survival.

Having found that peptide NT 109-153 could confer neuroprotection independently of phosphorylation I tested whether the peptide could be shortened with residues removed from the N terminal end. Accordingly I synthesized a 30 amino acid and a 20 amino acid version of this peptide, each containing an intact RGDSLAYGLR sequence, and tested them *in vivo* for the ability to protect the brain from ischemic injury following intranasal delivery. Interestingly, peptide NT 134-153, which is the shorter of the two, displayed greater neuroprotection. This result may reflect that the smaller molecular size of NT

134-153 results in superior delivery due to the fact that molecular size correlates inversely with delivery to the brain via the intranasal route [173, 174]. An important future direction will be to see whether truncated versions of peptide CT 154-198 (p) also confer enhanced neuroprotection.

Peptide NT 134-154 was selected for additional preclinical testing based on its greater efficacy when compared at an equal molar concentration to the other OPN peptides. I investigated the time window available for administration and found that NT 134-153 is capable of conferring neuroprotection when delivered at 1 and 3 hrs post MCAO, but not at 5 hrs. This experiment also revealed that NT 134-153 confers the greatest amount of neuroprotection when delivered during ischemia. This offers promise to patients scheduled for coronary artery bypass surgery, of which approximately 50% suffer permanent cognitive decline from intraoperative emboli [175].

A dose response experiment was performed to determine the potency of NT 134-153 and whether delivering a higher dose could increase its efficacy. A ten fold higher dose was not more neuroprotective than the previously identified protective dose and a ten fold lower dose failed to confer neuroprotection altogether. This data suggests that 17.5µg/kg, which is equivalent to the dose of 350ng used here, could be used for a preclinical trial in a non-human primate.

A future direction will be to perform a similar time window and dose response experiment with peptide CT 154-198 and test if combining NT 134-153 with CT 154-198

has an additive or synergistic effect. If an additive or synergistic effect is discovered then combining NT 134-153 and CT 154-198 into a single peptide is a potential means of targeting multiple pathways of neuroprotection with a single drug. By combining the peptides so that peptide CT 154-198 is positioned at the N terminus and peptide NT 134-153 is positioned at the C terminus the new peptide would have a free carboxylic acid on arginine 153 and as such, based on the data presented here, may be optimized for stroke treatment.

In summary:

- OPN does not require glycosylation to confer neuroprotection, although glycosylation is required for thrombin to cleave the intact molecule.
- Thrombin treated OPN is superior to the intact molecule in conferring neuroprotection.
- There exist at least two non-overlapping peptides within the sequence of OPN that confer neuroprotection when given alone.
- The sequence of one of these neuroprotective peptides is located between residues 154-198 and there is the requirement of phosphorylation at threonine 170, serine 176 and serine 180 for neuroprotective activity.
- The second neuroprotective peptide is located between residues 134 and 153, contains the integrin binding sequence RGDSLAYGLR and does not require phosphorylation for neuroprotective activity.

It is noteworthy that these peptides protect against stroke injury when delivered intranasally—a feature that offers substantial hope for their future therapeutic application. I anticipate that from these studies additional drugs based on the sequence of OPN may emerge as important components of future stroke therapy.

CHAPTER 3

THYRONAMINE AND 3-IODOTHYRONAMINE

INTRODUCTION

3.1 Hypothermia

Hypothermia is poised to become a successful treatment for stroke in humans. Two landmark prospective randomized controlled studies have been published demonstrating the benefit of mild hypothermia in improving neurologic outcome in patients suffering from cardiac arrest [48, 49]. Evidence from animal studies indicates that even mild hypothermia, lowering core temperature to 32-34^{o}C, provides substantial protection against cerebral ischemia. Current methods used to induce hypothermia involve cooling with ice, alcohol, cooling fans, specially designed cooling blankets and helmets and intravascular devices. These methods force body temperature below the homeostatic set point and induce shivering and vasoconstriction to oppose the drop in body temperature.

In laboratory studies hypothermia as a neuroprotectant is unsurpassed. Mild (32^{o}C) intra-ischemic hypothermia reduces global ischemic injury and provides lasting behavioral and histological protection in both young and old animals and remains the gold standard for studies of neuroprotection [176]. Since cooling during ischemia is not usually possible much research has been conducted to determine whether post-ischemic hypothermia is also beneficial. Early studies suggested that post-ischemic hypothermia was ineffective. This appears to be due to the application of too brief a period of cooling (2-3hrs) [177]. Subsequent preclinical tests with greater durations ($\geq$ 6 hours) of hypothermia have demonstrated that post-ischemic hypothermia is effective and that the therapeutic window

expands as the duration of hypothermia is increased. For example with cooling periods of 48 hours significant long term protection of CA1 hippocampal neurons can be achieved in the rat global ischemia model even when cooling is delayed by 12 hours [178].

The mechanisms by which hypothermia protects against ischemic injury are numerous and include reductions in metabolic rate, free radical formation, reperfusion injury, and glutamate release. No single action of hypothermia appears to be responsible for its marked neuroprotective actions.

Specific molecular mechanisms also contribute to neuroprotection in the hypothermic animal. Following focal cerebral ischemia, mild hypothermia has been shown to increase Bcl-2 expression, decrease Bax expression and attenuate cytochrome c release from the mitochondria [179, 180]. Hypothermia also prevents responses to ischemia that would otherwise promote apoptosis such as increased expression of transformation related protein 53 and attenuation of Akt activity [181, 182].

Hypothermia can be used as a preconditioning stimulus. It has been shown that hypothermia induced tolerance to ischemia is initiated within 6 hours, peaks at approximately 1 or 2 days and is reversed by 7 days after preconditioning stimulation. Hypothermia induced tolerance is dependent on *de novo* protein synthesis and involves direct changes in the brain neuropil. Intraoperative ischemia is an unavoidable complication of many types of surgery, and preconditioning induction of hypothermia is

a potentially valuable strategy for limiting cerebral injury during such predictable periods of risk.

The mechanism by which hypothermic preconditioning protects the brain almost certainly overlaps with the mechanism by which acute induction of hypothermia protects the brain, but is unlikely to be identical. Acute administration of hypothermia can directly protect neurons post ischemia by reducing metabolic rate [183]. It has been demonstrated that for each $1^{o}C$ decrease in temperature there is a 10% reduction in tissue metabolic requirements and free radical production (the Q10 effect) [183]. This process can benefit neurons when hypothermia is induced during or after ischemia but not when hypothermia is induced before ischemia as it is too temporally remote to the injury process. Instead, the protective effect of hypothermic preconditioning may rely on cellular reprogramming and direct biochemical changes in the intracellular and extracellular milieu [69].

In support of this postulate, hypothermia-induced preconditioning depends on *de novo* protein synthesis, and in SHSY5Y cells it requires modification of proteins by SUMOylation [184, 185]. Transcription factors are the main targets of SUMO conjugation and SUMOylation of these proteins generally causes transcriptional suppression. SUMOylation could in part explain the suppression of gene transcription common to multiple preconditioning stimuli [69, 186].

Hypothermia causes cardiac output to be reduced, which may cause a mild ischemic challenge in the brain. Therefore hypothermic preconditioning could work by acting as an

indirect method of inducing ischemic preconditioning. However, this cannot be the case when mild levels of hypothermia are used as the preconditioning stimulus since cardiac output is not reduced. Also, hypothermia of the brain appears as effective as whole body hypothermia, another scenario where cardiac output is not reduced.

Current methods of inducing hypothermia involve forced cooling. This causes shivering, a catecholamine surge and, in rodents, an increase in brown fat thermogenesis as the body tries to maintain homeostasis. These responses make the induction of hypothermia challenging, as they are effective at combating all but the most severe attempts to reduce temperature. These side effects make the induction of hypothermia an unpleasant experience for patients, especially in light of the fact that hypothermia must be carried out for days to derive maximum benefit. Sedatives can be used to reduce patient discomfort but pharmacokinetics change dramatically as temperature alters, making it difficult and often times dangerous to ascertain the correct dosage. Thus an improved method of inducing hypothermia would be extremely advantageous.

3.2 Thyronamine and 3-iodothyronamine

Anapyrexia (regulated hypothermia) refers to the condition in which core body temperature is lowered in response to a decrease in the thermoregulatory set-point. Anapyrexia occurs in some species in response to food restriction, poisoning, hypoglycemia, hypoxia, hemorrage, dehydration and infection. Regulated hypothermia exists as a means to diminish metabolic demands during conditions of severe energy

depletion, tissue injury or infection. A novel means of inducing anapyrexia may be through treatment with 3-iodothyronamine (T_1AM) or thyronamine (T_0AM), which are naturally occurring metabolites of thyroid hormone (TH).

Thyroxine (T4) is the principal secreted form of TH and constitutes 95% of all TH found in the circulation of humans [187]. In target tissues T4 is de-iodinated to 3,5,3,'-triiodothyronine (T3) which is the more active form of TH and has a higher affinity for the TH nuclear receptors TRα and TRβ [188]. T4 and T3 control a wide range of physiological processes including metabolism, thermogenesis, brain development, and cardiac function. As such, individuals with elevated TH present with increased metabolic rate, body temperature and heart rate compared to individuals with normal levels of circulating TH. T4 and T3 are slow acting and take hours to days to affect these physiological processes by altering gene transcription.

It has been proposed [189] that TH is further deiodinated and decarboxylated to give 3-iodothyronamine (T_1AM) and thyronamine (T_0AM) (Fig 3.1). These derivates are present in the brain, peripheral organs and blood of mammals [189]. The non-selective enzyme aromatic amino acid decarboxylase (AADC) promotes the efficient decarboxylation of a wide variety of aromatic amino acids and along with the de-iodinases has been proposed to be responsible for the enzymatic conversion of T4 into T_1AM and T_0AM.

It was recently shown that synthetic T_1AM and T_0AM injected into mice have the opposite effect to T4 and T3, rapidly inducing hypothermia via a mechanism independent

of gene transcription. T_1AM and T_0AM are not ligands for traditional nuclear TH receptors but are agonists of heterologously expressed trace amine associated receptor 1 (TAAR1), a G-protein coupled receptor (GPCR) that is activated by phenylethylamine, tyramine as well as amphetamine and its congeners [190]. Although T_1AM and T_0AM can dose-dependently couple TAAR1 to the production of cAMP, it is not yet clear whether TAAR1 is an endogenous receptor for the thyronamines T_1AM and T_0AM.

The specific number and placement of iodine atoms influences the potency of T_1AM and T_0AM. T_1AM is a more potent agonist of TAAR-1 than T_0AM. The addition of a single iodine atom to the 3-position of T_0AM results in an approximate 10-fold increase in agonist potency for TAAR-1. All other combinations of iodines on the thyronamine skeleton result in decreased potency [191].

T_1AM and T_0AM induce profound hypothermia in mice within 30 minutes of ip administration [189]. This hypothermic response occurs with no apparent long-term adverse effects and, importantly, there is no evidence of shivering or piloerection, suggesting that T_1AM/ T_0AM -induced hypothermia is not opposed by the body's natural homeothermic response to cold temperatures.

T_1AM and T_0AM have been characterized only recently and consequently little is known about their mode of action. However, based on their unique ability to induce rapid and long lasting hypothermia I postulated that T_1AM and T_0AM would provide a pharmacologic means to achieve hypothermia that could be used in the setting of

ischemia. Furthermore, hypothermia that is not countered by homeostatic attempts to raise body temperature would represent a significant improvement over existing methods of inducing hypothermia, thus T_1AM and T_0AM represent attractive candidate neuroprotectants for ischemia.

For my dissertation I have focused on T_1AM due to its greater potency, however, wherever possible I have performed experiments with both T_1AM and T_0AM as a means of characterization and relative comparison.

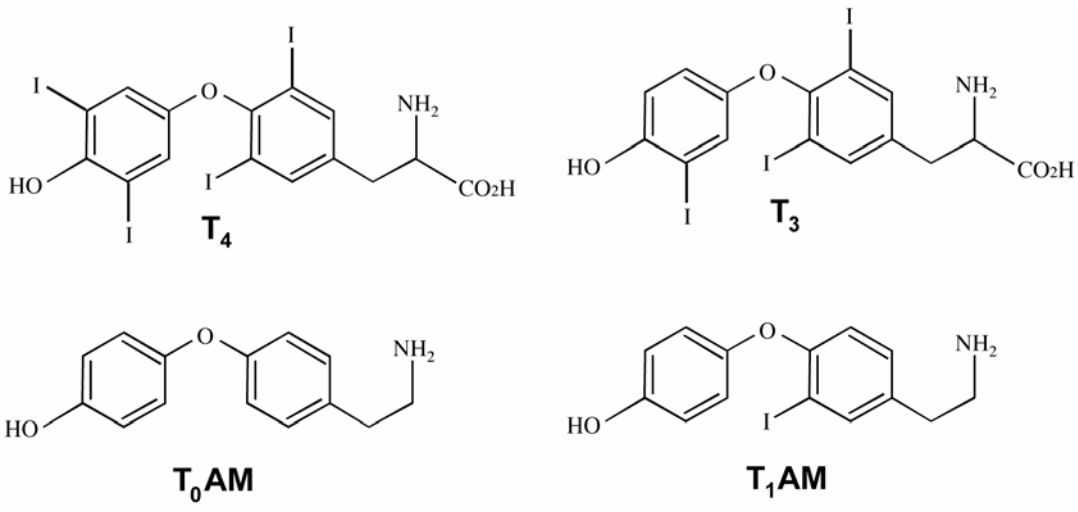

Figure 3.1 Chemical structures of the thyroid hormones T4 and T3 and naturally occurring metabolites, T_0AM and T_1AM.

3.3 SAR analysis of T_1AM

My collaborators Dr Thomas Scanlan and Dr David Grandy at OHSU have previously performed a structure activity analysis of T_1AM. The structural requirements for T_1AM to activate TAAR1 and induce hypothermia are as follows [191]:

i) A basic amino group at Cα is necessary.

ii) Monomethylation of the amine can be beneficial although larger alkyl groups and bis-alkylation are deleterious.

iii) mTAAR1 and rTAAR1 differ with respect to their tolerance of changes in the diaryl linker, both in length and functionality.

iv) Within the thyronamine scaffold, an iodine or methyl substituent at the 3-position is optimal.

v) H at the 4'-position vs OH is optimal, and substituents larger than OH are deleterious.

Scanlan and Grandy discovered that only 1 synthetic thyronamine, Compound 91, was more potent than T_1AM at inducing hypothermia. However, Compound 91 exhibits toxicity within a week of injection, a side effect not seen with T_1AM. This toxicity could be due to the lack of a 4'-OH, which may play a role in thyronamine clearance.

3.4 Hypothesis

I hypothesize that the thyronamines, T_1AM and T_0AM induce deep protracted hypothermia that may provide neuroprotection as an antecedent and acute treatment for brain ischemia.

3.5 Research Design

To perform a preclinical investigation of T_1AM I first tested the hypothesis that acute administration of T_1AM is neuroprotective. To test whether neuroprotection is conferred, in part, via the induction of hypothermia, I blocked the hypothermic effect of T_1AM. These experiments represent the first use of an endogenous cryogen as a means of inducing hypothermia to treat stroke.

To investigate whether acute treatment with T_1AM can directly protect neurons from ischemic injury in the absence of hypothermia, I tested T_1AM *in vitro* where pharmacological induction of hypothermia is not possible.

To test the hypothesis that T_1AM could be used as a stimulus for inducing hypothermic preconditioning, I administered T_1AM two days prior to MCAO. To determine whether preconditioning administration of T_1AM requires the induction of hypothermia I repeated this experiment while blocking the hypothermic effect of T_1AM. This experiment is the first to show hypothermic preconditioning in the mouse. Furthermore, this is the first demonstration of hypothermic preconditioning using a cryogen rather than physical methods of inducing hypothermia.

I tested preconditioning administration of T_1AM *in vitro* where cell temperature is determined by ambient temperature and hence pharmacological induction of hypothermia

is not possible. This allowed me to discover whether T_1AM can precondition neurons against ischemic injury in the absence of its hypothermic effect.

Finally, in order to discover whether T_1AM has side effects that would preclude its use in humans I monitored neurological function for 48 hours post injection of T_1AM.

RESULTS

3.6 Acute administration of T_1AM and T_0AM induces hypothermia and marked neuroprotection against stroke injury.

To investigate whether acute administration of T_1AM and T_0AM protects against ischemic injury mice were injected ip, with 50mg/kg of T_1AM or T_0AM 1 hour following MCAO. This dose of T_1AM and T_0AM was selected based on previous work showing 50mg/kg caused a level and duration of hypothermia that is protective in experiments using physical hypothermia [189]. This dose of T_1AM and T_0AM caused an immediate reduction in rectal temperature to an average of 31^{o}C within 30 minutes of injection and was well tolerated, causing a temporary reduction in spontaneous activity in injected mice but no other discernable behavioral change (Fig 3.2a, Table 3.1a and b).

The reduction in body temperature occurred in the absence of shivering or piloerection and by 24 hours post injection the body temperature of the T_1AM and T_0AM treated mice had returned to the same level as the vehicle-injected mice. The animals administered T_1AM and T_0AM had significantly reduced infarct volumes compared to mice injected with vehicle only, showing a 35% and 32% reduction, respectively (Fig 3.2b).

To determine whether the neuroprotective effect of T_1AM and T_0AM required a reduction in body temperature additional mice were injected with T_1AM or T_0AM and a drop in body temperature was blocked by placing the animals on an adjustable heating

pad following MCAO. The body temperature of the mice was monitored hourly and the setting of the heating pad adjusted to maintain body temperature of the T_1AM/ T_0AM injected animals at the same temperature as vehicle-injected animals. Blockade of T_1AM or T_0AM -induced hypothermia eliminated the protective effects of these drugs (Fig 3.2b) indicating that the neuroprotective effect of T_1AM and T_0AM depends, in part, on the induction of hypothermia.

Table 3.1a Criteria for Neurological Scoring

Behavior	Score	Description
Hair & grooming	0	Normal
	1	Localized disorder, especially around eyes and nose
	2	Generalized disorder, ruffled and/or dry fur
Ears	0	Normal position
	1	Transient lope-eared
	2	Steady lope-eared
Eyes	0	Normal
	1	Rheumy
	2	Dark discharge
	3	Semi-closed
	4	Closed
Posture	0	Normal
	1	Hunched and unstable
	2	Upright; Head and/or body rests on ground
	3	Lies on side; can assume prone position with strain
	4	Passive; lies as place
Spontaneous activity	0	Normal
	1	Calm; quiet; explores slowly
	2	Inert; somnolent; not exploring
	3	Lethargic; some movements in place
	4	No spontaneous movements
Epileptic behavior	0	Normal
	3	Hyperactive; timid and apprehensive
	6	Aggressive appearance; hyperexcited
	9	Extremely hyperexcited or focal seizures
	12	Partially or fully developed Grand Mal seizures
Gait	0	Normal
(open bench top)	1	Stiff:Inflexible
	2	Limping
	3	Trembling: drifting: falling
	4	Does not walk

Table 3.1b Neurological scoring for 48 hours post injection of T_1AM and T_0AM.

		Hours post Injection								
Behavior	**Treatment**	**0**	**1**	**2**	**3**	**4**	**5**	**6**	**24**	**48**
Hair & grooming	Vehicle	0	0	0	0	0	0	0	0	0
	T_1AM	0	0	0	0	0	0	0	0	0
	T_0AM	0	0	0	0	0	0	0	0	0
Ears	Vehicle	0	0	0	0	0	0	0	0	0
	T_1AM	0	0	0	0	0	0	0	0	0
	T_0AM	0	0	0	0	0	0	0	0	0
Eyes	Vehicle	0	0	0	0	0	0	0	0	0
	T_1AM	0	0	0	0	0	0	0	0	0
	T_0AM	0	0	0	0	0	0	0	0	0
Posture	Vehicle	0	0	0	0	0	0	0	0	0
	T_1AM	0	0	0	0	0	0	0	0	0
	T_0AM	0	0	0	0	0	0	0	0	0
Spontaneous activity	Vehicle	0	0	0	0	0	0	0	0	0
	T_1AM	0	3.5	3	2.75	3	2	0.75	0	0
	T_0AM	0	3.75	3	2.5	2.25	1.25	0.5	0	0
Epileptic behavior	Vehicle	0	0	0	0	0	0	0	0	0
	T_1AM	0	0	0	0	0	0	0	0	0
	T_0AM	0	0	0	0	0	0	0	0	0
Gait	Vehicle	0	0	0	0	0	0	0	0	0
(open bench top)	T_1AM	0	0	0	0	0	0	0	0	0
	T_0AM	0	0	0	0	0	0	0	0	0

Table 3.1 Mice were injected i.p. with vehicle, 50mg/kg T_1AM or 50mg/kg T_0AM and assessed hourly for the first 6 hours post injection and at 24 and 48 hours post injection. The scores represent the average score of 8 mice for each treatment.

Figure 3.2 Acute administration of T_1AM and T_0AM causes hypothermia and protection against ischemic injury. **A)** Temperature reduction following administration of T_1AM or T_0AM post stroke. Mice were i.p injected with vehicle or 50mg/kg of T_1AM or T_0AM 1 hour post reperfusion. Temperature was measured every hour for 6 hours post stroke and immediately before sacrifice (24 hours post stroke). In two separate groups of animals temperature reduction following T_1AM and T_0AM injection was prevented by maintaining animals on an adjustable heating pad. **B)** Infarct volume following T_1AM, T_0AM, T_1AM hypothermia blocked and T0AM hypothermia blocked treatment following MCAO. N = 8 per group. Error bars represent standard deviation. * p value = <0.05 compared to vehicle injected.

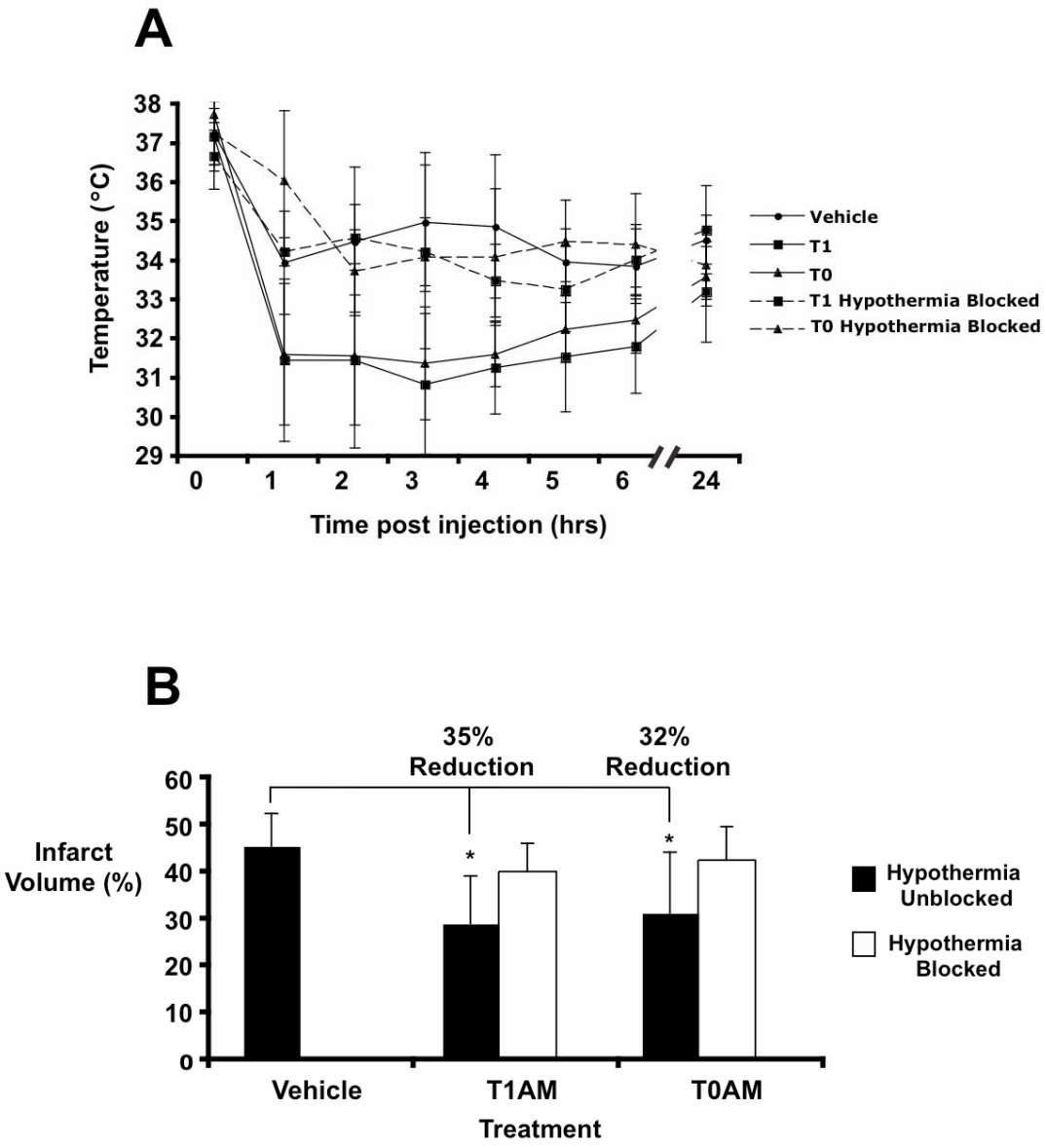
A
Temperature (°C)
38
37
36
35
34
33
32
31
30
29
0
1
2
3
4
5
6
24
Time post injection (hrs)
Vehicle
T1
T0
T1 Hypothermia Blocked
T0 Hypothermia Blocked
B
35%
Reduction
32%
Reduction
Infarct
Volume (%)
60
50
40
30
20
10
0
*
*
Vehicle
T1AM
T0AM
Treatment
Hypothermia
Unblocked
Hypothermia
Blocked

3.7 Acute administration of T_1AM and T_0AM *in vitro* does not confer neuroprotection against ischemic injury.

The acute effects of T_1AM and T_0AM were explored at the cellular level using primary neuronal cultures subjected to ischemic injury modeled *in vitro*. Escalating doses (5nM-500µM) of T_1AM or T_0AM were applied to primary mouse neuronal cultures immediately following exposure to 3 hours of oxygen and glucose deprivation (OGD). Under these *in vitro* conditions, T_1AM and T_0AM do not induce hypothermia. Figure 3.3 shows that treatment of primary neurons *in vitro* with T_1AM or T_0AM failed to provide protection from cell death induced by OGD. Furthermore, high doses (50µM, 500µM) of T_1AM and T_0AM were cytotoxic to the neuronal cultures in the absence of OGD. Treatment with 5nM of OPN peptide NT 109-153 (p) was used as a positive control. Collectively, these *in vivo* and *in vitro* experiments suggest that acute administration of T_1AM and T_0AM confers neuroprotection via a mechanism that depends on hypothermia.

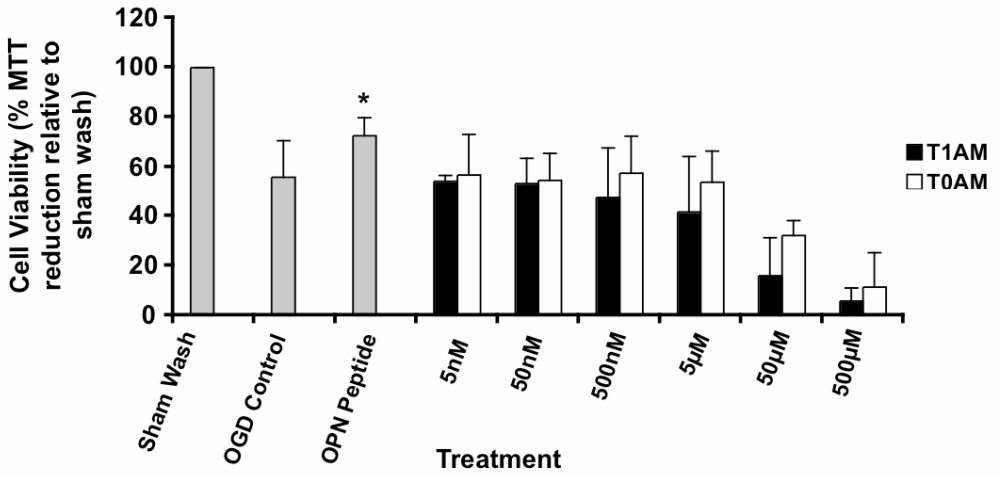

Figure 3.3 T_1AM and T_0AM acute administration *in vitro*. Experiments were performed on mouse primary neuronal cultures. Cells were treated with the indicated doses of T_1AM or T_0AM immediately after OGD. Cell viability assays were performed 24 hours post OGD (N=3). Treatment with 5nM OPN peptide (NT 109-153 (p)) was used as a positive control. Error bars represent standard deviation. * p value = <0.05 compared to OGD control.

3.8 Preconditioning with T_1AM, but not T_0AM confers protection against stroke injury.

To test whether T_1AM and T_0AM precondition the brain against ischemic injury via an antecedent stimulus of brief hypothermia, mice were given an ip injection of vehicle, T_1AM (50mg/kg) or T_0AM (50mg/kg) two days prior to 60 min MCAO. The body temperature of mice injected with T_1AM or T_0AM dropped within 30 minutes (Fig 3.4a) and animals remained hypothermic for 8 hours and were normothermic by the time of MCAO challenge. Mice preconditioned with T_1AM showed a significant reduction in infarct size (34%) compared to vehicle-treated animals. Mice preconditioned with T_0AM showed modest neuroprotection, which did not reach significance (Fig 3.4b). To test whether the effect of preconditioning with T_1AM depends on hypothermia, the T_1AM - induced drop in body temperature was blocked by maintaining the mice on a heating pad. Under these conditions, T_1AM administration failed to precondition mice and confer neuroprotection against stroke challenge given two days later. Thus, preconditioning with T_1AM appears to depend, in part, on hypothermia.

Figure 3.4 Preconditioning with T_1AM and T_0AM. Preconditioning with T_1AM but not T_0AM induces delayed tolerance to ischemic injury. **A)** Temperature reduction post injection with T_1AM and T_0AM. Mice were injected with 50mg/kg of T_1AM or T_0AM 2 days prior to MCAO. Temperature was measured for 8 hours post injection. In a separate group injected with 50mg/kg T_1AM, mice were prevented from becoming hypothermic by maintaining them on an adjustable heating pad and maintaining their temperature as close to that of vehicle injected mice as possible (T1AM hypothermia blocked). **B)** Infarct volume following T_1AM and T_0AM preconditioning treatment and T_1AM hypothermia blocked preconditioning treatment. N = 8 each group. Error bars represent standard deviation. * p value = <0.05 compared to vehicle injected.

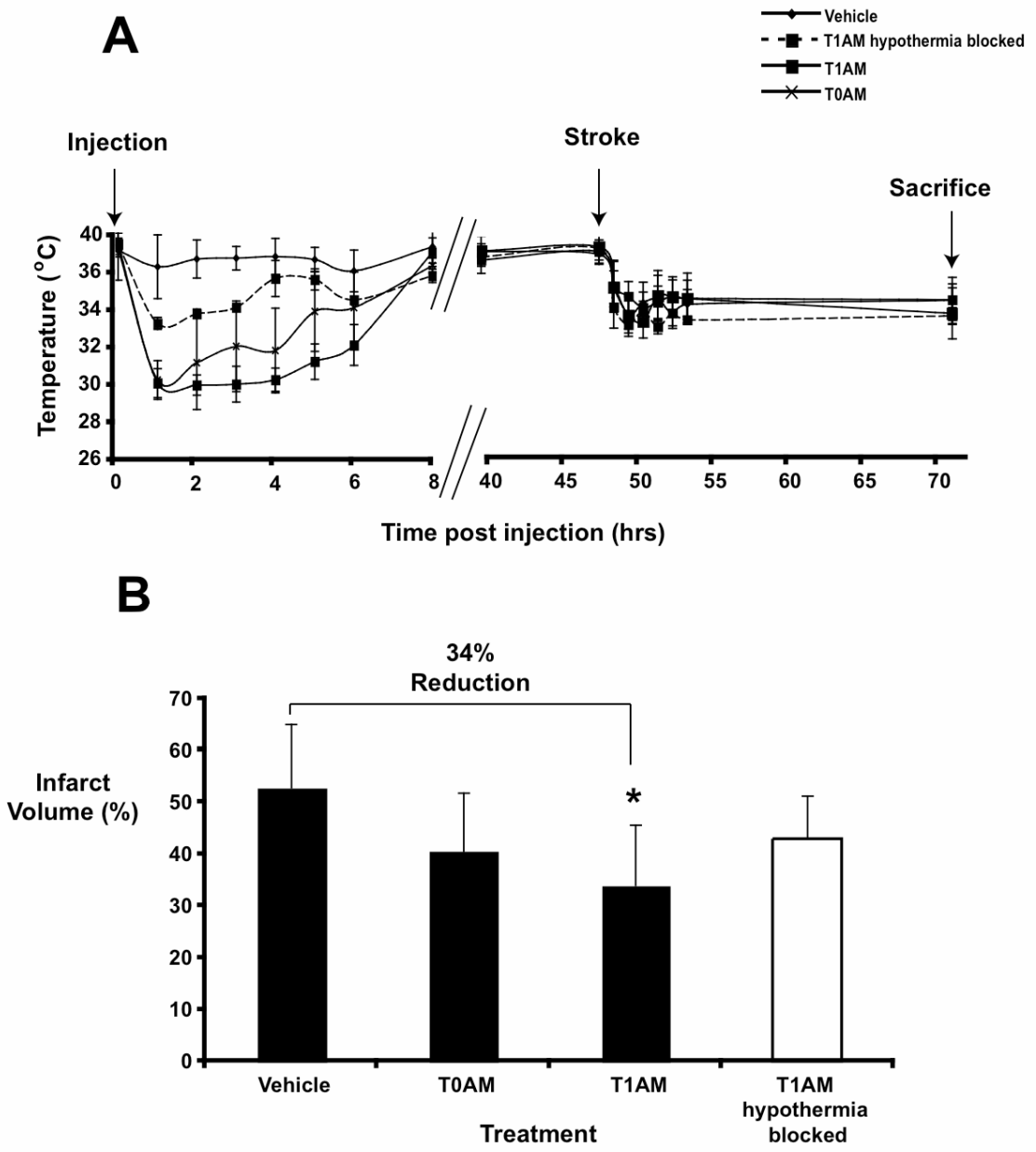
A
Vehicle
T1AM hypothermia blocked
T1AM
T0AM
Injection
Stroke
Sacrifice
Temperature (°C)
40
36
34
32
30
28
26
0
2
4
6
8
40
45
50
55
60
65
70
Time post injection (hrs)
B
34%
Reduction
Infarct
Volume (%)
70
60
50
40
30
20
10
0
*
Vehicle
T0AM
T1AM
T1AM
hypothermia
blocked
Treatment

3.9 Preconditioning administration of T_1AM and T_0AM *in vitro* does not confer neuroprotection against ischemic injury.

Further support for the requirement of hypothermia in T_1AM preconditioning was evinced by testing whether T_1AM pre-treatment of primary neuronal cultures induces protection against subsequent OGD-induced cell death. Primary mouse neuronal cultures were pretreated with doses of T_1AM and T_0AM ranging from 5nM to 500µM, two days before exposure to 3 hours OGD. None of the test doses of T_1AM or T_0AM was found to be protective (Fig 3.5).

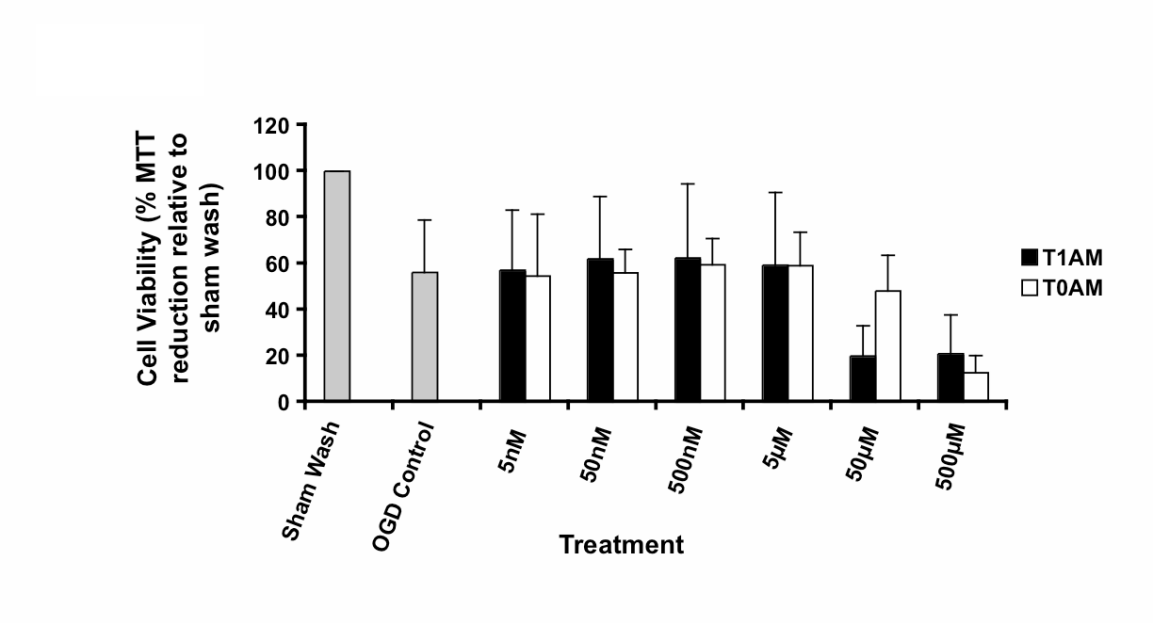

Figure 3.5 T_1AM and T_0AM preconditioning in vitro. Experiments performed on mouse primary neuronal cultures treated with the indicated doses of T_1AM and T_0AM 2 days prior to OGD. Cell viability assays were performed 24 hours post OGD (N=3). Error bars represent standard deviation.

3.10 Discussion

Physical hypothermia has been shown to be neuroprotective in various experimental paradigms of stroke [192-195]. Furthermore combining cerebroprotective drugs with hypothermia shows synergistic effects [192]. However, the application of physical hypothermia is technically challenging and may result in serious adverse side effects as a consequence of the body's homeostatic response. Drug induced hypothermia could serve as an alternative to physical hypothermia but depends on the identification of drug candidates with suitable pharmacodynamics. I have tested whether T_1AM and T_0AM could be applied as cryogens for the induction of therapeutic hypothermia as a treatment for stroke. I found that drug-induced hypothermia using T_1AM and T_0AM is protective against ischemic damage warranting further experiments looking at the effect of these drugs in primates.

I first tested whether ***acute*** administration of T_1AM and T_0AM could protect against ischemic damage via hypothermia. Mice were ip injected 1 hour post MCAO with a dose of T_1AM or T_0AM chosen for the ability to induce a putatively protective level of hypothermia in healthy animals. I found that both drugs were capable of conferring neuroprotection and by blocking the hypothermic actions of each drug I was able to verify that protection was due to hypothermia. I also tested each drug for the ability to protect against cell death *in vitro*, where the induction of hypothermia is not possible and found T_1AM and T_0AM do not confer neuroprotection.

A drawback of delayed tolerance is that for most preconditioning stimuli only a minor change in intensity or duration will lead to injury. For example, 1 minute of global ischemia is insufficient to elicit tolerance, whereas 2 to 5 minutes of ischemia elicits selective neuronal death [196]. This lack of a safety margin greatly reduces the therapeutic usefulness of ischemic preconditioning. However, hypothermia as a preconditioning stimulus is unique in that it has a broad safety margin [184]. Consequently hypothermia can serve as an effective preconditioning stimulus without presenting a direct risk to neurons. T_1AM treatment two days prior to ischemia provided significant protection from ischemic injury, an effect that was lost when the drop in body temperature was prevented. This suggests that T_1AM preconditioning protects the brain from ischemic injury as a result of the protective effects of hypothermia. In support of this hypothesis preconditioning administration of T_1AM to neurons in culture did not protect against OGD induced cell death.

In summary, these studies show that the thyronamines T_1AM and T_0AM confer protection against ischemic brain damage when administered acutely after stroke. In addition, this is the first demonstration that a cryogen (T_1AM) may be administered as a prophylactic therapy in situations of anticipated ischemic injury. T_1AM and T_0AM induce hypothermia—a condition which is required for these compounds to achieve their therapeutic neuroprotective effect in both acute therapy and preconditioning. The studies presented here using modeled ischemia *in vitro* support the requirement for hypothermia in T_1AM and T_0AM induced neuroprotection.

On the basis of the structural similarity between thyronamines and dopamine, it is conceivable that T_1AM and T_0AM activate a cognate thyronamine GPCR such as TAAR1, thus constituting a new signaling pathway that rapidly results in hypothermia. TAAR1 is a 7-transmembrane GPCR related to catecholamine and 5-hydroxytryptophan receptors. TAAR-1 is an excellent candidate receptor for T_1AM and T_0AM given the chemical similarity between thyronamines and biogenic amines, and because TAAR-1 belongs to the biogenic amine GPCR subfamily whose endogenous agonist remains to be established [189]. My studies do not address the specific ligand/receptor interactions of T_1AM or T_0AM; however, such information is of obvious importance to this field.

Intra-ischemic hypothermia remains the gold standard for therapeutic studies of potential neuroprotectants. However, cooling during ischemia is not usually possible, thus substantial effort has been directed towards the potential benefit of post-ischemic hypothermia [197]. Preclinical tests with hypothermic durations of 6 hours or more have demonstrated that post-ischemic hypothermia is effective and that the therapeutic window expands as the duration of hypothermia is increased; when cooling lasts for 48 hours, significant long term protection of CA1 hippocampal neurons can be achieved even when cooling is delayed by 12 hours [198]. Here I have shown that T_1AM and T_0AM can confer neuroprotection when treatment is delayed by 1 hour and it is likely that the time window available for T_1AM and T_0AM administration will mirror the time window available for other hypothermia treatments.

Post-ischemic hypothermia can also be used to extend the time window available for administering additional neuroprotective agents. Mild post-ischemic hypothermia has been used successfully in rats to prolong the therapeutic window for Bcl-2 gene therapy from 1.5 to 5 hours [199]. Thus, acute administration of T_1AM and T_0AM could be a means of extending the time window available for administration of other neuroprotectants.

I have shown that T_1AM provides antecedent protection to ischemia--an effect that requires hypothermia. This suggests that T_1AM triggers hypothermia-induced tolerance to ischemia. Hypothermia-induced ischemic tolerance is initiated within 6 hours, peaks at approximately 1 or 2 days and is reversed by 7 days after preconditioning stimulation [184]. It is likely that a hypothermic threshold must be reached for successful preconditioning to occur. My findings support this possibility as T_0AM failed to induce the same depth and duration of hypothermia as T_1AM and failed to confer antecedent protection to ischemia. This is also supported by a recent study by Yunoki et al, where the magnitude of tolerance induced by hypothermic preconditioning was shown to depend on the depth and duration of the hypothermic stimulus [200].

While there is precedence for investigating the neuroprotective effect of drug-induced hypothermia, the studies presented here are the first to apply endogenous molecules to induce hypothermia as a treatment for stroke. The synthetic cannabinoid HU-120 has been used to induce hypothermia and protect against ischemia in rats [201]. However, at doses that induce hypothermia, HU-120 has toxic side effects that limit its application for humans. Other studies with hypothermia-inducing cannabinoids have been more

encouraging. The synthetic cannabinoid WIN 55,212-2 can induce therapeutic hypothermia with fewer side effects than H

U-120, however effective treatment with WIN 55,212-2 requires continuous intravenous infusion for the hypothermic effect to be maintained [202]. A recent study demonstrates that hydrog

en sulfide can be used to reduce temperature in rodents [203], however this approach may have limited benefit in brain ischemia as hydrogen sulfide enhances NMDA receptor function, which could lead to increased excitotoxicity [204].

HU-120 and WIN 55,212-2 appear to induce hypothermia by binding directly to hypothalamic CB1 receptors and altering the homeostatic temperature set point [202]. Hydrogen sulfide likely induces hypothermia less specifically, via inhibition of complex IV in the electron transport chain which causes global hypometabolism [203]. I postulate that T_1AM and T_0AM induce hypothermia in a manner that more closely resembles the synthetic cannabinoids, working through a specific receptor, such as TAAR1, and inducing anapyrexia (regulated hypothermia).

In conclusion, T_1AM and T_0AM can be used to induce a therapeutic level of hypothermia and, because both are endogenous metabolites of thyroxine, they may be tolerated with fewer side effects than artificially engineered compounds. These unique molecules have developmental potential as cryogens for the treatment of stroke, where rapid and prolonged cooling offers outstanding therapeutic benefit to patients.

CHAPTER 4

COMBINING ACUTE AND ANTECEDENT THERAPY

INTRODUCTION

4.1 An introduction to combinatorial therapy

Stroke is a heterogeneous disorder with a complex pathophysiology. It can be ischemic or hemorrhagic, involve small or large blood vessels and be exacerbated by hypotension, fever and hyperglycemia. It is influenced by age, gender, racial background, comorbibities and concurrent medications. Cell death following stroke results from the complex interplay of excitotoxicity, acidosis, inflammation, oxidative stress, peri-infarct depolarization and apoptosis. In light of this complexity, it is likely that effective stroke therapy will require a combinatorial approach such as has been used successfully for the treatment of cancer, HIV infection, and tuberculosis.

The fact that no single drug class has proven efficacious in humans also argues that effective stroke therapy will require a combinatorial approach. Several experimental studies of combination drug therapy for stroke have shown that drugs that target different pathways can act together to have a synergistic or additive effect. For example tirilazad mesylate, a scavenger of free radicals, has been successfully combined with MK-801, a glutamate receptor antagonist. Tirilazad mesylate has also been successfully combined with insulin, which reduces hyperglycemia following acute stroke and diazepam, a GABA-ergic drug that inhibits nitric oxide formation in the brain. Nimodipine, a calcium channel blocker, has been successfully combined with MK-801. FGF, which strengthens antiapoptotic pathways in neurons has been successfully combined with citicoline, an

essential intermediate in the biosynthetic pathway of neuronal membranes that inhibits membrane phosphlipases and can restore Na+/K+ ATPase function [205-211]. Additional studies have shown that the effect of a single drug can be enhanced or the time window available for administration extended if applied in combination with hypothermia. For example Matsumoto et al found synergistic effects of s-emopamil, which reduces brain edema, and nimopidine with hypothermia and Zhao et al used hypothermia to extend the time window available for Bcl-2 gene therapy [182, 199, 212, 213].

The mechanisms by which acute and antecedent therapies confer neuroprotection are quite different. This is evinced by the fact that many antecedent neuroprotectants are actually harmful if administered acutely. For example TNFα can be used to precondition against ischemic injury but will worsen outcome if administered immediately post stroke [38, 77, 214]. In light of this difference in mechanism there is the possibility that combining acute and antecedent neuroprotection will have an additive or synergistic effect.

No such combinatorial experiment has been published and is particularly relevant for the large number of patients scheduled for cardiac artery bypass surgery. These patients could be treated in the days leading up to surgery with a preconditioning stimulus such as T_1AM, and acutely during, or just after surgery with OPN. In such a patient population 50% of patients suffer cognitive decline post surgery, presumably as a result of intraoperative emboli, and so such a combinatorial approach could of enormous benefit.

4.2 Hypothesis

That OPN and T_1AM confer neuroprotection via two distinct mechanisms offers the possibility that when used in combination an additive or even synergistic neuroprotective effect may result. Therefore, I hypothesize that treatment with T_1AM and OPN will result in greater neuroprotection than treatment with either molecule alone.

4.3 Research Design

I tested the effect of antecedent administration of T_1AM 2 days prior to stroke and acute nasal administration of an OPN peptide mimetic (peptide 109-153 (p)) during stroke.

4.4 Results

To determine whether acute treatment with OPN and antecedent treatment with T_1AM would be more neuroprotective than either treatment alone, mice were injected ip two days prior to surgery with T_1AM (50mg/kg) or vehicle (100µl volume) and temperature was monitored for 6 hours post injection. Two days later intranasal administration of OPN peptide 109-154 (p) or vehicle was performed ten minutes after initiating 60 minute MCAO. Mice were administered 50µl per mouse of OPN peptide or vehicle, given in nose drops (5µl/drop) over a 20 minute period (total OPN dose = 857ng). Intraperitoneal injection of 50mg/kg of T_1AM 2 days prior to MCAO induced profound hypothermia (Fig 4.1). T_1AM treatment alone reduced infarct volume by 27.5% compared to vehicle injected animals. Intranasal administration of peptide 109-153 (p) during MCAO was also neuroprotective and reduced infarct volume by 53.02% compared to vehicle treated animals. Treatment with both T_1AM preconditioning and acute administration of peptide 109-153 (p) reduced infarct volume by 63.56% compared to animals that were treated with vehicle alone. While this amount of neuroprotection is greater than treatment with peptide 109-153 (p) alone, or T_1AM alone, the increase is not significant.

Figure 4.1 Antecedent administration of T_1AM 2 days prior to stroke and acute nasal administration of an OPN peptide mimetic (peptide 109-153 (p)) during stroke. Mice were ip injected with T_1AM or vehicle two days prior to 60 minute MCAO. Mice were intranasally administered peptide 109-153 (p) or vehicle 10 minutes after initiating MCAO **A.)** Temperature following ip injection of T_1AM or vehicle. Data shown are mean + SEM. **B.)** Infarct volume 24 hours following MCAO visualized by TTC staining. Data shown are mean + SD. * p value < 0.05 compared to Veh/Veh treated, n = 8 per group, numbers above each bar refer to % reduction in infarct volume associated with each treatment.

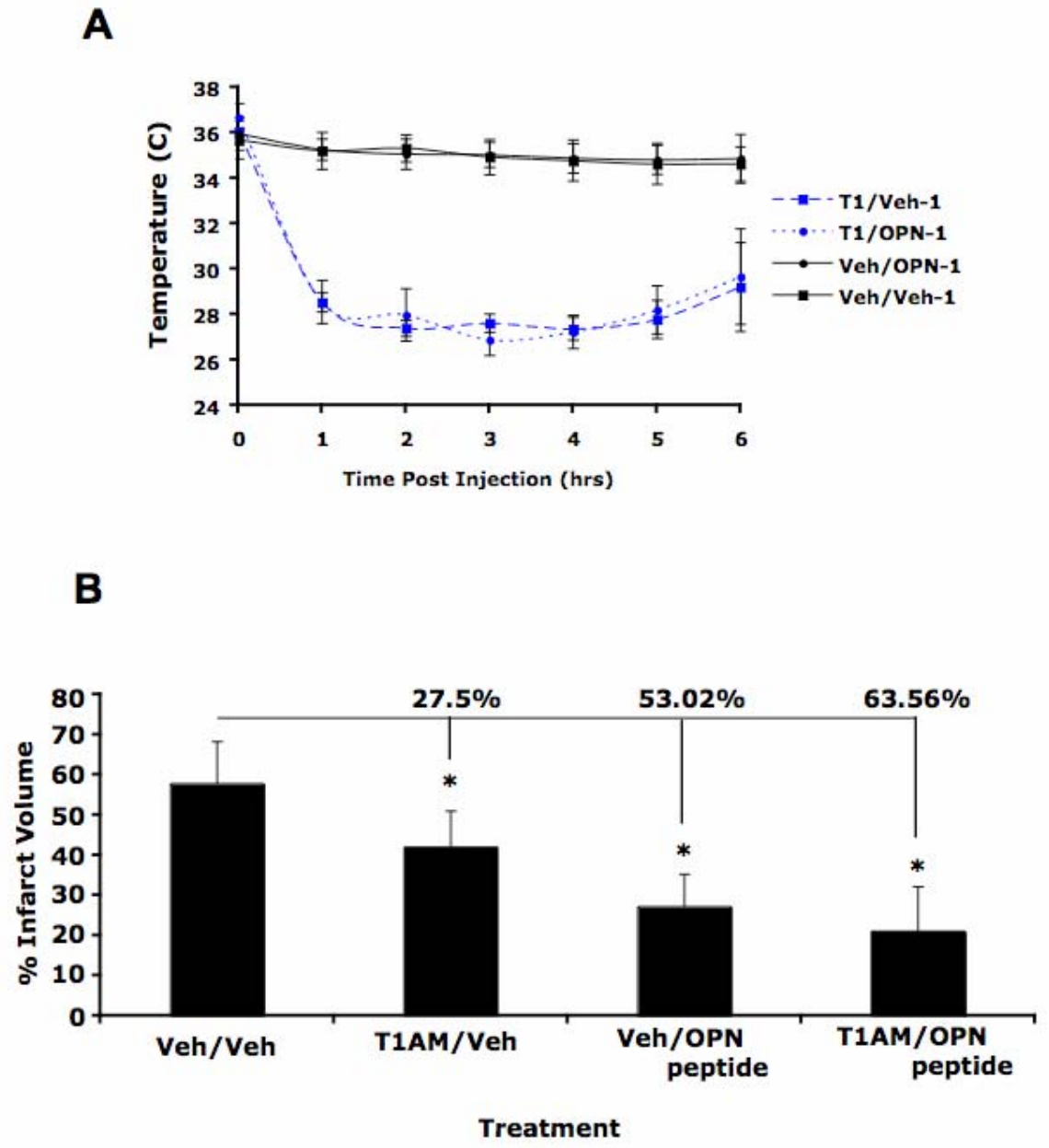
A
Temperature (C)
38
36
34
32
30
28
26
24
0
1
2
3
4
5
6
Time Post Injection (hrs)
T1/Veh-1
T1/OPN-1
Veh/OPN-1
Veh/Veh-1
B
% Infarct Volume
80
70
60
50
40
30
20
10
0
27.5%
53.02%
63.56%
*
*
*
Veh/Veh
T1AM/Veh
Veh/OPN peptide
T1AM/OPN peptide
Treatment

4.5 Discussion

Deep systemic hypothermia will cause increased peripheral vascular resistance, increased cardiac afterload, bradycardia, acidosis, increased blood viscosity, cerebrovascular constriction and abnormalities in blood coagulation [215, 216]. Taking into consideration both the side effects and the unrivaled neuroprotective proficiency of hypothermia an attractive means of employing hypothermia therapy is to use hypothermia as an antecedent stimulus that can be combined with an acute neuroprotectant that has fewer side effects. Accordingly I combined antecedent treatment with T_1AM with acute treatment with OPN. Such a strategy would benefit patients scheduled to undergo cardiac artery bypass surgery. In such a patient population, 50% of patients suffer cognitive decline post surgery as a result of intraoperative emboli. Such a patient population would better tolerate side effects that result from hypothermia by applying hypothermia at a time point remote to surgery. During surgery however, there are no contraindications that would preclude intranasal administration of OPN mimetics.

Antecedent hypothermia, induced by T_1AM, caused a reduction in infarct volume of 64% when combined with intranasal administration of an OPN mimetic (peptide 109-154 (p)). When the peptide was used alone there was a reduction in infarct volume of 53% and when hypothermic preconditioning alone via injection of T_1AM, was applied there was a reduction in infarct volume of 27%. Although combined administration of an OPN mimetic with hypothermic preconditioning may be more effective than either treatment alone, the increase in protection observed in this experiment was not statistically

significant, therefore, although outcome appears improved in the combined treatment group my data does not confirm my primary hypothesis.

Despite the lack of evidence of an additive or synergistic protective effect of OPN combined with T_1AM, this experiment provides evidence that acute and antecedent therapy used in combination does not exacerbate stroke injury. Additionally, previous studies have shown that a common outcome of combinatorial therapy is that neuroprotective drugs become effective at lower doses, obviating the need for elevated dosage or repeat administration. This could arise from the fact that a drug that targets an early mechanism of damage, such as the release of glutamate, could dampen the activation of later pathological mechanisms that may be targeted by additional drugs. The failure of several neuroprotective trials has been attributed to dose limiting toxicity and a repeat of this experiment could reveal that the combination used here permits a lower dose of an OPN peptide mimetic to be administered.

On the basis of the complexity of events in cerebral ischemia and the disappointing results from single-agent trials, it may be unrealistic to expect that a single neuroprotective drug will demonstrate benefit in humans. Rather, effective neuroprotection may require rational combinatorial therapy that combines drugs with different mechanisms of action. In the future there will likely be others that challenge the particular strategy of combined therapy I have tested here, and I believe that ultimately this approach will lead to a benchmark breakthrough for the treatment of stroke.

CHAPTER 5

PERSPECTIVES

There is an urgent need for development of stroke treatments as currently there are no neuroprotective drugs available for stroke patients. Many of the reasons that explain the difficulty in advancing drugs have been discussed in earlier chapters. However, one of the most concerning reasons for past failure of neuroprotective drugs is a lack of quality control in preclinical research. Many past studies have not implemented operating procedures that limit the generation of false positive or false negative results. For example many prior studies have not been randomized or blinded and have failed to set proper inclusion and exclusion criteria. The use of inappropriate statistics and inadequate control of physiological parameters have also plagued numerous studies [217].

Past studies have also failed to develop a method of drug delivery during the early stages of preclinical development that would be viable for humans. Drugs have failed repeatedly because they cannot pass through the BBB or because blood flow is too low in the ischemic territory to allow adequate delivery and dispersal. Intranasal administration bypasses these problems of delivery that have beset other neuroprotective drugs and represents a milestone for the preclinical development of OPN. Delivery may be less of a problem for the preclinical development of T_1AM because T_1AM does not appear to act on the CNS to induce hypothermia. I have found that intranasal administration of T_1AM does not result in hypothermia and my collaborators Dr David Grandy and Dr Thomas Scanlan report that icv administration of T_1AM also does not result in hypothermia (unpublished observations). This suggests that T_1AM acts in the periphery.

Data from several trials suggest that the degree of therapeutic benefit of a neuroprotectant is directly related to the promptness of treatment, however it is extremely difficult to provide treatment for many stroke patients within the first three hours after the onset of symptoms. Therefore, the time window for penumbral survival needs to be extended. One method by which this could be done is by initiating therapies that do not require imaging or precise stroke subtyping before patients reach the hospital. The induction of hypothermia with a cryogen such as T_1AM could be performed in the ambulance on route to the emergency room and is one method by which this could be achieved. Therefore, not only is T_1AM neuroprotective in its own right, it could also enable the neuroprotective potential of other drugs.

My studies with OPN show that there are at least two neuroprotective peptides contained within the parent molecule. An exciting direction for future preclinical research with OPN will be to test chimeric peptides that are comprised of sequences from both CT 154-198 (p) and NT 134-153. For example, a chimeric protein that consists of the RGDSLAYGLR sequence of NT 134-153 attached to the C terminal end of peptide CT 154-198 (p) may provide neuroprotection by ligating integrin receptors and CD44 and result in greater neuroprotection than using either peptide alone. This chimeric peptide combines the CD44 binding sequence of OPN with the RGDSLAYLGR sequence in the post thrombin cleavage orientation, thus representing an OPN like molecule that has been optimized for use as a stroke treatment. An advantage of combining the two peptides into a single molecule is that it is unclear at this time whether the US Food and Drug

Administration will allow a stroke trial with two unapproved drugs. Combining the two peptides creates a monotherapy that may have multiple effects on the ischemic cascade.

There are additional measures that can be taken to increase the likelihood of success of OPN and T_1AM therapies for stroke. For example both drugs would benefit by evaluation in a non-human primate stroke model prior to testing in humans. A primate trial benefits human trial design by enabling a more accurate estimation of cohort size than is possible from a rodent model alone. Additionally, if OPN or T_1AM fail to confer neuroprotection in a non-human primate then there is leeway to discover the reason for failure and adapt the treatment paradigm accordingly.

T_1AM is likely to reduce temperature at a slower rate in primates than in rodents. Our observations from rats support this contention where we find that although rats respond to T_1AM and T_0AM by lowering body temperature, the rate of reduction is slower than in mice. This is due to the larger size and greater thermal inertia of rats and means that T_1AM may need to be complemented with a physical means of initially reducing temperature in primates. However, even if T_1AM is only used to maintain hypothermia in humans it could still be of enormous benefit to patients by reducing the need for general anesthesia during prolonged hypothermia therapy. Currently general anesthesia is the greatest problem for hypothermia therapy due to the accompaniment of respiratory arrest, reduced blood pressure, unresponsiveness, and EEG suppression. Thus, respiratory control and drugs for stabilizing blood pressure are necessary, a bedside evaluation of neurologic state is impossible and frequent CT scans are required.

A non-human primate trial will also reveal the bioavailability, toxicity and pharmacokinetics of OPN and T_1AM in a species more closely related to humans. This will facilitate dose selection for a human trial and could reveal sooner potential contraindications that would preclude using either one of these drugs in humans.

Combination therapy maximizes opportunites for tissue salvage and represents a promising new direction for stroke research. Here, I tested one means of combining OPN and T_1AM, using T_1AM as an antecedent therapy and OPN as an acute treatment. Although this experiment did not reveal an additive or synergistic effect, combining these drugs in a different way may yet prove efficacious. For example, T_1AM may prove effective as a means of extending the time window available for OPN administration. Alternately, T_1AM could be used simultaneously with OPN to target multiple pathways of acute neuroprotection concurrently.

In conclusion I have demonstrated that OPN and T_1AM both have the ability to ameliorate injury following stroke and have performed preclinical experiments to advance each towards clinical trial. OPN peptide NT 124-153 and T_1AM are now at a stage where they could be tested in a primate model of stroke and it is here that their full potential as a treatment for stroke in humans will likely be revealed.

CHAPTER 6

MATERIALS AND METHODS

Mice

C57Bl/6 mice (male, 8-10 wks, 20-24g) were obtained from the National Cancer Institute or from Jackson Laboratories. All procedures met NIH guidelines with the approval of the Oregon Health & Science University Institutional Animal Care and Use Committee.

Recombinant mouse OPN

Osteopontin was obtained from EMD Biosciences /Calbiochem, San Diego, CA, USA, Cat. No. 499260. This OPN is produced by the NSO murine myeloma cell line. For all experiments OPN was dissolved in artificial cerebrospinal fluid.

Peptides

OPN peptides were custom synthesized by Invitrogen (Carlsbad, CA, USA) or Genscript (CA, USA). Phosphorylated residues are indicated by: S(p) or T(p). A schematic diagram of OPN and the location of peptides NT 109-153 (N terminal) and CT 154-198 (C terminal) within the full-length sequence is shown in Figure 3.9. **Peptide sequences are as follows:**

NT 109-153 (p)

S(p)DES(p)HHS(p)DES(p)DETVTASTQADTFTPIVPTVDVPNGRGDSLAYGLR

NT 109- 153

SDESHHSDESDETVTASTQADTFTPIVPTVDVPNGRGDSLAYGLR

NT 124- 153

ASTQADTFTPIVPTVDVPNGRGDSLAYGLR

NT 134-153

IVPTVDVPNGRGDSLAYGLR

CT 154 –198 (p)

SKSRSFQVSDEQYPDAT(p)DEDLTS(p)HMKS(p)GESKESLDVIPVAQLLSM

CT 154 –198

SKSRSFQVSDEQYPDATDEDLTSHMKSGESKESLDVIPVAQLLSM

SCRAMBLED (scrambled sequence of NT 109- 153)

NVPGDVVITPDSEHSGLDSRAAQTSSEDHSGAYRLFPDTTTVDET

T_1AM and T_0AM

T_1AM and T_0AM were obtained by chemical synthesis as previously described and dissolved in 75% saline/25% DMSO at a concentration of 12.5mg/ml [218].

An in vitro model of ischemia: Oxygen and Glucose Deprivation

To determine whether OPN and T_1AM are neuroprotective, one of the methods I employed was an *in vitro* model of ischemia, oxygen-glucose deprivation (OGD). This model utilizes mouse or rat cortical neuronal cultures (60-70% neurons) that when exposed to 180 minutes or 120 minutes of OGD respectively, show 45-60% cell death as assessed by propidium iodide (PI) staining or MTT assay. Following exposure to OGD a subset of cells within this culture system show shrunken cell bodies and nuclei (Fig 6.1a). In contrast, other cells have classic apoptotic features, such as blebbing of nuclei and packaging of cellular contents (Fig 6.1a). Cells with each of these types of morphology stain positive for propidium iodide (Fig 6.1a). Within the culture there is also a robust increase in cleavage of the cell death pathway associated protein, caspase 3 (Fig 6.1b)

and cell death can be reduced by the caspase 3 inhibitor Ac-DEVD-CHO (10 μM) (Fig 6.1c). These data suggest that following OGD cells within this model die by apoptotic and necrotic cell death mechanisms, similar to the response to injury that occurs in the ischemic penumbra, the target of neuroprotection research.

Figure 6.1 Effect of 120 minutes of OGD on neuronal cultures. a) Light microscopic images of control and OGD-treated cells showing different morphologies of cell death. Cells were stained with PI and then counterstained with DAPI. Images were taken using a 40 x objective (scale bar = 10 μm). b) Increased cleavage of caspase 3 following 120 minutes of OGD, as determined by western blotting. There is an increase of caspase 3 cleavage fragment 6 hours following 120 minutes of OGD. Data shown is a representative blot of 3 independent experiments. c) Cell death following 120 minutes of OGD is reduced by the caspase 3 inhibitor Ac-DEVD-CHO. Cells were incubated with Ac-DEVD-CHO (10 μM) for 24 hours prior to OGD. Data shown are mean ± SD (n=5) ** denotes $P < 0.01$ vs. effect of 120 minutes of OGD alone (one-way ANOVA with Bonferroni's post hoc test). These experiments appear in our paper titled "Neuroprotection by Osteopontin in Stroke". [119]

a

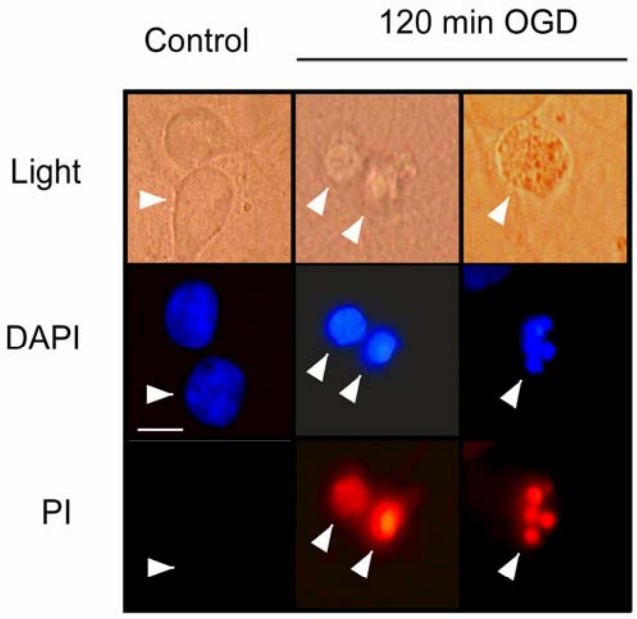
Control
120 min OGD
Light
DAPI
PI

b

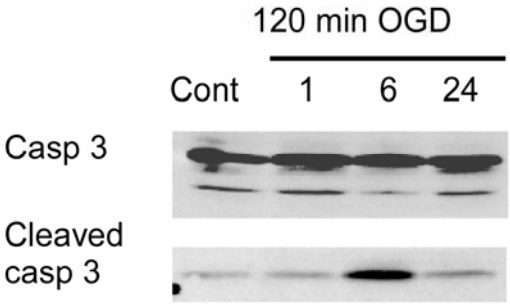
120 min OGD
Cont
1
6
24
Casp 3
Cleaved
casp 3

c

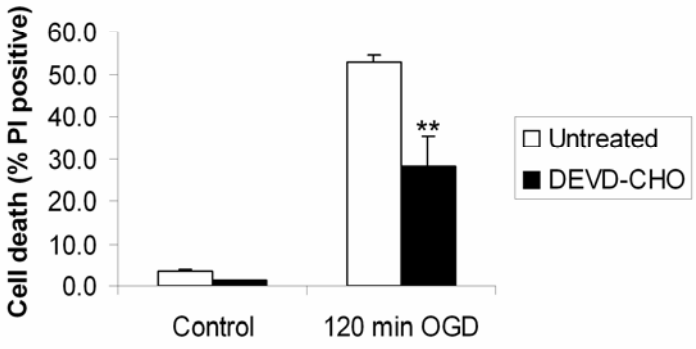
Cell death (% PI positive)
60.0
50.0
40.0
30.0
20.0
10.0
0.0
**
Untreated
DEVD-CHO
Control
120 min OGD

Rat Neuronal cell culture

Cortical neuronal cultures were prepared from 1 day old Sprague Dawley rat pups using the method of Goslin [219] as previously described [220]. Briefly, cortices were dissected from 10-12 rat pups, dissociated with papain (Worthington Biochemicals, Lakewood, NJ, USA) and grown in Neurobasal-A/B27/glutamax media (Invitrogen, Carlsbad, CA, USA) for 7 days, when cultures consist of ~60% neurons as assessed by NeuN staining. Cells were plated out at a density of 500,000 cells per coverslip (for cell staining), 50,000 cells per well (for cell viability assays) and 5,000,000 cells per 10 cm culture dish (for western blotting).

Mouse Neuronal cell culture

Cortical neuronal cultures were prepared from anesthetized E16 C57BL/6 mice. Cerebral cortices were dissected and incubated in 0.05% (wt/vol) trypsin-EDTA for 15 minutes at 37^{o}C. Tissue was then triturated and cells plated on poly-L-ornithine coated 96-well plates or 25mm x 25mm glass coverslips at a density of 50,000 per well or 500,000 per coverslip. Cells were cultured in Neurobasal medium supplemented with L-glutamine and B27. Cultures consisted of 50-60% neurons as assessed by NeuN staining on glass coverslips. Oxygen and glucose deprivation was performed on day 7 of culture using cells in 96 well plates.

Oxygen and glucose deprivation

Oxygen and glucose deprivation (OGD) was performed by washing the cells with phosphate buffered saline (PBS) (0.5 mM $CaCl_2$, 1.0 mM $MgCl_2$; pH 7.4) and placing

culture dishes in an anaerobic chamber for 120 minutes for rat cultures and 180 minutes for mouse cultures (Coy Laboratories, USA);(85 % N_2, 5% H_2, 10 % CO_2; 35 ºC). OGD was terminated by removing cells from the chamber, replenishing with Neurobasal A media and replacing them back into the normoxic incubator.

Propidium Iodide cell death assay

Twenty four hours following OGD coverslips containing cortical cells were incubated with propidium iodide (1.5 µg/ ml) for 2 minutes, washed with PBS and fixed with 4% formaldehyde. Cells were then mounted onto glass slides using Vectashield mounting medium containing 4',6-diamidino-2-phenylindole (DAPI) (Vector Labs, Burlingame, CA, USA). Cell viability was determined as the ratio of propidium iodide-stained cells to the total number of DAPI-stained cells, visualized using a fluorescence microscope (Leica GMBH, Bannockburn, IL, USA).

MTT cell viability assay

Twenty four hours following OGD cells were incubated in 200µl MTT solution (0.5 mg/ml in media) for 1 hour at 37°C. Incubation was stopped by removing media and adding 100µl of DMSO. Absorbance was read at 550 nm. Data are expressed as percentage of cell death compared to control cultures that did not undergo OGD.

OPN treatment of in vitro cultures

Mouse recombinant OPN (0.01-1.0 µg/ml) was added to media and incubated with cells for either 24 hours prior to, or 24 hours following 120 minute OGD. To probe the biochemical basis for neuroprotection by OPN LY294002, U0126 (both 10 µM);(Cell

Signaling Technology, Beverly, MA, USA), cycloheximide (1.0 μM);(Sigma, St. Louis, MO, USA) and GRGDSP (10 nM);(Sigma-Genosys, The Woodlands, TX, USA) were incubated with cells for 10 min prior to addition of 0.1 μg/ml OPN (5nM) to the cultures. For testing the effect of treatment of OPN with thrombin cells were treated with thrombin treated OPN (5nM) or untreated OPN (5nM) for 24 hr post 120 min OGD. For testing the neuroprotective potential of OPN peptides cells were treated with 5nM intact OPN, or an equimolar dose of the indicated peptide for 24 hr post 120 min OGD.

Western blotting from neuronal cultures

Western blotting was performed as previously described [221]. Tissue samples were lysed in a nondenaturing buffer containing the protease inhibitors phenylmethylsulfonylfluride (100 μg/ ml), aprotinin (1 μg/ml), leupeptin (1 μg/ml), pepstatin (1 μg/ml), NaF (50 mM) and Na_3VO_4 (2 mM). Protein concentration was determined by Bradford reagent spectrophotometrically at A^{595}. Protein samples (50 μg) were denatured in a gel-loading buffer at 100°C for 5 min and then loaded onto 12% SDS-polyacrylamide gels. Proteins were transferred to polyvinylodene difluoride membranes and incubated with primary antibodies at 4 ^{o}C overnight; anti-phospho-Akt, anti-phospho p42/p44 MAPK, full length and cleaved caspase 3 (Cell Signaling Technology, Beverly, MA, USA), α-tubulin (Santa Cruz Biotechnology, Santa Cruz, CA, USA). Membranes were incubated with anti-rabbit or anti-mouse IgG conjugated to horseradish peroxidase (Cell Signaling Technology, Beverly, MA, USA) followed by chemiluminesense detection (NEN Life Science Products, Boston, MA, USA) and then exposed to Kodak film (Biomax). Images were

captured using a Dage 72 camera and gel bands analyzed using gel scanning integrated optical density software (Bioquant, Nashville, TN, USA).

Thrombin cleavage of OPN

Recombinant mouse OPN (800ul at 100µg/ml) (EMD Biosciences /Calbiochem, San Diego, CA, USA) was mixed with thrombin agarose beads (100ul) (Thrombin CleanCleave Kit, Sigma) for 72 hr at 37^{o}C with shaking. Removal of thrombin was achieved by centrifugation (500xg for 5 min) and collection of the supernatant. The supernatant was purified further via passage through a 0.2um filter-that removed any remaining thrombin agarose beads (diameter of 45µm) and allowed OPN and its cleaved fragments to pass through. Thrombin is covalently bound to the agarose beads with no detectable leakage of thrombin from the beads with a detection limit of <5 picomoles/ml, thus the cleaved fragments were not contaminated with residual thrombin.

Western blotting of recombinant mouse OPN treated with thrombin

Protein was denatured in a gel-loading buffer at 100°C for 5 min and then loaded onto a 12% SDS-polyacrylamide gel. Protein was then transferred to a polyvinylodene difluoride membrane and incubated with primary goat anti-mouse OPN antibody (Sigma, Saint Louis, MO, USA) at 4^{o}C overnight. Membranes were rinsed and incubated with donkey anti-goat IgG conjugated to horseradish peroxidase followed by chemiluminesence detection (NEN Life Science Products, Boston, MA, USA).

Adhesion assay with HEK 293 Cells

96 well plates were coated with recombinant mouse OPN (thrombin treated or untreated) at 2µg/ml in phosphate buffered saline (PBS) overnight at 4^oC. Plates were washed three times with PBS and blocked with 200ul/well of PBS-0.5% BSA at room temperature for 1hr. HEK 293 cells were plated in adhesion buffer (PBS, 50mM HEPES, 0.1% BSA, 0.1% glucose 0.05mM $MnCl_2$) at a density of $1x10^5$ cells per well. Cells were incubated at 37^o for 45 min and then washed in PBS to remove non-adherent cells. Sigma FAST p-nitrophenylphosphate (50 ul) was added to each plate for 2 hr at 37^oC and plates were read at 405nM. The percentage of cells remaining in each well (adherent cells) was calculated using a standard curve generated from a control plate containing known quantities of cells in each well ranging from 0-250,000. The experiment was performed three times and the results averaged.

An in vivo model of ischemia: Middle Cerebral Artery Occlusion

To model stroke *in vivo* I employed a model of focal ischemia, MCAO (Fig 6.2). This technique involves transecting the external carotid artery, temporarily tying off the common carotid artery and using the external carotid artery to pass a suture through the internal carotid artery to occlude the junction of the anterior and middle cerebral arteries. The suture can be left in place for a variable duration of time and then removed to allow reperfusion. This technique does not require craniotomy, models focal occlusion of a large cerebral artery, and can be done with a high throughput approach. MCAO causes cell death in striatum and overlying frontal, parietal, temporal, and occipital cortex, but also variable damage in the thalamus, cervicomedullary junction, substantia nigra, and

hypothalamus. Occlusions of the middle cerebral artery represent the most typical type of stroke that is seen in human patients. In addition the MCAO model provides the advantages that it gives infarcts of consistent and reproducible size and provides latitude for infarct size to be increased or decreased depending on the negative or positive effect of a drug candidate being tested [143].

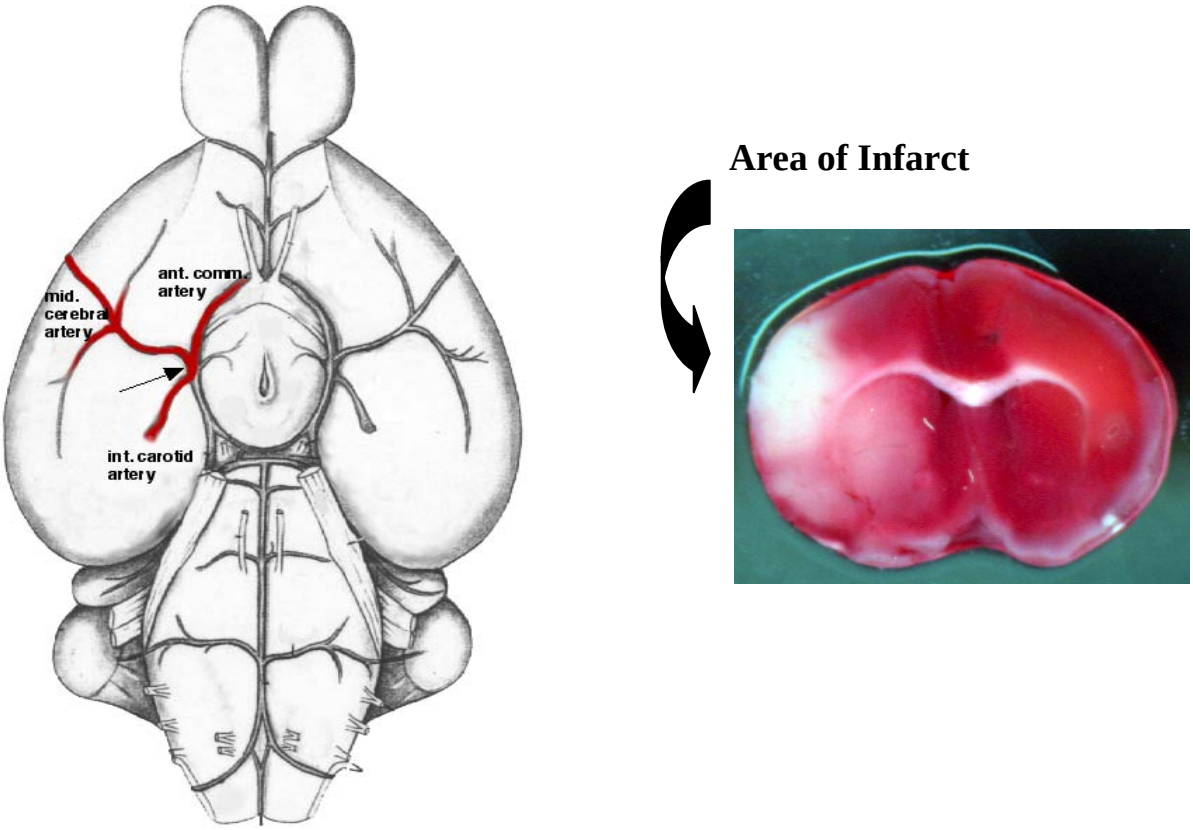

Figure 6.2 The MCAO model. The middle cerebral artery is occluded by a suture. This provides a transient blockade. When the suture is removed reperfusion occurs. The infarcted region (appearing white) can be measured by triphenyltetrazolium chloride (TTC) staining 24, 72 or 96 hrs following stroke.

Surgery

Cerebral focal ischemia was induced by middle cerebral artery occlusion (MCAO) as previously published [222]. Briefly, mice were anesthetized by halothane inhalation (4%/ l O_2) and maintained with 1.5%/ l O_2. The middle cerebral artery was blocked by threading silicone-coated 7-0 monofilament nylon surgical suture through the external carotid to the internal carotid and finally blocking its bifurcation into the MCA and anterior cerebral artery. The filament was maintained intraluminally while the mice were maintained under anesthesia. The filament was then removed, thereby restoring blood flow. Cerebral blood flow (CBF) was monitored throughout the surgery by laser Doppler flowmetry (Periflow 5000; Perimed, Sweden). Body temperature was monitored throughout surgery using a rectal thermometer (Hi-Lo Temp 8200 Patient Temperature Monitor, Sensortek Inc, Lake forest, CA, USA). Following surgery, mice were kept on a thermal barrier pad with free access to soft food and were sacrificed after either 24, 72 or 96 hours.

Infarct measurement

Mice were deeply anesthetized with isoflurane, then perfused via the ascending aorta with saline, containing 2 U/ml heparin at a flow rate of 9 ml/ min. Brains were rapidly removed, placed on a tissue slicer (Stoelting, Wood Dale, IL, USA) and covered with soft agarose. The olfactory bulb and cerebellum were removed and discarded. The remaining brain was sectioned into 1 mm slices beginning from the rostral end. To visualize the region of infarction, sections were placed in 1.5% 2,3,5-triphenyltetrazolium chloride (TTC) in 0.9% phosphate-buffered saline and stained for 15 min at 37°C [223]. After

staining, the sections were transferred to 10% paraformaldehyde. Images of the sections were scanned, and the area of the infarct and the ipsilateral hemisphere were measured using NIH image 1.62 or ImageJ software. The measurements were multiplied by the section thickness (1mm) and then summed over the entire brain to yield volume measurements. Ischemic damage data are presented as percent injury of the ipsilatateral hemisphere [(infarct volume)/(ipsilateral hemisphere volume) x 100] rather than absolute volume. This equation corrects for hemispheric edema, which is found in both infarcted and healthy tissue within the ipsilateral hemisphere [224]. This direct infarct assessment method is appropriate for *percent* infarct volume measurements as presented herein whereas the indirect method [225] is used for *absolute* measurements of infarct size (i.e. mm3).

Intracerebral ventricular injections

OPN, human albumin (ZLB Bioplasma AG, Berne, Switzerland) or vehicle (artificial cerebrospinal fluid (aCSF)) was injected into the left lateral ventricle (coordinates: 0 mm bregma, 1 mm lateral, and 2.5 mm ventral) using a 27 gauge needle. Total injection volume was 1ul per mouse.

Temperature measurement following OPN administration

Body temperature was measured at 3, 6, 24, 48, 72 and 96 hours following icv administration of OPN (5µg/kg) or vehicle. In a second group of animals, body temperature was measured at 1, 3, 6, 24 and 48 hours following administration of either aCSF or OPN in mice subjected to MCAO.

Blood glucose measurement following OPN administration

Blood glucose was measured (One Touch SureStep, Lifescan, Milpitas, CA, USA) 1 hour and 24 hours following icv administration of OPN (5µg/kg) or aCSF.

Intranasal administration of OPN

Intranasal administration was performed as follows: mice were placed on their backs and administered either aCSF, OPN, thrombin treated OPN or OPN peptides, given in nose drops (5ul/drop) over a 20 min period, alternating drops every 2-5 min between the left and right nares. For studies of neuroprotection the total volume delivered was 50µl. Nasal administration of thrombin cleaved OPN (5µg) was begun 10 min after initiating MCAO. OPN peptides were delivered intranasally either 10 min after initiating MCAO or at 1, 3 or 5 hrs post MCAO. For all experiments except the dose response experiment, the dose administered of each peptide was molar equivalent to 5µg of thrombin cleaved OPN (table 1). For the dose response experiment of NT 134-153, the peptide was delivered 1 hr after initiating MCAO at a dose ten fold higher and ten fold lower than the previously identified protective dose (350ng).

Treatment	Mol Weight	Dose (ng)	Volume (µl)	Molarity (µM)
aCSF	-	-	50	-
Thrombin cleaved OPN	30,000	5000	50	3.33
Peptide NT 109-153 (p)	5142	857	50	3.33
Peptide NT 109-153	4776	796	50	3.33
Peptide CT 154-198 (p)	5227	871	50	3.33
Peptide CT 154-198	4987	831	50	3.33
Peptide NT 134-153	2100	350	50	3.33
Peptide NT 124-153	3119	520	50	3.33
Scrambled Peptide	4776	796	50	3.33

Table 6.1: Dose of each peptide that is equal on a molar basis to 50µg of thrombin cleaved OPN.

Detection of OPN in the brain following Nasal Administration

Immunofluorescent detection of OPN in the brain was performed on mice given 2µg (20ul) of OPN or aCSF. Mice were sacrificed 2 hr post administration (n = 3 each group). Brains were sliced on a cryostat to a section thickness of 20µm. OPN antibody = MPIIIB10 (Developmental Studies Hybridoma Bank, Iowa City, IA, USA). Secondary antibody = mouse anti-mouse IgG conjugated to Cy 3. Tissue was mounted in Vectashield mounting medium containing DAPI.

ELISA detection of OPN in the brain was performed on mice that received 5µg (50µl) of OPN or aCSF. CSF was tapped from mice sacrificed at 30 min, 1 hr and 2 hrs post administration by puncturing the cisterna magna with a 27-gauge needle connected to a syringe (n = 3 each group). OPN concentration was calculated using an ELISA kit for mouse osteopontin (Assay Designs TiterZyme EIA kit for mouse osteopontin, Ann Arbor, MI, USA) following the manufacturers directions. This kit will only detect full

length OPN, thus, only the concentration of intact OPN could be evaluated in the brain following intranasal administration.

Neurological Assessment

To determine the behavioral consequences of T_1AM and T_0AM administration mice were i.p injected with 100µl of vehicle, T_1AM (50mg/kg) or T_0AM (50mg/kg) and observed hourly for the first six hours post injection and at 24 and 48 hours post injection (N=8 each group). Mice were scored according to the criteria outlined in Table 3.4a.

Temperature Measurement

The successful completion of this thesis required the adoption of a strategy for safely and non-invasively measuring mouse temperature. The use of telemetry is time consuming, involves invasive surgery and is costly. The use of rectal probes can be traumatic and stressful. Rectal thermometer measurements can fluctuate due to the mechanical process used to acquire readings. As an alternative means of monitoring mouse temperature I employed the novel method of using a Raytek infrared thermometer (emissivity set to 0.98 and offset: 2.9^0C) [226]. To validate this type of body temperature measurement I compared readings from a rectal probe and the infrared thermometer from recently sacrificed mice (n=8). I found a high correlation between the two methods with an average difference between the two devices of 0.48^oC (Fig 6.3).

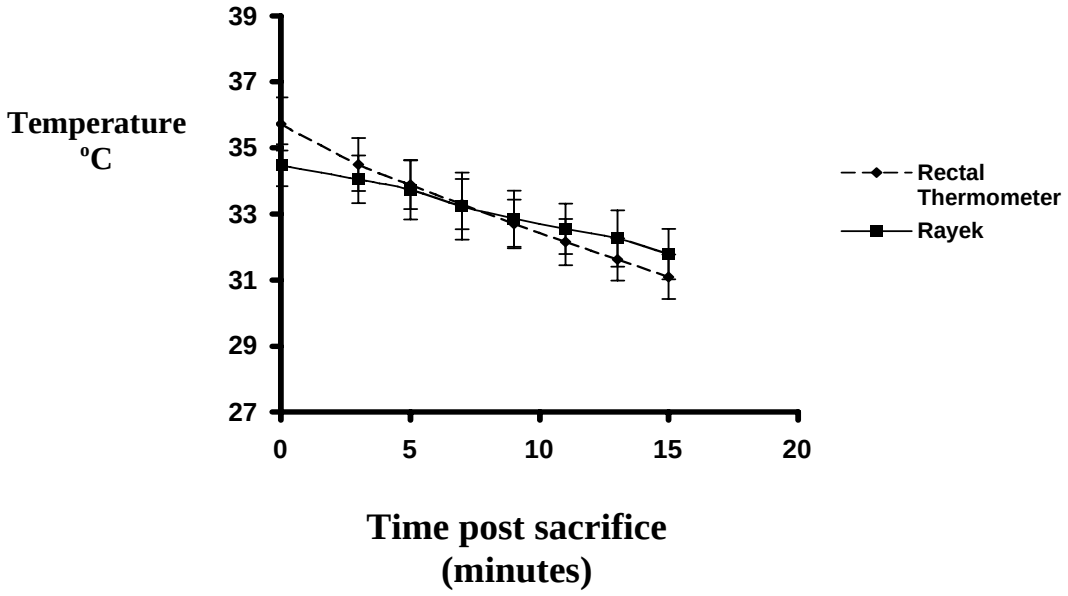

Figure 6.3 Comparison of temperature readings obtained using a rectal and infrared thermometer. Mice were sacrificed and temperature recorded for 15 minutes.

Acute administration of T_1AM and T_0AM

Mice were injected ip with 100µl of vehicle, T_1AM (50mg/kg) or T_0AM (50mg/kg) 1 hour following termination of ischemia and placed in a cage on a heating pad. Cage temperature was maintained at 28^oC, thereby allowing the temperature of the drug-treated animals to fall. For the T_1AM and T_0AM 'hypothermia blocked' group of animals, mice were kept in a separate cage on an adjustable heating pad which was continually adjusted to keep drug treated animals at the same temperature as vehicle injected animals, which were closely monitored by infrared thermometry.

Preconditioning administration of T_1AM and T_0AM

Mice were injected ip with 100µl vehicle, T_1AM (50mg/kg) or T_0AM (50mg/kg) 2 days prior to MCAO. Injections took place between 9.00am and 10.00am. Following injection mice were maintained at ambient temperature (22^oC) and their temperature recorded for 6 hours post injection. For the T_1AM 'hypothermia blocked' group of animals, mice were kept in a separate cage on an adjustable heating pad which was continually adjusted to keep drug treated animals at the same temperature as vehicle injected animals, which were closely monitored by infrared thermometry, as above. Following surgery all preconditioned mice were kept in cages maintained at 28^oC and temperature was recorded every hour for the first 6 hours post surgery (48-54 hours post injection) and immediately before sacrifice (72 hours post injection).

T_1AM and T_0AM treatment of in vitro cultures

For acute administration, T_1AM or T_0AM was added to the culture media at the indicated concentrations immediately post OGD and remained present for 24 hours, at which point cell viability was assessed. OPN peptide NT 109-153 (p) was used as a positive control. For preconditioning administration, T_1AM and T_0AM were added to the culture media at the indicated concentrations 2 days prior to OGD. T_1AM and T_0AM were removed at the time of OGD by washing with PBS.

Statistical analysis

Unless otherwise indicated data are shown as means ± SD of n determinations. Data from cell viability assays and *in vivo* stroke experiments were analyzed by one-way ANOVA followed by Bonferroni's multiple comparison test, using Graphpad Prism version 4.0 (Graphpad software, San Diego, CA, USA).

APPENDIX I

A PRIMATE MODEL OF STROKE

My goal is to develop OPN and T_1AM into drugs for stroke patients. This will require testing OPN and T_1AM in a primate model of stroke and my laboratory has completed a pilot study that provides a foundation upon which to test OPN and T_1AM in the rhesus macaque (*Macaca mulatta*). As a result of this pilot study an entirely new model of experimental stroke has been developed for this species.

Although neuroprotection is conventionally assessed in animal stroke models by histological evaluation of the lesion, this is not possible in human trials and instead MRI is usually employed as the method of visualizing ischemic damage. To bridge this gap between methods of assessing neurological outcome, and thus bridge one of the most significant gaps between preclincal and clinical stroke trials, we incorporated MRI into our primate stroke model. Very few studies have compared histology and MRI in primate stroke models. Although good correspondence between MRI and histological lesion volume has been found in marmosets, cynomolgus monkeys and baboons following MCAO, to our knowledge this is the first study to compare MRI to histological lesion volume in the rhesus [227-229].

To model stoke in the rhesus macaque we selected a transorbital approach to gain access to the cerebral vasculature, an approach that has been successfully used in macaques, squirrel monkeys and baboons. A comprehensive review of this approach, including a comparison with other methods can be found in, “Models of focal cerebral ischemia in the nonhuman primate” by Shunichi Fukuda and Gregory del Zoppo [230].

There are two alternatives to the transorbital approach, both of which are less desirable. One alternative is an *intracranial* approach, which requires a craniotomy. The transorbital approach is preferable to this method because it minimizes pain and discomfort, recovery time is more rapid, and it does not leave the subject with a cranial defect or disturbed deep brain tissue that may alter vascular structures.

An additional advantage of the transorbital method over the intracranial method is that it can be used to reach an intracranial vessel without exposing cerebral tissue to atmospheric conditions, a factor that can cause ultrastructural abnormalities to neurons and glial cells [230]. Also, this method does not cause damage to the brain by retractors and does not damage the blood brain barrier, leading to edema.

The other alternative to a transorbital approach is an interventional approach, requiring the injection or placement of emboli (silicone cylinders or balloons) into the vessel to be occluded via the carotid or femoral artery. However, the use of silicone cylinders and balloons to occlude a vessel such as the middle cerebral artery (MCA) is less precise than directly reaching the vessel via the orbit.

This study is not the first to model stroke in the rhesus macaque using the transorbital approach. The model was originally developed in the 1970s where researchers occluded the MCA for 2 hours using this technique [231, 232]. However, 2 hours of occlusion led to heterogeneous lesion size. For example, in a study of 9 animals, Crowell et al report that following 2 hours of MCAO, 4 primates had no apparent infarct, 2 had only microscopic

evidence of necrosis, 1 had a small infarct confined to the internal capsule and 2 had a large infarct in the territory supplied by the MCA [232]. Since the 1970s there has only been one additional study performed in the rhesus using this model. This 2001 study also occluded the MCA for 2 hours but did not report infarct volume following surgery, using metabolic signs as a readout of ischemic damage instead [233].

Although the transorbital approach has not been extensively used in the rhesus macaque, its use has been more widespread in the closely related cynomolgus monkey (*Macaca fascicularis*). In this species a length of occlusion of the MCA of 3 hours has been used, which generates a cortical infarct with a volume of 1ml [234, 235]. Although this is less than 5% of the total volume of the ipsilateral hemisphere, this model has been used to assess the efficacy of potential stroke therapeutics, for example the immunosuppressive drug tacrolimus (FK506) [236].

Due to the lack of a well defined model of transorbital occlusion of the MCA in the rhesus we began our pilot study by occluding the MCA for different durations. Our goal was to identify a length of ischemia that would generate a reproducible infarct of a suitable volume with which to test OPN and T_1AM.

Two animals were subjected to a single clip MCA occlusion:1 animal with a 4 hour occlusion time (#18816) and 1 animal with a 3 hour occlusion time (#19522) (Table A.1). The results by MRI scan performed 3 days later indicated that the infarcts were modest

and likely to be too small to be appropriate for testing the use of interventional neuroprotection.

We performed MCAO on two additional animals to determine whether a modified procedure involving a 4 hour double clip placement (1 clip on the orbitalfrontal branch of the middle cerebral artery and 1 clip on the M1 segment of the middle cerebral artery just distal from the orbitalfrontal branch) would generate a more extensive lesion. The two animals were treated identically and subjected to MRI scans immediately post surgery and 72 hours later. The lesions involved the caudate and putamen with very small involvement of the insular cortex. The first animal showed substantial hemiparesis on the affected side by 24 hours and this deficit resolved only modestly by 72 hours post surgery. The animal's brain showed a midline shift on the MRI scan at 72 hours; which was likely due to edema. There was evidence of hemorrhage in the necrotic region of the brain lesion, which may have contributed to the edema and neurological deficit. The lesion size was ~13% of the hemisphere. The second animal displayed a modest hemiparesis that resolved during the 3 day recovery period. The lesion involved the caudate and putamen and represented ~7% of the hemisphere (Table A.1).

The fact that this double clip procedure of extensive duration failed to result in motor cortex damage yet produced a sizable lesion in the caudate/putamen area led us to postulate that there may be an anatomical difference that makes the cortex of the rhesus macaque resistant to MCAO. By searching the literature and dissecting the brains of cull animals, we discovered that there is a significant difference in the cerebral vasculature of

this species compared to the cerebral vasculature of humans [237]. In the brain of the rhesus macaque, there exists only a single pericallosal artery which feeds oxygenated blood to both hemispheres, while in humans, there are two pericallosal arteries, each feeding a different hemisphere (Figure A.1).

In humans, each pericallosal artery is a continuation of one of the anterior cerebral arteries (ACA) as they continue superiorly and posteriorly and feed the medial surface of the cerebral hemispheres. In the rhesus macaque, the two anterior cerebral arteries come together to form a single pericallosal trunk [237]. This results in greater collateral circulation between the two hemispheres and likely explains why little cortical damage occurs when the middle cerebral artery (MCA) is occluded in rhesus macaques.

Knowledge of this vascular incongruity led us to test a new model of multiple arterial occlusion, as a means of circumventing the challenge of contralateral circulation. We were concerned that MCA occlusion combined with ACA occlusion may be too severe a model of ischemia so we first performed a trial surgery with a MCA occlusion plus an internal carotid artery occlusion for 90 minutes. The resulting infarct was very small and the animal displayed virtually no neurological impairment (#21208, Table A.1).

We next performed a 90 minute surgery using a single clip on the anterior cerebral artery (A2) just after it joins the contralateral side and a clip at the M1 segment of the MCA just distal to the orbital-frontal branch. This double-clip ACA + MCA occlusion produced a visable infarct with neurological deficits that were moderate in severity (#22410, Table A.1). Importantly, the infarct involved the temporal cortex, which achieved the desired

effect and parallels outcome in humans. Of note, the MRI scans performed on this animal revealed abnormally large ventricles within the brain.

Based on the favorable outcome of animal 22410 we performed 2 more animals with the same conditions. Both animals exhibited large infarcts and severe neurological deficits (#20291 & #20622, Table A.1) and one died 45 hours following surgery likely due to brain edema. It is possible that the abnormally large ventricles of 22410 protected this animal from the injurious effects of edema by providing extra space within the cranium to accommodate brain swelling. Due to the severity of infarct and neurological deficit in animals 20291 and 20622, we decreased time for subsequent animals to 60 minutes.

Animals 22064 and 22394 were subjected to double-clip ACA + MCA occlusion for 60 minutes and MRI scans and TTC staining revealed infarcts of ~23% that involved the temporal cortex and the caudate-putamen area. The neurological deficits were moderate with a marked hemiparesis on the affected side. Importantly, the modest infarct volume of ~23% provides latitude for infarct size to be increased or decreased depending on the negative or positive effect of a drug candidate being tested.

We repeated this model of multiple arterial occlusion in a further 3 animals and found that it generated infarcts of a consistent and reproducible size when assessed by TTC, cresyl violet and MRI imaging (Figure A.2, Table A.2). Although a sixth animal (#22035) subjected to this model had a much smaller infarct volume and a higher neurological score following surgery than the other 5 animals, Dr. West noted that this

animal had a very shallow orbit and the ACA was located very deep, which precluded him from being able to verify that the ACA was completely occluded following placement of the clip. From this data we surmise that 60 minutes of occlusion of the MCA and ACA provides an appropriate stroke model in the rhesus with which to conduct preclinical trials of stroke therapeutics.

Within the above data there was a strong linear relationship between infarct measurements taken using MRI T2, cresyl violet and TTC staining, with no statistical difference between the results obtained by each of these methods ($P > 0.05$). Graphs showing this linear relationship are provided in figure A.3 along with representative images from each technique. This suggests that each method is suitable for producing accurate measurements of cerebral infarction following ischemic stroke in the rhesus macaque. There was also a high correlation between measurements of neurological scoring and evaluation of infarct volume and graphs showing the linear nature of this relationship can be found in figure A.4. This suggests that neurological score is a valuable predictor of the severity of stroke in this model.

Stroke causes a defined response in the blood of human patients characterized by lymphocytopenia and an increase in the number of circulating neutrophils and monocytes [238]. As a means of corroborating that our model of multiple arterial occlusion in the rhesus causes changes in the periphery representative of human stroke, we performed an analysis of the white blood cell response to stroke in our pilot animals. We found pronounced lymphocytopenia, neutrophilia, and an increase in the number of circulating

monocytes, which mirrors the response seen in humans and further validates the new stroke model (Figure A.5).

In conclusion, we have developed and validated a new model of ischemic stroke that is tailored for the rhesus macaque. We have incorporated MRI into our model to facilitate taking OPN and T_1AM treatment to the next stage of clinical testing. We are now ready to begin a primate preclinical trial with OPN and T_1AM and believe that the groundwork has been set to accurately ascertain the full neuroprotective potential of each of these neuroprotectants as a treatment for stroke.

Primate #	Sex	MCAO duration (hrs)	Time of death post MCAO (hrs)	TTC Infarct volume (mm3)	TTC Infarct vol. % of ipsilat. Hem.	T2 MRI Infarct vol. % of ipsilat. Hem.	Neurological Score (0-100) hrs post MCAO		
							24	48	72
19522	M	3	72	472	1	4.5	85	95	92
18816	M	4	72	3933	8.4	2.6	50	60	90
20909	M	4 (2clip MCA)	72	5915	13.8	10.9	25	30	30
20263	M	4 (2 clip MCA)	72	3512	7.4	7.4	50	87	89
21208	M	1.5 (2 clip MCA & ICA)	48	2276	5.6	0.7	96	100	N/D
22410	M	1.5 (2clip MCA & ACA)	48	14284	18.3	32.9	35	45	N/D
20291	M	1.5 (2clip MCA & ACA)	48	15326	36.4	47.3	25	27	N/D
20622	M	1.5 (2clip MCA & ACA)	48	16612	34.8	41.6	27	Dead	N/D

Table A.1. Infarct volume and neurological scoring following single and multiple arterial occlusion. N/D = Not done.

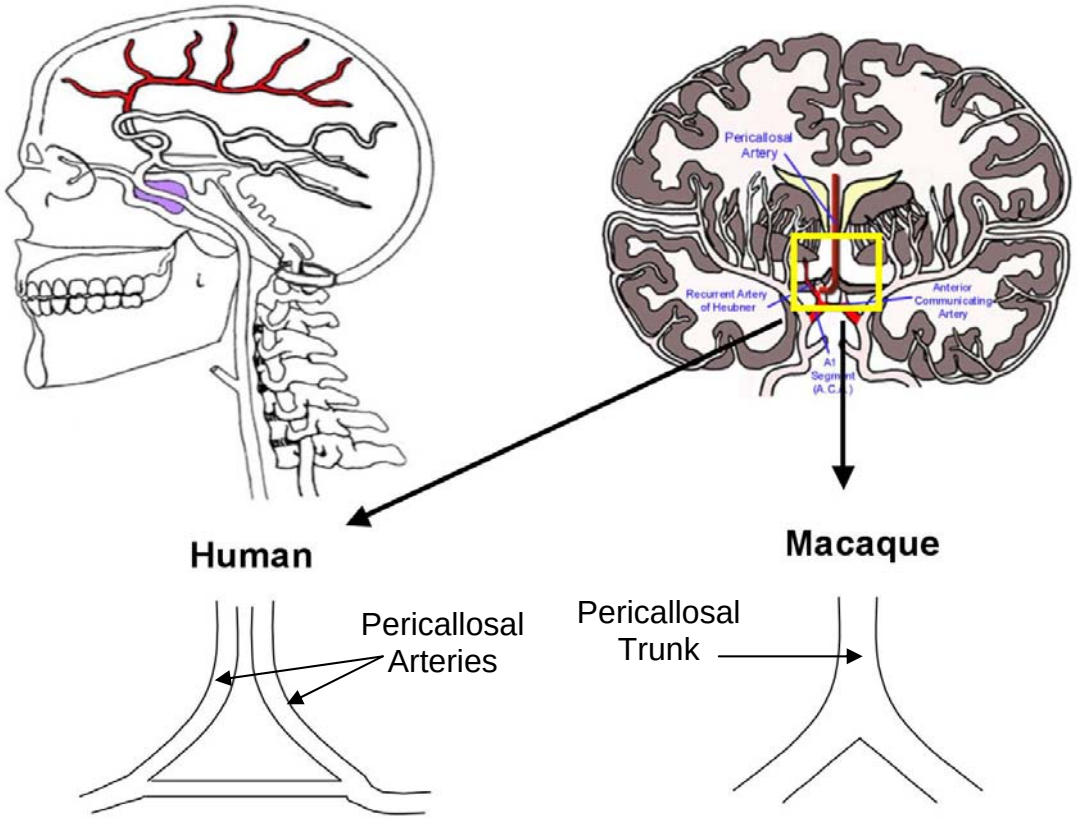

Figure A.1. A comparison of the anatomy of the pericallosal artery in the rhesus macaque and human. Upper images show the territory supplied by the pericallosal artery and the location of the artery in the human brain. Lower images show the difference in the anatomy of the pericallosal vasculature. In the rhesus macaque the pericallosal arteries have fused into a single trunk [237]. The upper images were taken from the Loyola University Medical Education Network website: (http://www.meddean.luc.edu/lumen/MedEd/Neuro/neurovasc/navigation/peri.htm)

Primate #	Sex/Age (Years/ days)	TTC Infarct volume (mm3)	TTC Infarct vol. % of ipsilat. Hem.	T2 MRI Infarct vol. % of ipsilat. Hem.	Neurological Score (0-100) hrs post MCAO	
					24	**48**
23530	M (10/252)	14155	30	26.6	35	32
22689	M (5/221)	15223	31.7	25.7	25	31
22035	M (6/181)	5843	13.1	9.2	75	82
21766	M (6/364)	10849	23	27.0	25	33
22394	M (5/259)	10263	23.2	24.2	28	36
22064	M (6/7)	9995	21.1	23.3	33	41
	Average	**11055**	**23.6**	**23**	**37**	**43**

Table A.2. Infarct volume and neurological scoring following 60 minutes of multiple arterial occlusion (MCA & ACA).

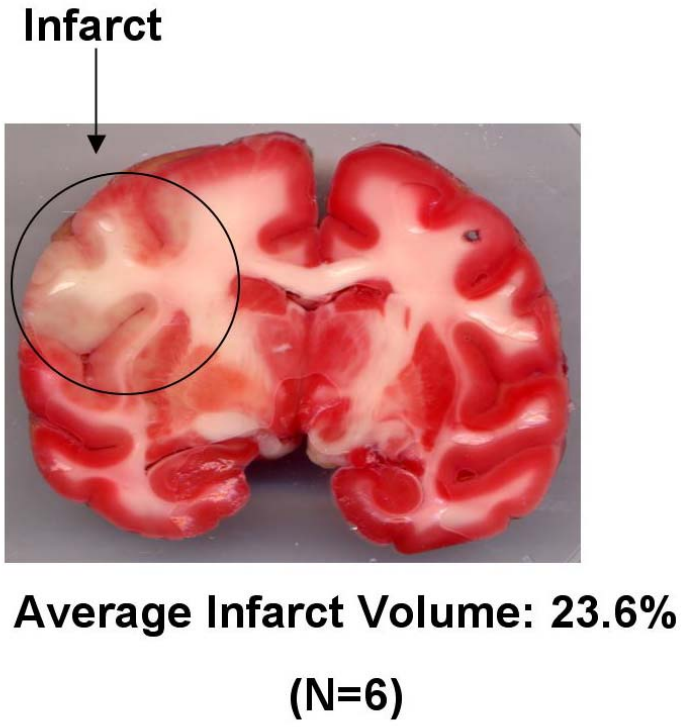

Figure A.2. Representative section following 60 minutes of multiple arterial occlusion. Section has been stained with TTC 48 hours following ischemia. Sixty minutes of occlusion of the MCA and ACA results in an average infarct volume of 23.6% as assessed by TTC staining (N = 6)

Figure A.3. Correlation between MRI T2, cresyl violet and TTC measurement of infarct volume. Top panels: MRI T2, cresyl violet and TTC image of the same section from an individual that underwent 60 minutes of MCA and ACA occlusion. Bottom graphs: The linear relationship between MRI T2, cresyl violet and TTC staining. The Pearson correlation coefficient is provided for each graph. In the lower two graphs 2 animals have been excluded from the data set due to these animals undergoing a modified TTC staining protocol (45 minutes immersion in TTC instead of 15 minutes).

MRI T2	Cresyl Violet	TTC
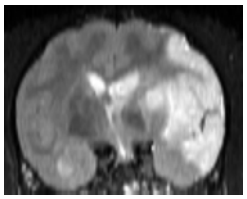	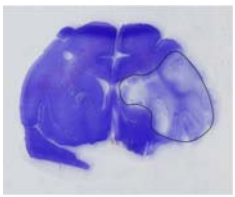	

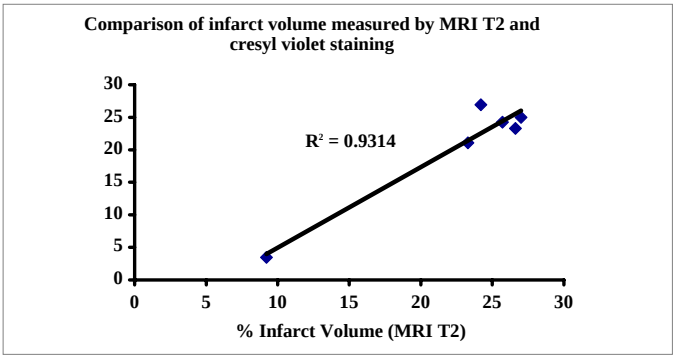

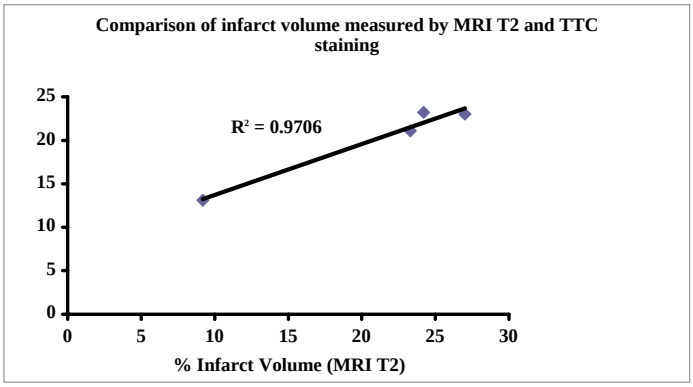

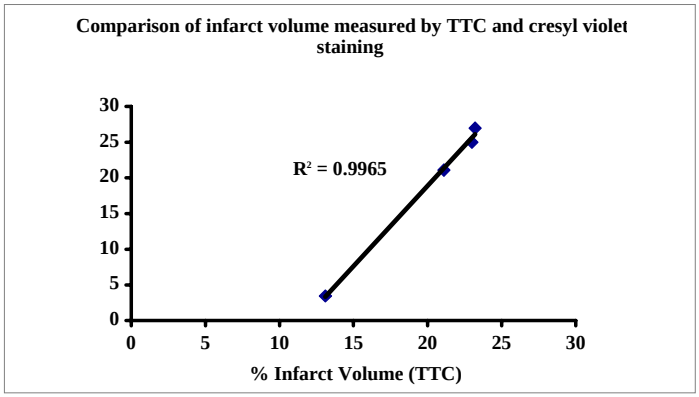

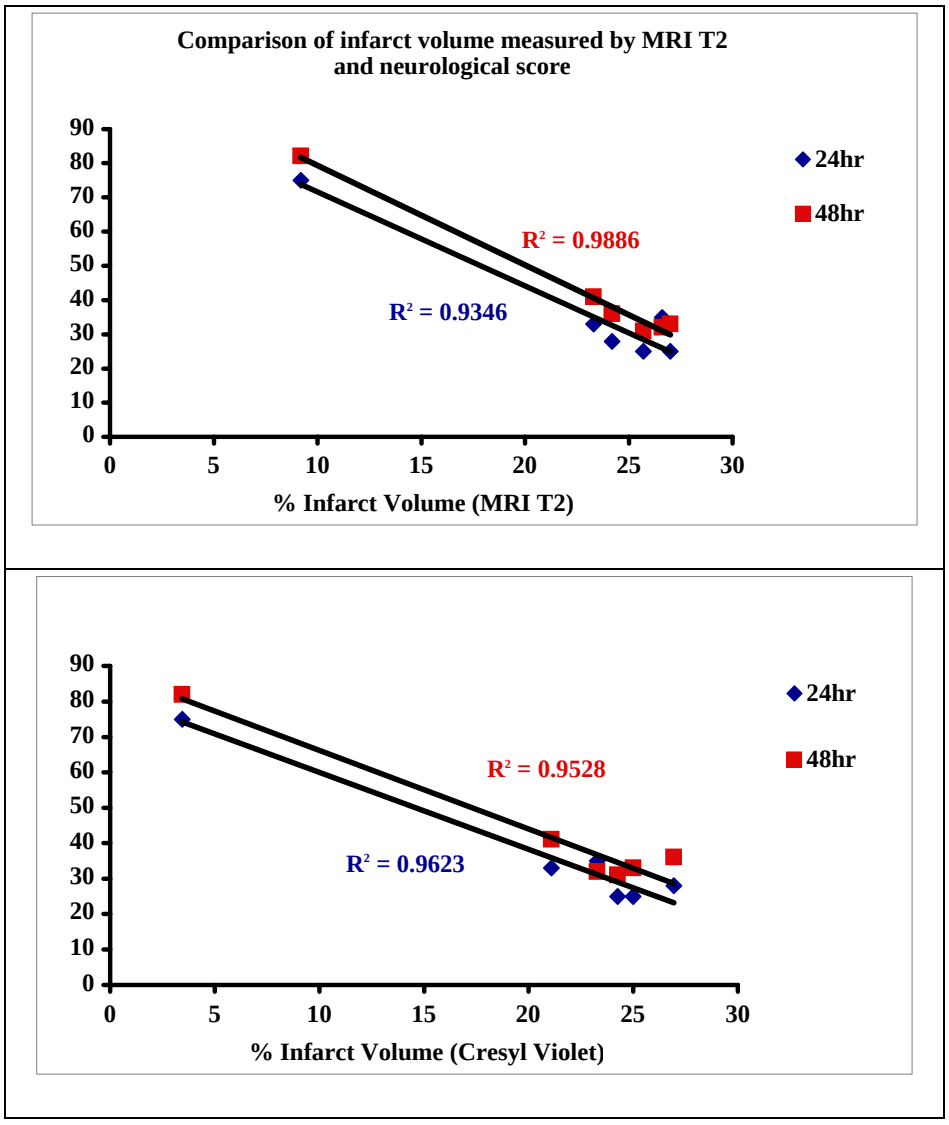

Figure A.4. Correlation between neurological scoring at 24 and 48 hours post stroke and infarct volume (measured by MRI T2 and cresyl violet staining). The Pearson correlation coefficient is provided for each graph.

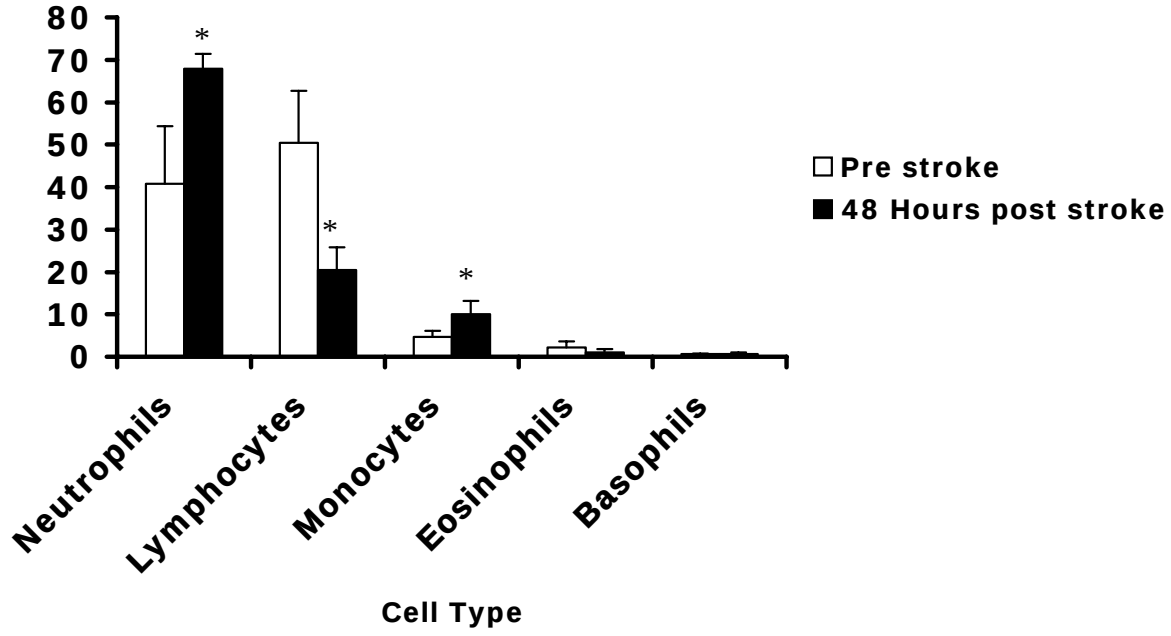

Figure A.5 The white blood cell response to stroke in the rhesus macaque. A complete blood count was performed on blood drawn immediately prior to stroke and at 48 hours post stroke. Data shown are mean $\pm$ SD. * p value < 0.05 compared to pre-stroke samples. N = 6.

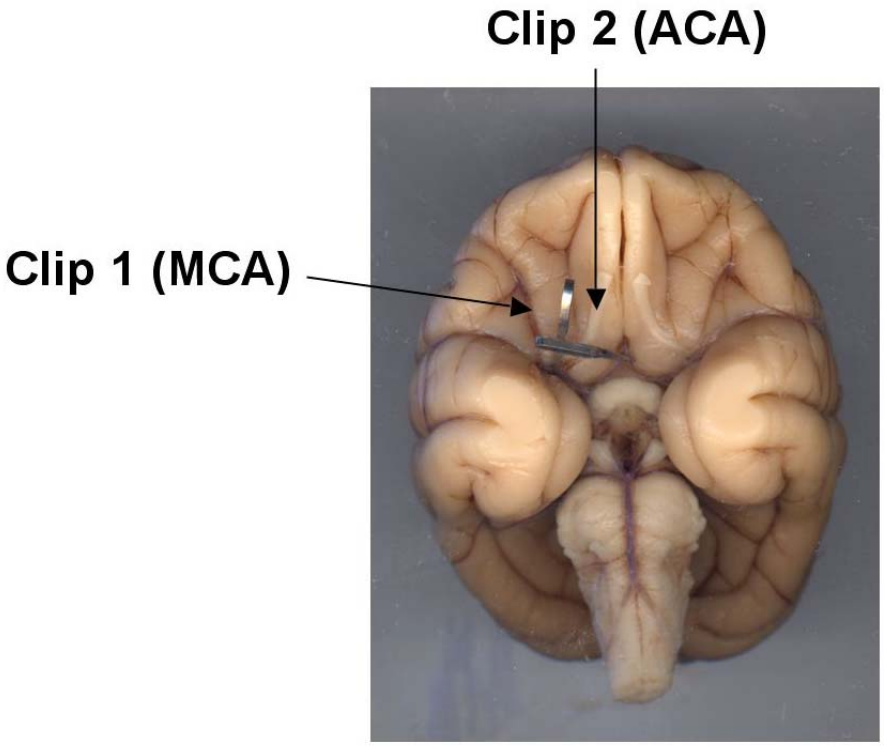

Figure A.6. Clip placement for a model of multiple arterial occlusion in the rhesus macaque. Multiple arterial occlusion of the MCA and ACA was performed with the animal in a stereotaxic frame using the microsurgical transorbital approach of Hudgins and Garcia [239].

EXPERIMENTAL STROKE PROCEDURE

Preoperative care

Animals were food restricted for 12 hours and examined to ensure that the overall health of each animal was adequate to withstand the procedure. Anesthesia was induced with ketamine HCl (15-25 mg/kg IM), followed by maintenance anesthesia with isoflurane gas vaporized in 100% oxygen and delivered via cuffed orotracheal tube. Hair was clipped from the surgical site, followed by sterile preparation with povidone iodine scrub and solution. A percutaneous cephalic or saphenous intravenous catheter was placed to allow for blood sampling as well as intraoperative fluid administration. One sample of blood (10cc) was drawn prior to middle cerebral artery occlusion for CBC analysis. Rectal temperature was monitored. Indirect monitoring of arterial blood pressure was performed by placing a pediatric cuff on the lower arm or leg. Heart rate and rhythm was monitored by insertion of an esophageal stethoscope. Pulse oximetry was continuously monitored along with evaluation of mucous membrane color. Venous blood gases were analysed at the beginning and at the end of surgery. EEG monitoring was done to confirm successful occlusion and reperfusion. Loss of palpebral and corneal reflexes, degree of muscle relaxation, rate and depth of breathing, and lack of somatic response to surgical stimuli were used to ascertain adequacy of anesthesia.

Middle Cerebral Artery Occlusion Surgery

Surgery was performed once on each animal. Surgical implementation was carried out in a fully equipped surgical suite at the Oregon National Primate Research Center (ONPRC) by Drs. Alex West and Nik Lessov with assistance from surgical services personnel. All surgery was conducted under aseptic conditions.

A transorbital approach was used. Anatomically, the anterior cerebral artery (ACA) and the middle cerebral artery (MCA) lie directly posterior to the orbit. To gain access to these vascular structures, enucleation was followed by transection of the optic nerve and ophthalmic artery. Bleeding was controlled with electrocoagulation. Angiography has demonstrated that the MCA and ACA remain patent after these procedures. A small craniotomy (~1 cm diameter) was made by removal of the medial sphenoid wing and portions of the adjacent middle fossa with a high-speed pneumatic drill and bone rongeurs. Under microscopic view (300-mm objective lens), the optic strut was removed as well as part of the medial bone adjacent to the planum sphenoidale to open the optic foramen and maximize visualization of the both anterior cerebral arteries. The dura was then opened in a semicircular fashion and retracted anteriorally. The Sylvian fissure was then opened with an arachnoid knife and microscissors to identify the top of the ICA, the anterior cerebral artery (ACA), and the MCA. Microsurgical technique enables exposure of the MCA from the surrounding arachnoid membranes and branching vessels. When dissection of the MCA and the lentoculostriate artery (LS) bundles was complete, a neurosurgical clip was placed around the MCA proximal to the take-off of the LSA. For the final model of multiple arterial occlusion the first clip was placed on the ACA

junction if clearly visualized or across both A1 arteries. The second clip was then placed on the MCA just proximal to the fronto-polar branch (Figure A.4). Direct occlusion was visualized by a high power-operating microscope. The occlusion time varied between 60 minutes and 4 hours. At the end of this period of occlusion, the neurosurgical clip(s) were removed, (MCA first). The wound was then irrigated with copious amounts of saline and observed for any signs of bleeding. The dural flap was then positioned to cover the defect. A small periorbital tissue patch was then placed over the dural opening. Surgicell along with bone wax was placed over the defect with final application of Vetbond. The wound was closed with a single layer of 2-0 silk suture with bacitracin ointment applied. The femoral arterial line was removed and the wound closed with absorbable suture.

MRI scan immediately pre and post experimental stroke

While under anesthesia animals were subjected to a pre-stroke and acute stroke MRI scan. Subjects were transported to the Imaging facility at ONPRC. The subject was positioned in the MRI unit and wrapped in a towel with continued delivery of isoflurane gas (0.75-1.0% in oxygen delivered at 1.0 L/min) for maintenance anesthesia via precision vaporizor located approximately 2.5 meters from magnet. A pulse monitor was attached to the tail, toe, or finger to monitor pulse rate. Respiratory rate was monitored by observing the in-and-out movement of the anesthesia bag. Upon completion of the acute MRI procedure, the animal was disconnected from the non-rebreathing tube and moved back to the prep-room for recovery. In the prep room, the pulse rate, respiratory rate, oxygen saturation, and end-tidal carbon dioxide levels were monitored throughout anesthetic recovery. Once the endotracheal tube had been removed and the subject was

able to sit up unassisted, the subject was moved to a transfer box for transport back to their home cage.

Postoperative care

Administration of analgesics and daily health checks were performed by trained personnel from surgical services. Postoperative analgesia was afforded by hydromorphone HCl by either intramuscular (1.0 mg) or oral (2.0 mg) route, and buprenorphine (0.3 mg IM). Observation for species-specific behaviors, as well as food and water consumption, and urine and feces production was performed.

Neurological assessment, magnetic resonance imaging (MRI), blood sampling and euthanasia

48 or 72 hours following stroke surgery, each animal was given a neurological assessment, anesthetized for MRI and had blood drawn just prior to euthanasia (described below).

Neurological Assessment

The neurological assessment was performed by a trained observer. The assessment was observational only with no active involvement by the observer with the subject. Animals were assessed with the 100-point Spetzler scale, with higher scores representing better functional outcomes. Motor function was graded from 1 to 75, according to severity of hemiparesis in the extremities and face. Hemiparesis in the extremities was scored as 10 = severe hemiparesis, 25 = mild hemiparesis, 55 = favors normal side, and 70 = normal.

Hemiparesis in the face was scored as 1 = normal or one-sided paralysis and 5 = normal facial movement. Behavior and alertness was scored from 0 to 20, with 0 = dead, 1 = comatose, 5 = aware but inactive, 15 = aware but less active, and 20 = normal. Visual field deficits were assigned 1 if present or 5 if absent.

MRI Scan 48 (and 72) hours post stroke

Subjects were transported to the Imaging facility at ONPRC. Anesthesia was induced in the prep-room with a 3mg/kg intramuscular injection of Telazol (Tiletamine/Zolazepam). Once induced, eye ointment was applied to the eye and an endotracheal tube was placed. The pulse rate, respiratory rate, oxygen saturation, and end-tidal carbon dioxide were recorded in the prep room. If all values were normal, the subject was moved from the prep room and positioned in the MRI unit. The subject was wrapped in a towel and a long non-rebreathing tube was connected to the endotracheal tube. Isoflurane gas (.75-1.0% in oxygen delivered at 1.0 L/min) was delivered for maintenance anesthesia via precision vaporizor located approximately 2.5 meters from magnet. A pulse monitor was attached to the tail, toe, or finger to monitor pulse rate. Respiratory rate was monitored by observing the in-and-out movement of the anesthesia bag. Upon completion of the MRI procedure, the patient was disconnected from the non-rebreathing tube and transferred to the necropsy room for euthanasia.

Euthanasia

Following MRI, the animal was further anesthetized with sodium pentobarbital delivered intravenously at 25mg/kg. After depth of anesthesia was ensured by evaluation of

corneal, palpebral and gag reflexes, the abdominal cavity was opened, the animal was exsanguinated via the distal aorta and blood was collected for CBC analysis. Following euthanasia by exsanguination, the thoracic cavity was opened and the common trunk/carotid arteries were cannulated. Ice-cold saline was used to perfuse the cephalic structures. This technique permits regional chilling of the head and its contents. The skull was then opened and the brain carefully removed, placed in ice-cold saline and subsequently processed for infarct measurements.

TTC staining of brain

Each brain was immersed in ice-cold saline and placed in a macaque brain mold at 4^{o}C. The brain was sectioned into 15 slices, each 4mm thick and transferred to 10cm plates containing 1.5% TTC. The brain was incubated at 37^{o}C for 15 minutes and then placed in 10% formalin. Each section was scanned and the infarct volume calculated using the same formula used to calculate infarct volume in the rodent.

Cresyl Violet staining of brain

Following scanning and evaluation of infarct volume using TTC, each section was cryopreserved in 10% formalin containing 30% sucrose and frozen. Sections were then mounted on a sliding microtome and further sectioned to a thickness of 50µm. One 50µm section from each 4mm section was stained for 3 minutes in cresyl violet solution (1g cresyl violet *sigma C5042*, 400ml water, pH 3.6) before being washed twice in distilled water. Sections were then dehydrated by immersion for 4 minutes in 95% ethanol, followed by 2 minutes in 100% ethanol. Sections were then placed for 4 minutes in

xylenes, coverslipped and dried overnight, prior to scanning and assessment of infarct volume.

REFERENCES

1. Stephenson J. Rising stroke rates spur efforts to identify risks, prevent disease. *JAMA*. 1998;279:1239-1240
2. Fisher M, Bogousslavsky J. Further evolution toward effective therapy for acute ischemic stroke. *JAMA*. 1998;279:1298-1303
3. Pancioli A, Broderick J, Kothari R, Brott T, Tuchfarber A, Miller R, Khoury J, Jauch E. Public perception of stroke warning signs and knowledge of potential risk factors. *JAMA*. 1998;279:1288-1292
4. AHA. 2001 heart and statistical update. *American Heart Association*. 2000
5. Caplan L. *Caplan's stroke. A clinical approach*. Butterworth Heinemann; 2000.
6. Adams F. *The genuine works of hippocrates: Translated from the greek*. Baltmore: Williams and Wilkins; 1939.
7. McDevitt E, Carter S, Gatje B. Use of anticoagulants in treatment of cerebral vascular disease. *JAMA*. 1958;166:592-596
8. del Zoppo G. Microvasculature responses to cerebral ischemia/inflammation. *Annals of the New York Academy of Science*. 1997;823:132-147
9. Gonzalez R, Hirsch J, Koroshetz W, Lev M, Schaefer P. *Acute ischemic stroke. Imaging and intervention*. Springer; 2006.
10. Edvinsson L, Krause D, N. *Cerebral blood flow and metabolism*. Lippincott Williams and Wilkins; 2002.
11. Hsu C, Y. *Ischemic stroke: From basic mechanisms to new drug development*. Karger; 1998.

12. Olney J. Brain lesions, obesity, and other disturbances in mice treated with monosodium glutamate. *Science*. 1969;164:719-721

13. Simon R. Acidotoxicity trumps excitotoxicity in ischemic brain. *Archives of Neurology*. 2006;63:1368-1370

14. Pignataro G, Simon R, Xiong Z. Prolonged activation of asic1a and the time window for neuroprotection in cerebral ischaemia. *Brain*. 2007;130:151-158

15. Sugawara T, Chan P. Reactive oxygen radicals and pathogenesis of neuronal death after cerebral ischemia. *Antioxidants & Redox Signaling*. 2003;5:597-607

16. Halliwell B. Free radicals, antioxidants, and human disease: Curiousity, cause, or consequence? *Lancet*. 1994;344:721-724

17. Kerr J. A histochemical study of hypertrophy and iscaemic injury of rat liver with special reference to changes in lysosomes. *Journal of Pathology and Bacteriology*. 1965;90:419-435

18. Kerr J, Wyllie A, Currie A. Apoptosis: A basic biological phenomenon with wide-ranging implications in tissue kinetics. *British Journal of Cancer*. 1972;26:239-257

19. Antonsson B, Montessuit S, Sanchez B. Bax is present as a high molecular weight oligomer/complex in the mitochondrial membrane of apoptotic cells. *Journal of Biological Chemistry*. 2001;276:11615-11623

20. Adams J, Cory S. Life or death decisions by the bcl-2 protein family. *Trends in the Biochemical Sciences*. 2001;26:61-66

21. Kroemer G, Reed J. Mitochondrial control of cell death. *Nature Medicine*. 2000;6:513-519

22. Edwards EA, Dean LM. Effects of crowding of mice on humoral antibody formation and protection to lethal antigenic challenge. *Psychosomatic Medicine*. 1977;39:19-24

23. Hengartner M. The biochemisty of apoptosis. *Nature*. 2000;407:770-776

24. Miyashita T, Reed J. Tumor suppressor gene p53 is a direct transcriptional activator of the human bax gene. *Cell*. 1995;80:293-299

25. Namura S, Zhu J, Fink K, Endres M, Srinivasan A, Tomaselli KJ, Yuan J, Moskowitz MA. Activation and cleavage of caspase-3 in apoptosis induced by experimental cerebral ischemia. *Journal of Neuroscience*. 1998;18:3659-3668

26. Zoppo GJd. Microvasculature responses to cerebral ischemia/inflammation. *Annals of the New York Academy of Science*. 1997;823:132-147

27. Zoppo Gd, Ginis I, Hallenbeck JM, Iadecola C, Wang X, Feurstein GZ. Inflammation and stroke: Putative role for cytokines, adhesion molecules and inos in brain response to ischemia. *Brain Pathology*. 2000;10:95-112

28. Chen J, Graham S, Chan P, Lan J, Zhou R, Simon R. Bcl-2 is expressed in neurons that survive focal ischemia in the rat. *Neuroreport*. 1995;6:394-398

29. Ellerby L, Ellerby H, Park S. Shift of the cellular oxidation reduction potential in neural cells expressing bcl-2. *Journal of Neurochemistry*. 1996;67:1259-1267

30. Graham S, Chen J. Programmed cell death in cerebral ischemia. *Journal of Cereberal Blood Flow and Metabolism*. 2001;21:99-109

31. Guan Q, Pei D, Liu X, Wang X, Xu T, Zhang G. Neuroprotection against ischemic brain injury by sp600125 via suppressing the extrinsic and intrinsic pathways of apoptosis. *Brain Reseach*. 2006;1092:36-46

32. Guan QH, Pei D, Zong Y, Xu T, Zhang G. Neuroprotection against ischemic brain injury by a small peptide inhibitor of c-jun n terminal kinase (jnk) via nuclear and non-nuclear pathways. *Neuroscience*. 2006;139:609-627

33. Zhao H, Yenari M, Cheng D, Sapolsky R, Steinberg G. Bcl-2 overexpression protects against neuron loss within the ischemic margin following experimental stroke and inhibits cytochrome c translocation and caspase 3 activity. *Journal of Neurochemistry*. 2003;85:1026-1036

34. Shinoura N, Satou R, Yoshida Y, Asai A, Kirino T, Hamada H. Adenovirus mediated transfer of bcl-x(l) protects neuronal cells from bax-induced apoptosis. *Experimental Cell Research*. 2000;254:221-231

35. Gong C, Qin Z, Betz AL, Liu XH, Yang GY. Cellular localization of tumor necrosis factor alpha following focal cerebral ischemia in mice. *Brain Research*. 1998;801:1-8

36. Nawashiro H, Brenner M, Fukui S, Shima K, Hallenbeck J. High susceptibility to cerebral ischemia in gfap-null mice. *Journal of Cerebral Blood Flow and Metabolism*. 2000;20:1040-1044

37. Nawashiro H, Martin D, Hallenbeck JM. Neuroprotective effects of tnf binding protein in focal cerebral ischemia. *Brain Research*. 1997;778:265-271

38. Shohami E, Ginis I, Hallenbeck JM. Dual role of tumor necrosis factor alpha in brain injury. *Cytokine Growth Factor Review*. 1999;10:119-130

39. Ali C, Nicole O, Docagne F, Lesne S, Mackenzie E, Nouvelot A, Buisson A, Vivien D. Ischemia-induced interleukin-6 as a potential endogenous

neuroprotective cytokine against nmda receptor mediated excitotixicity in the brain. *Journal of Cereberal Blood Flow & Metabolism*. 2000;20:956-966

40. Greenberg D, Jin K. Experienceing vegf. *Nature Genet*. 2004;36:792-793

41. Bruce AJ, Boling W, Kindy MS, Peschon J, Kraemer PJ, Carpenter MK, Holtsberg FW, Mattson MP. Altered neuronal and microglial responses to excitotoxic and ischemic brain injury in mice lacking tnf receptors. *Nature Medicine*. 1996;2:788-794

42. Zhang Z, Zhang L, Jiang Q, Zhang R, Davies K, Powers C. Vegf enhances angiogenesis and promotes blood brain barrier leakage in the ischemic brain. *Journal of Clinical Investigation*. 2000;106:829-838

43. Gonzalez B, Leroux P, Lamacz M, Bodenant C, Balazs R, Vaudry H. Somatostatin receptors are expressed by immature cerebellar granule cells. *PNAS*. 1992;89:9627-9631

44. Strong A, Smith S, Whittington D, Meldrum B, Parsons A. Factors influencing the frequency of fluorescence transients as markers of peri-infarct depolarizations in focal cerebral ischemia. *Stroke*. 2000;31:214-222

45. Gill R, Andine P, Hillered L, Persson L, Hagberg H. The effect of mk-801 on cortical spreading depression in the penumbral zone following focal ischemia in the rat. *Journal of Cereberal Blood Flow and Metabolism*. 1992;12:371-379

46. Chen Q, Chopp M, Bodzin G, Chen H. Temperature modulation of cerebral depolarization during focal cerebral ischemia in rats: Correlation with ischemic injury. *Journal of Cereberal Blood Flow and Metabolism*. 1993;13:389-394

47. Dirnagl U, Iadecola C, Moskowitz M. Pathobiology of ischaemic stroke: An integrated view. *TINS*. 1999;22:391-397

48. Bernard S, Gray T, Buist M. Treatment of comatose survivors of out of hosital caridac arrest with induced hypothermia. *New England Journal of Medicine*. 2002;346:557-563

49. listed) Na. Mild therapeutic hypothermia to improve the neurologic outcome after cardiac arrest. *New England Journal of Medicine*. 2002;346:549-556

50. Plum F. Neuroprotection in acute ischemic stroke. *JAMA*. 2001;285:1760-1761

51. DeGraba T, Pettigrew L. Why do neuroprotective drugs work in animals but not humans? *Neurology Clinic*. 2000;18:475-493

52. investigators TR. A randomized trial of tirilazad mesylate in patients with acute stroke (ranttas). *Stroke*. 1996;27:1453-1458

53. group TAns. Clinical trial of nimodipine in acute ischemic stroke. *Stroke*. 1992;23:3-8

54. Wahlgren N, Ranasinha K, Rosolacci T, Franke C, Van Erven P, Ashwood T, Claesson L. Clomethiazole acute stroke study (class): Results of a randomized, controlled trial of clomethiazole verus placebo in1360 acute stroke patients. *Stroke*. 1999;30:21-28

55. Diener H, Cortens M, Ford G, Grotta J, Hacke W, Kaste M, Koudstaal P, Wessel T. Lubeluzole in acute ischemic stroke treatment: A double blind study with an 8-hour inclusion time window comparing a 10-mg daily dose of lubeluzole with placebo. *Stroke*. 2000;31:2543-2551

56. Davis S, Lees K, Albers G, Diener H, Marabi S, Karlsson G, Norris J. Selfotel in acute ischemic stroke: Possible neurotoxic effects of an nmda antagonist. *Stroke*. 2000;31:347-354

57. Albers G, Goldstein L, Hall D, Lesko L. Aptiganel hydrochloride in acute ischemic stroke: A randomized controlled trial. *Journal of the American Medical Association*. 2001;286:2673-2682

58. Lees K, Asplund K, Carolei A, Davis S, Diener H, Kaste M, Orgogozo J, Whitehead J. Glycine antagonsit (gavestinel) in neuroprotection in patients with acute stroke: A randomized controlled trial. *Lancet*. 2000;355:1949-1954

59. Donnan G, Dewey H, Davis S. Mri and stroke: Why has it taken so long? *The Lancet*. 2007;369:252-254

60. Sorensen A, Copen W, Ostergaard L, Buonanno F, Gonzalez R, Rordorf G, Rosen B, Schwamm L, Weisskoff R, Koroshetz W. Hyperactute stroke: Simultaneous measurement of relative cerebral blood volume, relative cerebral blood flow, and mean tissue transit time. *Radiology*. 1999;210:519-527

61. Nandagopal K, Dawson TM, Dawson VL. Critical role for nitric oxide signaling in cardiac and neuronal ischemic preconditioning and tolerance. *The Journal of Pharmacology & Experimental Therapeutics*. 2001;297:474-478

62. Chen J, Graham SH, Zhu RL, Simon RP. Stress proteins and tolerance to focal cerebral ischemia. *Journal of Cerebral Blood Flow and Metabolism*. 1996;16:566-577

63. Chen J, Simon R. Ischemic tolerance in the brain. *Neurology*. 1997;48:306-311

64. Murry C, Jennings R, Reimer K. Preconditioning with ischemia: A delay of lethal cell injury in ischemic myocardium. *Circulation*. 1986;74:1124-1136

65. Li G, Vasquez J, Gallagher K, Lucchesi B. Myocardial protection with preconditioning. *Circulation*. 1990;82:609-619

66. Bolli R. The late phase of preconditioning. *Circulation Research*. 2000;87:972-983

67. Lawson CS, Downey JM. Preconditioning: State of the art myocardial protection. *Cardiovascular Research*. 1993;27:542-550

68. Stenzel-Poore MP, Stevens SL, Simon RP. Genomics of preconditioning. *Stroke*. 2004;35:2683-2686

69. Stenzel-Poore MP, Stevens SL, Xiong Z, Lessov NS, Harrington CA, Mori M, Meller R, Rosenzweig HL, Tobar E, Shaw TE, Chu X, Simon RP. Effect of ischemic preconditioning on genomic response to cerebral ischemia: Similarity to neuroprotective strategies in hibernation and hypoxia-tolerant states. *The Lancet*. 2003;362:1028-1037

70. Marini AM, Paul SM. N-methyl-d-aspartate receptor-mediated neuroprotection in cerebellar granule cells requires new rna and protein synthesis. *Proceedings of the National Academy of Sciences of the USA*. 1992;89:6555-6559

71. Barone FC, White RF, Spera PA, Ellison J, Currie RW, Wang X, Feuerstein GZ. Ischemic preconditioning and brain tolerance. Temporal histological and functional outcomes, protein synthesis requirement, and interleukin-1 receptor antagonist and early gene expression. *Stroke*. 1998;29:1937-1951

72. Khan S, Lopez-Chua C, Zhang J, Fisher L, Sorensen E, Denhardt D. Soluble osteopontin inhibits apoptosis of adherent endothelial cells deprived of growth factors. *Journal of Cellular Biochemistry*. 2002;85:728-736

73. Wegener S, Gottschalk B, Jovanovic V, Knab R, Fiebach J, Schellinger P, Kucinski T, Jungehulsing G, Brunecker P, Muller B, Banasik A, Amberger N, Wernecks K, Siebler M, Rother J, Villringer A, Weih M. Transient ischemic attacks before stroke: Preconditioning the human brain? A multicenter magnetic resonance imaging study. *Stroke*. 2004;35:616-621

74. Riepe M, Ludolph A. Chemical preconditioning: A cytoprotective strategy. *Molecular and Cellular Biochemistry*. 1997;174:249-254

75. Brambrink A, Schneider A, Noga H, Astheimer A, Gotz B, Korner I, Heimann A, Welschof M, Kempski O. Tolerance-inducing dose of 3-nitropropionic acid modulates bcl-2 and bax balance in the rat brain: A potential mechanism of chemical preconditioning. *Journal of Cerebral Blood Flow and Metabolism*. 2000;20:1425-1436

76. Vannucci R, Towfighi J, Vannucci S. Hypoxic preconditioning and hypoxic-ischemic brain damage in the immature rat: Pathologic and metabolic correlates. *Journal of Neurochemistry*. 1998;71:1215-1220

77. Nawashiro H, Tasaki K, Ruetzler CA, Hallenbeck JM. Tnf-alpha pretreatment induces protective effects against focal cerebral ischemia in mice. *Journal of Cerebral Blood Flow & Metabolism*. 1997;17:483-490

78. Rosenbaum J, Han Y, Park J, Kennedy M, Planck S. Tumor necrosis factor-a is not essential in endotoxin induced eye inflammation: Studies in cytokine receptor deficient mice. *Journal of Rheumatology*. 1998;25

79. Stenzel-Poore M, Simon RP. Lipopolysaccharide (lps) preconditioning in stroke; a look into the neuroprotective signature. In: Krieglstein J, Klumpp S, eds. *Pharmacology of cerebral ischemia*. Stuttgart: Medpharm Scientific Publishers; 2004:379-385.

80. Tasaki K, Ruetzler CA, Ohtsuki T, Martin D, Nawashiro H, Hallenbeck JM. Lipopolysaccharide pre-treatment induces resistance against subsequent focal cerebral ischemic damage in spontaneously hypertensive rats. *Brain Research*. 1997;748:267-270

81. Dawson DA, Furuya K, Gotoh J, Nakao Y, Hallenbeck JM. Cerebrovascular hemodynamics and ischemic tolerance: Lipopolysaccharide-induced resistance to focal cerebral ischemia is not due to changes in severity of the initial ischemic insult, but is associated with preservation of microvascular perfusion. *Journal of Cerebral Blood Flow and Metabolism*. 1999;19:616-623

82. Nishida M, Carley WW, Gerritsen ME, Ellingsen O, Kelly RA, Smith TW. Isolation and characterization of human and rat cardiac microvascular endothelial cells. *American Journal of Physiology*. 1993;264:H639-H652

83. Denhardt D, Guo X. Osteopontin: A protein with diverse functions. *FASEB Journal*. 1993;7:1475-1482

84. Katagiri YU, Sleeman J, Fujii H, Herrlich P, Hotta H, Tanaka K, Chikuma S, Yagita H, Okumura K, Murakami M, Saiki I, Chambers AF, Uede T. Cd44

variants but not cd44s cooperate with beta1-containing integrins to permit cells to bind to osteopontin independently or arginine-glycine-aspartic acid, thereby stimulating cell motility and chemotaxis. *Cancer Research*. 1999;59:219-226

85. Denhardt D, Noda M, O'Regan A, Pavlin D, Berman J. Osteopontin as a means to cope with environmental insults: Regulation of inflammation, tissue remodeling, and cell survival. *Journal of Clinical Investigation*. 2001;107:1055-1061

86. Denhardt D, Giachelli C, Rittling S. Role of osteopontin in cellular signaling and toxicant injury. *Annual Review of Pharmacology and Toxicology*. 2001;41:723-749

87. Smith LL, Giachelli CM. Structural requirements for alpha 9 beta 1-mediated adhesion and migration to thrombin-cleaved osteopontin. *Experimental Cell Research*. 1998;242:351-360

88. Yokosaki Y, Matsuura N, Sasaki T, Murakami I, Schneider H, Higashiyama s, Saitoh Y, Yamakido Y, Taooka Y, Sheppard D. The integrin alpha(9)beta(1) binds to a novel recognition sequence (svvyglr) in the thrombin-cleaved amino-terminal fragment of osteopontin. *Journal of Biological Chemistry*. 1999;274:36328-36334

89. Helluin O, Chan C, Vilaire G, Mousa S, DeGrado WF, Bennett JS. The activation state of alphavbeta3 regulates platelet and lymphocyte adhesion to intact and thrombin-cleaved osteopontin. *Journal of Biological Chemistry*. 2000;175:18337-18343

90. Barry ST, Ludbrook SB, Murrison E, Horgan CM. Analysis of the alpha4beta1 integrin-osteopontin interaction. *Experimental Cell Research*. 2000;258:342-351

91. Yamamoto N, Sakai F, Kon S, Morimoto J, Kimura C, Yamazaki H, Okazaki I, Seki N, Fujii T, Uede T. Essential role of the cryptic epitope slayglr within osteopontin in a murine model of rheumatoid arthritis. *Journal Clinical Investigation*. 2003;112:181-188

92. Green PM, Ludbrook SB, Miller DD, Horgan CMT, Barry ST. Structural elements of the osteopontin svvyglr motif important for the interaction with alpha4 integrins. *FEBS letters*. 2001;503:75-79

93. Giancotti FG, Ruoslahti E. Integrin signaling. *Science*. 1999;285:1028-1032

94. Rice J, Courter D, Giachelli C, Scatena M. Molecular mediators of avb3-induced endothelial cell survival. *Journal of Vascular Research*. 2006;43:422-436

95. Gary D, Mattson M. Integrin signaling via the pi3-kinase-akt pathway increases neuronal resistance to glutamate-induced apoptosis. *Journal of Neurochemistry*. 2001;76:1485-1496

96. Mosher DF. A role for fibronectin in self-repair after ischemic injury. *Nature Medicine*. 2001;7:290-292

97. Sakai T, Johnson K, Murozono M, Sakai K, Magnuson M, Wieloch T, Cronberg T, Isshiki A, Erickson H, Fassler R. Plasma fibronectin supports neuronal survival and reduces brain injury following transient focal cerebral ischemia but is not essential for skin-wound healing and hemostasis. *Nature Medicine*. 2001;7:324-330

98. Ichikawa H, Itota T, Nishitani Y, Torii Y, Inoue K, Sugimoto T. Osteopontin-immunoreactive primary sensory neurons in the rat spinal and trigeminal nervous systems. *Brain Research*. 2000;863:276-281

99. Shin S, Cha J, Chun M, Chung J, Lee M. Expression of osteopontin mrna in the adult rat brain. *Neuroscience Letters*. 1999;273:73-76

100. Wang X, Louden C, Yue T, Ellison JA, Barone FC, Solleveld HA, Feuerstein GZ. Delayed expression of osteopontin after focal stroke in the rat. *Journal of Neuroscience*. 1998;18:2075-2083

101. Wang H, Zhan Y, Xu L, Feuerstein GZ, Wang X. Use of suppression subtractive hybridization for differential gene expression in stroke. Discovery of cd44 gene expression and localization in permanent focal stroke in rats. *Stroke*. 2001;32:1020-1027

102. Scatena M, Almeida M, Chaisson M, Fausto N, Nicosia R, Giachelli C. Nf-κb mediates αvβ3 integrin-induced endothelial cell survival. *Journal of Cell Biology*. 1998;141:1083-1093

103. Pinkstaff J, Lynch G, Gall C. Localization and seizure-regulation of integrin β1 mrna in adult rat brain. *Molecular Brain Research*. 1998;55:265-276

104. Ellison JA, Velier JJ, Spera P, Jonak ZL, Wang X, Barone FC, Feuerstein GZ. Osteopontin and its integrin receptor alphavbeta3 are upregulated during formation of the glial scar after focal stroke. *Stroke*. 1998;29:1698-1707

105. Giachelli C, Lombardi D, Johnson R, Murry C, Almeida M. Evidence for a role of osteopontin in macrophage infiltration in response to pathological stimuli in vivo. *American Journal of Pathology*. 1998;152:353-358

106. Matsumoto M, Sakao Y, Akira S. Inducible expression of nuclear factor il-6 increases endogenous gene expression of macrophage inflammatory protein-1

alpha osteopontin and cd14 ina monocytic leukemia cell line. *International Immunology*. 1998;10:1825-1835

107. Guo H, Cai C, Schroeder R, Kuo P. Osteopontin is a negative feedback regulator of nitric oxide synthesis in murine macrophages. *Journal of Immunology*. 2001;166:1079-1086

108. Singh K, Sirokman G, Communal C, Robinson K, Conrad C, Brooks W, Bing O, Colucci W. Myocardial osteopontin expression coincides with the development of heart failure. *Hypertension*. 1999;33:663-670

109. Wang D, Yamamoto S, Hijiya N, Benveniste E, Gladson C. Transcriptional regulation of the human osteopontin promoter: Functional analysis and DNA-protein interactions. *Oncogene*. 2000;19:5801-5809

110. Samdani AF, Dawson TM, Dawson VL. Nitric oxide synthase in models of focal ischemia. *Stroke*. 1997;28:1283-1288

111. Liu T, Clark RK, McDonnell PC. Tumor necrosis factor alpha expression in ischemia neurons. *Stroke*. 1994;25:1481-1488

112. Buttini M, Appel K, Sauter A, Gebicke-Haerter PJ, Boddeke HW. Expression of tumor necrosis factor alpha after focal ischemia in the rat. *Neuroscience*. 1996;7:1-16

113. Barone FC, Feuerstein GZ. Inflammatory mediators and stroke: New opportunities for novel therapeutics. *Journal of Cerebral Blood Flow & Metabolism*. 1999;19:819-834

114. Cuttle L, Zhang X-J, Endre Z, Winterford C, Gobe G. Bcl-x_l translocation in renal tubular epithelial cells in vitro protects distal cells from oxidative stress. *Kidney International*. 2001;59:1779-1788

115. Padanilam BJ, Martin DR, Hammerman MR. Insulin-like growth factor i-enhanced renal expression of osteopontin after acute ischemic injury in rats. *Endocrinology*. 1996;137:2133-2140

116. Persy VP, Verstrepen WA, Ysebaert DK, De Greef KE, De Broe ME. Differences in osteopontin up-regulation between proximal and distal tubules after renal ischemia/reperfusion. *Kidney International*. 1999;56:601-611

117. Liaw L, Birk DE, Ballas CB, Whitsitt JS, Davidson JM, Hogan BLM. Altered wound healing in mice lacking a functional osteopontin gene (spp1). *Journal of Clinical Investigation*. 1998;101:1468-1478

118. Noiri E, Dickman K, Miller F, Romanov G, Romanov V, Shaw R, Chambers A, Rittling S, Denhardt D, Goligorsky M. Reduced tolerance to acute renal ischemia in mice with a targeted disruption of the osteopontin gene. *Kidney International*. 1999;56:74-82

119. Meller R, Stevens SL, Minami M, Cameron JA, King S, Rosenzweig H, Doyle K, Lessov NS, Simon RP, Stenzel-Poore MP. Neuroprotection by osteopontin in stroke. *Journal of Cereberal Blood Flow and Metabolism*. 2005;25:217-225

120. Schroeter M, Zickler P, Denhardt D, Hartung H, Jander S. Increased thalamic neurodegeneration following ischaemic cortical stroke in osteopontin deficient mice. *Brain*. 2006;129:1426-1437

121. Ellison JA, Barone FC, Feuerstein GZ. Matrix remodeling after stroke: De novo expression of matrix proteins and integrin receptors. *Annals of the New York Academy of Sciences*. 1999;890:204-222

122. Murry C, Giachelli C, Schwartz S, Vracko R. Macrophages express osteopontin during repair of myocardial necrosis. *American Journal of Pathology*. 1994;145:1450-1462

123. Reddy K, Mangale S. Integrin receptors: The dynamic modulators of endometrial function. *Tissue Cell*. 2003;35:260-273

124. Pardridge W. *Peptide drug delivery to the brain*. New York: Raven Press; 1991.

125. Brownless J, Williams C. Peptidases, peptides and the mammalian blood-brain barrier. *Journal of Neurochemistry*. 1993;60:1089-1096

126. Lo E, Singhal A, Torchilin V, Abbott N. Drug delivery to damaged brain. *Brain Research Reviews*. 2001;38:140-148

127. Begley D. The blood brain barrier: Principles for targeting peptides and drugs to the central nervous system. *Journal of Pharmacy and Pharmacology*. 1996;48:136-146

128. Brightman M. *Physiology and pharmacology of the blood brain barrier. Handbook of experimental pharmacology 103*. Berlin: Springer-Verlag; 1992.

129. Nabeshima S, Reese T, Landis D, Brightman M. Junctions in the meninges and marginal glia. *Journal of Comparative Neurology*. 1975;164:127-169

130. Kunz J, Krause D, Kremer M, Dermietzel R. The 140-kda protein of blood brain barrier associated pericytes is identical to aminopeptidase n. *Journal of Neurochemistry*. 1994;62:2375-2386

131. Taylor E. The impact of eflux transporters in the brain on the development of drugs for cns disorders. *Clinical Pharmokinetics*. 2002;41:81-92

132. Sadeque A, Wandel C, He H, Shah S, Wood A. Increased drug delivery to the brain by p-glycoprotein inhibition. *Clinical Pharmacological Therapeutics*. 2000;68

133. Illum L. Transport of drugs from the nasal cavity to the central nervous system. *Eur Journal of Pharmaceutical Science*. 2000;11:1-18

134. Kucheryanu V, Kryzhanovsky G, VS K, Yurasov V, Zhigaltsev I. *Intranasal fibroblast growth factors: Delivery into the brain exerts antiparkinsonian effect in mice*. Boston: Controlled release society; 1999.

135. Liu B, Hammer GD, Rubinstein M, Mortrud M, Low MJ. Identification of DNA elements cooperatively activating proopiomelanocortin gene expression in the pituitary gland of transgenic mice. *Molecular and Cellular Biology*. 1992;12:3978-3990

136. Frey W, Liu J, Chen X, Thorne R, Fawcett J, Ala T. Delivery of nerve growth factor to the brain via the olfactory route. *Drug Delivery*. 1997;4:87-92

137. Pietrowsky R, Struben C, Molle M, Fehm H, Born J. Brian potential changes after intranasal administration vs intravenous administration of vasopressin: Evidence for a direct nose to brain pathway for peptide effects in humans. *Biological Psychiatry*. 1996;39:332-340

138. Pietrowsky R, Thieman A, Kern W, Fehm H, Born J. A nose-brain pathway for psychotropic peptides: Evidence from a brain evoked potential study with cholecystokinin. *Psychoneuroendocrinology*. 1996;70:63-72

139. Kern W, Born J, Schreiber H, Fehm H. Central nervous system effects of intranasally administered insulin during euglycemia in men. *Diabetes*. 1999;48:557-563

140. Hinchcliffe M, Illum L. Intranasal insulin drug delivery and therapy. *Advanced Drug Delivery Reviews*. 1999;35:199-234

141. Liu X, Fawcett J, Thorne R, Frey W. Non-invasive intranasal insulin-like growth facotr-i reduces infarct volume and improves neurologic function in rats following middle cerebral artery occlusion. *Neuroscience Letters*. 2001;308:91-94

142. Liaw L, Birk DE, Ballas CB, Whitsitt JS, Davidson JM, Hogan BL. Altered wound healing in mice lacking a functional osteopontin gene (spp1). *Journal of Clinical Investigation*. 1998;101:1468-1478

143. Carmichael S. Rodent models of focal stroke: Size, mechanism and purpose. *The journal of the American Society of NeuroTherapeutics*. 2005;2:396-409

144. Guo H, Cai CQ, Schroeder RA, Kuo PC. Osteopontin is a negative feedback regulator of nitric oxide synthesis in murine macrophages. *Journal of Immunology*. 2001;166:1079-1086.

145. Zheng DQ, Woodard AS, Tallini G, Languino LR. Substrate specificity of alpha(v)beta(3) integrin-mediated cell migration and phosphatidylinositol 3-kinase/akt pathway activation. *Journal of Biological Chemistry*. 2000;275:24565-24574

146. Lin YH, Yang-Yen HF. The osteopontin-cd44 survival signal involves activation of the phosphatidylinositol 3-kinase/akt signaling pathway. *Journal of Biological Chemistry*. 2001;276:46024-46030

147. Das R, Mahabeleshwar GH, Kundu GC. Osteopontin stimulates cell motility and nuclear factor kappab-mediated secretion of urokinase type plasminogen activator through phosphatidylinositol 3-kinase/akt signaling pathways in breast cancer cells. *Journal of Biological Chemistry*. 2003;278:28593-28606

148. Thorne RG, Emory CR, Ala TA, Frey WH. Quantitative analysis of the olfactory pathway for drug delivery to the brain. *Brain Research*. 1995;692:278-282

149. Thorne RG, Pronk GJ, Padmanabhan V, Frey WH. Delivery of insulin-like growth factor-i to the rat brain and spinal cord along olfactory and trigeminal pathways following intranasal administration. *Neuroscience*. 2004;127:481-496

150. Thorne RG, Frey WH. Delivery of neurotrophic factors to the central nervous system: Pharmokinetic considerations. *Clinical Pharmokinetics*. 2001;40:907-946

151. Balin BJ, Broadwell RD, Salcman M, El-Kalliny M. Avenues for entry of peripherally administered protein to the cns in mouse, rat and squirrel monkey. *The Journal of Comparative Neurology*. 1986;251:260-280

152. Pantano P, Caramia F, Bozzao L, Dieler C, Kummer R. Delayed increase in infarct volume after cerebral ischemia: Correlations with thrombolytic treatment and clinical outcome. *Stroke*. 1999;30:502-507

153. Senger DR, Perruzzi CA, Papadopoulos-Sergiou A, Van De Water L. Adhesive properties of osteopontin: Regulation by a naturally occurring thrombin-cleavage in close proximity to the grgds cell-binding domain. *Molecular Biological Cell*. 1994;5:565-574

154. Kleinman JG, Worcester EM, Beshensky AM, Sheridan AM, Bonventre JV, Brown D. Upregulation of osteopontin expression by ischemia in rat kidney. *Annals of the New York Academy of Science*. 1995;760:321-323

155. Persy VP, Verstrepen WA, Ysebaert DK, De Greef KE, De Broe ME. Differences in osteopontin up-regulation between proximal and distal tubules after renal ischemia/reperfusion. *Kidney International*. 1999;56:601-611

156. Padanilam BJ, Martin DR, Hammerman MR. Insulin-like growth factor i-enhanced renal expression of osteopontin after acute ischemic injury in rats. *Endocrinology*. 1996;137:2133-2140

157. Noiri E, Dickman K, Miller F, Romanov G, Romanov VI, Shaw R, Chambers AF, Rittling SR, Denhardt DT, Goligorsky MS. Reduced tolerance to acute renal ischemia in mice with a targeted disruption of the osteopontin gene. *Kidney International*. 1999;56:74-82.

158. Denhardt DT, Lopez CA, Rollo EE, Hwang SM, An XR, Walther SE. Osteopontin-induced modifications of cellular functions. *Annals of the New York Academy of Science*. 1995;760:127-142

159. Bonni A, Brunet A, West AE, Datta SR, Takasu MA, Greenberg ME. Cell survival promoted by the ras-mapk signaling pathway by transcription-dependent and -independent mechanisms. *Science*. 1999;286:1358-1362

160. Pugazhenthi S, Nesterova A, Sable C, Heidenreich KA, Boxer LM, Heasley LE, Reusch JE. Akt/protein kinase b up-regulates bcl-2 expression through camp-response element-binding protein. *Journal of Biological Chemistry*. 2000;275:10761-10766.

161. Born J, Lange T, Kern W, McGregor G, Bickel U, Fehm H. Sniffing neuropeptides: A transnasal approach to the human brain. *Nature Neuroscience*. 2002;5:514-516

162. Liu XF, Fawcett JR, Thorne RG, DeFor TA, Frey WH. Intranasal administration of insulin-like growth factor-i bypasses the blood-brain barrier and protects against focal cerebral ischemic damage. *Journal of Neurological Sciences*. 2001;187:91-97

163. Dahlin M, Bergman U, Jansson B, Bjork E, Brittebo E. Transfer of dopamine in the olfactory pathway following nasal administration in mice. *Pharmaceutical Research*. 2000;17:737-742

164. Danuser B, Rebsamen H, Weber C, Krueger H. Lipopolysaccharide-induced nasal cytokine response: A dose-response evaluation. *European Archives of Oto-Rhino-Laryngology*. 2000;257:527-532

165. Jin K, Xie L, Childs J, Sun Y, Mao X, Loginova A, Greenberg DA. Cerebral neurogenesis is induced by intranasal administration of growth factors. *Annals of Neurology*. 2003;53:405-409

166. Liu F, Fawcett JR, Frey WH. Intranasal administration of the antioxidant myricetin reduces infarct volume and improves neurologic function following focal cerebral ischemia in rats. *Neurology*. 2002;58:A389

167. Agnihotri R, Crawford HC, Haro H, Matrisian LM, Havrda MC, Liaw L. Osteopontin, a novel substrate for matrix metalloproteinase-3 (stromelysin-1) and matrix metalloproteinase-7 (matrilysin). *Journal of Biological Chemistry*. 2001;276:28261-28267

168. Green PM, Ludbrook SB, Miller DD, Horgan CMT, Barry ST. Structural elements of the osteopontin svvyglr motif important for the interaction with alpha4 integrins. *FEBS letters*. 2001;503:75 -79

169. Larkin J, Renukaradhya GJ, Sriram V, Du W, Gervay-Hague J, Brutkiewicz RR. Cd44 differentially activates mouse nk t cells and conventional t cells. *Journal of Immunologyl*. 2006;177:268-279

170. Ayroldi E, Cannarile L, Migliorati G, Bartoli A, Nicoletti I, Riccardi C. Cd44 (pgp-1) inhibits cd3 and dexamethasone-induced apoptosis. *Blood*. 1995;86:2672-2678

171. Bates RC, Edwards NS, Burns GF, Fisher DE. A cd44 survival pathway triggers chemoresistance via lyn kinase and phosphoinositide 3-kinase/akt in colon carcinoma cells. *Cancer Research*. 2001;61:5275-5283

172. He B, Mirza M, Weber GF. An osteopontin splice variant induces anchorage independence in human breast cancer cells. *Oncogene*. 2006;25:2192-2202

173. Sakane T, Akizuki M, Taki Y, Yamashita S, Sezaki H, Nadai T. Direct drug transport from the rat nasal cavity to the cerebrospinal fluid: The relation to the molecular weight of drugs. *Journal of Pharmacy and Pharmacology*. 1995;47:379-381

174. Fisher A, Illum L, Davis S, Schacht E. Di-iodo-l-tyrosine-labetted dextrans as molecular size markers of nasal absorbtion in the rat. *Journal of Pharmacy and Pharmacology*. 1992;44:550-554

175. Newman MF, Kirchner JL, Phillips-Bute B, Gaver V, Grocott H, Jones RH, Mark DB, Reves JG, Blumenthal JA. Longitudinal assessment of neurocognitive

function after coronary-artery bypass surgery. *The New England Journal of Medicine*. 2001;344:395-402

176. Tiaho F, Nerbonne JM. Vip and secretin augment cardiac l-type calcium channel currents in isolated adult rat ventricular myocytes. *Pflugers Arch - Europena Journal of Physiology*. 1996;432:821-830

177. Dietrich W, Busto R, Alonso O, Globus M, Ginsberg M. Intraischemic but not postischemic brain hypothermia protects chronically following global forebrain ischemia in rats. *Journal of Cereberal Blood Flow & Metabolism*. 1993;13:541-549

178. Colbourne F, Corbett D. Delayed and prolonged post-ischemic hypothermia is neuroprotective in the gerbil. *Brain Research*. 1994;654:265-272

179. Prakasa B, Yoshida Y, Su M, Segura M, Kawamura S, Yasui N. Immunohistochemical expression of bcl-2, bax, and cytochrome c following focal cerebral ischemia and effect of hypothermia in rat. *Neuroscience Letters*. 2000;291:196-200

180. Yenari M, Iwayama S, Cheng D, Hua Sun G, Fujimura M, Morita-Fujimure Y, Chan P, Steinberg G. Mild hypothermia attenuates cytochrome c release but does not alter bcl-2 expression or caspase activation after experimental stroke. *Journal of Cereberal Blood Flow & Metabolism*. 2002;22:29-38

181. Ning X, Chen S, Xu C, Li L, Yao L, Qian K, Krueger J, Hyyti O, Portman M. Hypothermic protection of the ischemic heart via alterations in apoptotic pathways as assessed by gene array analysis. *Journal of Applied Physiology*. 2002;92:2200-2207

182. Zhao H, Shimohata T, Wang J, Sun G, Schaal D, Sapolsky R, Steinberg G. Akt contributes to neuroprotection by hypothermia against cerebral ischemia in rats. *The Journal of Neuroscience*. 2005;25:9794-9806

183. Leon L. Hypothermia in systemic inflammation: Role of cytokines. *Frontiers in Bioscience*. 2004;9:1877-1888

184. Nishio S, Chen ZF, Yunoki M, Toyoda T, Anzivino M, Lee KS. Hypothermia-induced ischemic tolerance. *Annals New York Academy of Sciences*. 1999;890:26-41

185. Lee Y-J, Miyake S-i, Wakita H, McMullen D, C, Azuma Y, Auh S, Hallenbeck J, M. Protein sumoylation is massively increased in hibernation torpor and is critical for the cytoprotection provided by ischemic preconditioning and hypothermia in shsy5y cells. *Journal of Cerebral Blood Flow & Metabolism*. 2006

186. Stenzel-Poore M, Stevens S, King J, RP S. Preconditioning reprograms the response to ischemic injury and primes the emergence of unique endogenous neuroprotective phenotypes: A speculative synthesis. *Stroke*. In Press

187. Mortoglou A, Candiloros H. The serum triiodothyronamine to thyroxine (t3/t4) ratio in various thyroid disorders and after levothyroxine replacement therapy. *Hormones*. 2004;3:120-126

188. Hiroi Y, Kim H-H, Ying H, Furuya F, Huang Z, Simoncini T, Noma K, Ueki K, Nguyen N-H, Scanlan T, Moskowitz M, Cheng S, Liao J. Rapid nongenomic actions of thyroid hormone. *Proceedings of the National Academy of Science*. 2006;103:14104-14109

189. Scanlan TS, Suchland KL, Hart ME, Chiellini G, Huang Y, Kruzich PJ, Frascarelli S, Crossley DA, Bunzow JR, Ronca-Testoni S, Lin ET, Hatton D, Zucchi R, Grandy DK. 3-iodothyronamine is an endogenous and rapid-acting derivative of thyroid hormone. *Nature Medicine*. 2004;10:638-642

190. Bunzow J, al e. Amphetamine, 3,4-methylenedioxymethamphetamine, lysergic acid diethylamide, and metabolites of catecholamine neurotransmitters are agonists of a rat trace amine receptor. *Molecular Pharmacology*. 2001;60:1181-1188

191. Hart BL. Biological basis of the behavior of sick animals. *Neuroscience and Biobehavior Reviews*. 1988;12:123-137

192. Dietrich W, Lin B, Globus M. Effect of delayed mk-801 treatment with or without immediate post-ischemic hypothermia on chronic neuronal survival after global forebrain ischemia. *Journal of Cereberal Blood Flow and Metabolism*. 1995;15:960-968

193. Barone F, Feuerstein G, White R. Brain cooling during transient focal ischemia provides complete neuroprotection. *Neuroscience Biobehavioral Reviews*. 1997;21:31-44

194. Maier CM, Ahern K, Cheng ML, Lee JE, Yenari MA, Steinberg GK. Optimal depth and duration of mild hypothermia in a focal model of transient cerebral ischemia: Effects on neurologic outcome, infarct size, apoptosis, and inflammation. *Stroke*. 1998;29:2171-2180

195. Meden P, Overgaard K, Pedersen H, Boysen G. Effect of hypothermia and delayed thrombolysis in a rat embolic stroke model. *Acta Neurologica Scandinavia*. 1994;90:904-910

196. Kitagawa K, Matsumoto M, Tagaya M, Hata R, Ueda H, Niinobe M. Ischemic tolerance phenomenon found in the brain. *Brain Research*. 1990;528:21-24

197. Thornhill J, Corbett D. Therapeutic implications of hypothermic and hyperthermic temperature conditions in stroke patients. *Canadian Journal of Physiology and Pharmacology*. 2001;79:254-261

198. Colbourne F, Sutherland G, Auer R. Electron microscopic evidence against apoptosis as the mechanism of neuronal death in global ischemia. *Journal of Neuroscience*. 1999;19:4200-4210

199. Zhao H, Yenari M, RM S, Steinberg G. Mild postischemic hypothermia prolongs the time window for gene therapy by inhibiting cytochrome c release. *Stroke*. 2004;35:572-577

200. Yunoki M, Nishio S, Ukita N, Anzivino MJ, Lee KS. Characteristics of hypothermic preconditioning influencing the induction of delayed ischemic tolerance. *Journal of Neurosurgery*. 2002;97:650-657

201. Leker RR, Gai N, Mechoulam R, Ovadia H. Drug-induced hypothermia reduces ischemic damage: Effects of the cannabinoid hu-210. *Stroke*. 2003;34:2000-2006

202. Bonfils PK, Reith J, Hasseldam H, Johansen FF. Estimation of the hypothermic component in neuroprotection provided by cannabinoids following cerebral ischemia. *Neurochemistry International*. 2006

203. Blackstone E, Morrison M, Roth MB. H2s induces a suspended animation-like state in mice. *Science*. 2005;308:518

204. Qu K, Chen CP, Halliwell B, Moore PK, Wong PT. Hydrogen sulfide is a mediator of cerebral ischemic damage. *Stroke*. 2006;37:889-893

205. Auer R. Combination therapy with u74006f (tirilazad mesylate), mk-801, insulin and diazepam in transient forebrain ischemia. *Neurology Research*. 1995;17:132-136

206. Lyden P, Lonzo L, Nunez S. Combination chemotherapy extends the therapeutic window to 60 minutes after stroke. *Journal of Neurotrauma*. 1995;12:223-230

207. Uematsu D, Araki N, Greenberg J, Sladky J, Reivich M. Combined therapy with mk-801 and nimodipine for protection of ischemic brain damage. *Neurology*. 1991;41:88-94

208. Schabitz W, Fuhai L, Katsumi I, Sandage B, Locke K. Synergistic effects of a combination of low-dose basic fibroblast growth factor and citicoline after temporary experimental focal ischemia. *Stroke*. 1999;30:427-432

209. Matsumoto M, Scheller M, Zornow M, Strnat M. Effects of s-emopamil, nimopidine, and mild hypothermia on hippocampal glutamate concentrations after repeated cerebral ischemia in rabbtits. *Stroke*. 1993;24:1228-1234

210. Meden P, Overgaard K, Pedersen H, Boysen G. Effect of early treatment with tirilazad (u74006f) combined with delayed thrombolytic therapy in rat embolic stroke. *Cerebrovascular Disease*. 1996;6:141-148

211. Meden P, Overgaard K, Sereghy T, Boysen G. Enhancing the efficacy of thrombolysis by ampa receptor blockade nbqx in a rat embolic stroke model. *Journal of Neurological Sciences*. 1993;119:209-216

212. Zausinger S, Scholler K, Plesnila N, Schmid-Elsaesser R. Combination drug therapy and mild hypothermia after transient focal cerebral ischemia in rats. *Stroke*. 2003;34:2246-2251

213. Kollmar R, Henninger N, Bardutzky J, Schellinger P, Schabitz W, Schwab S. Combination therapy of moderate hypothermia and thrombolysis in experimental thromboembolic stroke- an mri study. *Experimental Neurology*. 2004;190:204-212

214. Nawashiro H, Martin D, Hallenbeck JM. Inhibition of tumor necrosis factor and amelioration of brain infarction in mice. *Journal of Cerebral Blood Flow & Metabolism*. 1997;17:229-232

215. Leben J, Tryba M. Prevention of hypothermia during surgery. Contribution of convective heating system and warm infusion. *Annals New York Academy of Sciences*. 1997;813:807-811

216. Schubert A. Side effects of mild hypothermia. *Journal of Neurosurgery and Anesthesiology*. 1997;7:139-147

217. Dirnagl U. Bench to bedside: The quest for quality in experimental stroke research. *Journal of Cerebral Blood Flow & Metabolism*. 2006;1:1-14

218. Hara H, Friedlander RM, Gagliardini V, Ayata C, Fink K, Huang Z, Shimizu-Sasamata M, Yuan J, Moskowitz MA. Inhibition of interleukin 1beta converting

enzyme family proteases reduces ischemic and excitotoxic neuronal damage. *Proceedings of the National Academy of Science USA*. 1997;94:2007-2012

219. Goslin K. Rat hippocampal neurons in low-density culture. *Culturing nerve cells*. 1998:339-370

220. Stenzel-Poore MP, Stevens SL, Xiong Z, Lessov NS, Harrington CA, Mori M, Meller R, Rosenzweig HL, Tobar E, Shaw TE, Chu X, Simon RP. Effect of ischaemic preconditioning on genomic response to cerebral ischaemia: Similarity to neuroprotective strategies in hibernation and hypoxia-tolerant states. *Lancet*. 2003;362:1028-1037

221. Meller R, Skradski SL, Simon RP, Henshall DC. Expression, proteolysis and activation of caspases 6 and 7 during rat c6 glioma cell apoptosis. *Neuroscience Letters*. 2002;324:33-36.

222. Clark WM, Lessov NS, Dixon MP, Eckenstein F. Monofilament intraluminal middle cerebral artery occlusion in the mouse. *Neurology Research*. 1997;19:641-648.

223. Bederson JB, Pitts LH, Germano SM, Nishimura MC, Davis RL, Bartkowski HM. Evaluation of 2,3,5-triphenyltetrazolium chloride as a stain for detection and quantification of experimental cerebral infarction in rats. *Stroke*. 1986;17:1304-1308

224. Lin B, Globus MY, Dietrich WD, Busto R, Martinez E, Ginsberg MD. Differing neurochemical and morphological sequelae of global ischemia: Comparison of single- and multiple-insult paradigms. *Journal of Neurochemistry*. 1992;59:2213-2223

225. Swanson RA, Morton MT, Tsao-Wu G. A semiautomated method for measuring brain infarct volume. *Journal of Cerebral Blood Flow & Metabolism*. 1990;10:290-293

226. Warn PA, Brampton MW, Sharp A, Morrissey G, Steel N, Denning DW, Priest T. Infrared body temperature measurement of mice as an early predictor of death in experimental fungal infections. *Lab Animal*. 2003;37:126-131

227. Marshall J, Ridley R, Baker H, Hall L, Carpenter T, Wood N. Serial mri, functional recovery, and long-term infarct maturation in a non-human primate model of stroke. *Brain Research Bulletin*. 2003;61:577-585

228. Mack W, Komotar R, Mocco J, Coon A, Hoh D, King R, Ducruet A, Ransom E, Oppermann M, DeLaPaz R, Connolly E. Serial magnetic resonance imaging in experimental primate stroke: Validation of mri for pre-clinical cerebroprotective trials. *Neurology Research*. 2003;25:846-852

229. Roitberg B, Khan N, Tuccar E, Kompoliti K, Chu Y, Alperin N, Kordower J, Emborg M. Chronic ischemic stroke model in cynomolgus monkeys: Behavioral, neuroimaging and anatomical study. *Neurology Research*. 2003;25:68-78

230. Fukuda S, Del Zoppo G. Models of cerebral ischemia in the nonhuman primate. *ILAR*. 2003;44:96-104

231. Molinari G, Moseley J, Laurent M. Segmental middle cerebral artery occlusion in primates: An experimental method requiring minimal surgery and anesthesia. *Stroke*. 1974;5:334-339

232. Crowell R, Olsson Y, Klatzo I, Ommaya A. Temporary occlusion of the middle cerebral artery in the monkey: Clinical and pathological observations. *Stroke*. 1970;1:439-448

233. Frykholm P, Hillered L, Langstrom B, Persson L, Valtysson J, Watanabe Y, Enblad P. Increase in interstitial glycerol reflects the degree of ischameic brain damage: A pet and microdialysis study in a middle cerebral artery occlusion-reperfusion primate model. *Journal of Neurology, Neurosurgery and Psychiatry*. 2001;71:455-461

234. Takamatsu H, Tsukada H, Kakiuchi T, Nishiyama S, Noda A, Umemura K. Detection of reperfusion injury using pet in a monkey model of cerebral ischemia. *The Journal of Nuclear Medicine*. 1999;41:1409-1416

235. Takamatsu H, Tsukada H, Noda A, Kakiuchi T, Nishiyama S, Nishimura S, Umemura K. Fk506 attenuates early ischemic neuronal death in a monkey model of stroke. *The Journal of Nuclear Medicine*. 2001;42:1833-1840

236. Furuichi Y, Maeda M, Matsuola N, Mutoh S, Yanagiara T. Therapeutic time window of tacrolimus (fk506) in a nonhuman primate stroke model: Comparision with tissue plasminogen activator. *Experimental Neurology*. 2007;204:138-146

237. Coceani F, Gloor P. The distribution of the internal carotid circulation in the brain o the macaque monkey (macaca mulatta). *Journal of Comparative Neurology*. 1966;128:419-430

238. Dirnagl U, Klehmet J, Braun J, Harms H, Meisel C, Ziemssen T, Prass K, Meisel A. Stroke-induced immunodepression. *Stroke*. 2007;38:770

239. Hudgins W, Garcia J. Transorbital approach to the middle cerebral artery of the squirrel monkey: A technique for experimental cerebral infarction applicable to ultrastructural studies. *Stroke*. 1970;1:107-111